INTEGRATED MULTI-WELL RESERVOIR AND DECISION MODEL TO DETERMINE OPTIMAL WELL SPACING IN UNCONVENTIONAL GAS RESERVOIRS

A Thesis

by

RUBIEL RAUL ORTIZ PRADA

Submitted to the Office of Graduate Studies of
Texas A&M University
in partial fulfillment of the requirements for the degree of

MASTER OF SCIENCE

December 2010

Major Subject: Petroleum Engineering

Integrated Multi-Well Reservoir and Decision Model to Determine Optimal Well Spacing in Unconventional Gas Reservoir

INTEGRATED MULTI-WELL RESERVOIR AND DECISION MODEL TO DETERMINE OPTIMAL WELL SPACING IN UNCONVENTIONAL GAS RESERVOIR

A Thesis

by

RUBIEL RAUL ORTIZ PRADA

Submitted to the Office of Graduate Studies of
Texas A&M University
in partial fulfillment of the requirements for the degree of

MASTER OF SCIENCE

Approved by:

Chair of Committee,	Duane A. McVay
Committee Members,	Stephen A. Holditch
	Thomas A. Blasingame
Head of Department,	Stephen A. Holditch

December 2010

Major Subject: Petroleum Engineering

ABSTRACT

Integrated Multi-Well Reservoir and Decision Model to Determine Optimal Well Spacing in Unconventional Gas Reservoir.

(December 2010)

Rubiel Raul Ortiz Prada, B.S., Universidad Industrial de Santander, Colombia

Chair of Advisory Committee: Dr. Duane A. McVay

Optimizing well spacing in unconventional gas reservoirs is difficult due to complex heterogeneity, large variability and uncertainty in reservoir properties, and lack of data that increase the production uncertainty. Previous methods are either suboptimal because they do not consider subsurface uncertainty (e.g., statistical moving-window methods) or they are too time-consuming and expensive for many operators (e.g., integrated reservoir characterization and simulation studies).

This research has focused on developing and extending a new technology for determining optimal well spacing in tight gas reservoirs that maximize profitability. To achieve the research objectives, an integrated multi-well reservoir and decision model that fully incorporates uncertainty was developed. The reservoir model is based on reservoir simulation technology coupled with geostatistical and Monte Carlo methods to predict production performance in unconventional gas reservoirs as a function of well spacing and different development scenarios. The variability in discounted cumulative production was used for direct integration of the reservoir model with a Bayesian

decision model (developed by other members of the research team) that determines the optimal well spacing and hence the optimal development strategy. The integrated model includes two development stages with a varying Stage-1 time span. The integrated tools were applied to an illustrative example in Deep Basin (Gething D) tight gas sands in Alberta, Canada, to determine optimal development strategies.

The results showed that a Stage-1 length of 1 year starting at 160-acre spacing with no further downspacing is the optimal development policy. It also showed that extending the duration of Stage 1 beyond one year does not represent an economic benefit. These results are specific to the Berland River (Gething) area and should not be generalized to other unconventional gas reservoirs. However, the proposed technology provides insight into both the value of information and the ability to incorporate learning in a dynamic development strategy. The new technology is expected to help operators determine the combination of primary and secondary development policies early in the reservoir life that profitably maximize production and minimize the number of uneconomical wells. I anticipate that this methodology will be applicable to other tight and shale gas reservoirs.

DEDICATION

To my parents Raul and Raquel, who have offered me unconditional love and support throughout my life

ACKNOWLEDGEMENTS

I am grateful to all those who have contributed to this thesis, especially to my advisor, Dr. D.A. McVay, for his wise guidance and to Unconventional Gas Resources for providing the data set of Berland River area and for giving permission to use it in my thesis.

TABLE OF CONTENTS

Page

ABSTRACT iii

DEDICATION v

ACKNOWLEDGEMENTS vi

TABLE OF CONTENTS vii

LIST OF FIGURES ix

LIST OF TABLES xvi

1. INTRODUCTION 1

2. BACKGROUND AND LITERATURE REVIEW 5

3. OBJECTIVE 13

4. METHODOLOGY 14

5. BERLAND RIVER FIELD 18

    5.1. Geological Background 18
    5.2. Gething Formation 21

6. RESERVOIR MODEL 26

    6.1. Multi-Well Reservoir Model Specifications 26
    6.2. Reservoir Simulation Grid 29
    6.3. Reservoir Properties Maps 31
    6.4. Other Parameters 49
    6.5. Validation of Reservoir Model 51
    6.6. Multi-well Reservoir Results 52
    6.7. Recovery Efficiency 67
    6.8. Comparison of Multi-Well Reservoir Model and Single-Well Model. 67

7. DECLINE CURVE MODEL 75

Page

7.1. Overview 75
7.2. Decline Curve Model 76

8. INTEGRATED RESERVOIR AND DECISION MODEL 81

8.1. Overview 81
8.2. Decision Model 81
8.3. Integration of Reservoir with the Decision Model 86
8.4. Optimal Well Spacing Determination 93
8.5. Economic Considerations (Present Value Ratio) 102

9. CONCLUSIONS AND RECOMMENDATIONS 108

9.1. Conclusions 108
9.2. Recommendations for Future Work 110

NOMENCLATURE 112

REFERENCES 115

VITA 121

LIST OF FIGURES

		Page
Figure 1	Unconventional gas production in the United States now accounts for more than half of total gas production.	2
Figure 2	Location map showing the position of the study (Berland River) area relative to the Deep Basin of Alberta (Smith et al. 1984).	19
Figure 3	**a)** Stratigraphic correlation chart of Lower Cretaceous indicating the formation under study (Hietala and Connolly 1984) **b)** Stratigraphic column of the Lower Cretaceous in the Deep Basin are. (Smith et al. 1984).	20
Figure 4	Structure map of the study area at the Lower Cretaceous showing the configuration of the Deep Basin and the adjacent Peace River Arch (Smith et al. 1984).	22
Figure 5	Type logs of the various facies of the Gething Formation (Smith et al. 1984).	24
Figure 6	Net sand isopach map and paleography map of the Gething formation (Smith et al. 1984).	25
Figure 7	Top section of a net-to-gross ratio map showing the location of the individual wells to be simulated.	28
Figure 8	Top view of the simulated area by Schlumberger showing the wells used in their study. The regions enclosed in light purple represent the UGR asset.	30
Figure 9	An example of structure map, top of Gething D Formation for the study area in UGR's integrated reservoir study, meters sstvd (subsea true vertical depth). N – S yellow dashed line indicates a section in the North to South direction shown on Figure 10.	31

Page

Figure 10 Example North-South section indicated by the N-S dashed yellow line on map shown on Figure 9 for UGR's Berland River area showing the vertical layering of Gething D formation interval. The three vertical layers of Gething D formation are indicated by red color lines. 32

Figure 11 Variogram map for gas porosity. The white line shows the major direction of anisotropy. 36

Figure 12 Variogram map for net-to-gross ratio. The white line shows the major direction of anisotropy. 37

Figure 13 Variogram map for permeability. The white line shows the major direction of anisotropy. 38

Figure 14 An exponential variogram model for gas porosity. **a)** is the variogram in the major direction of anisotropy and **b)** is the variogram in the minor direction. 39

Figure 15 A Gaussian variogram model for NTG. **a)** is the variogram in the major direction of anisotropy and **b)** is the variogram in the minor direction. 40

Figure 16 A spherical variogram model for permeability. **a)** is the variogram in the major direction of anisotropy and **b)** is the variogram in the minor direction. 41

Figure 17 An example of a log including facies for a well of the area under study. The facies log is presented on Track 4. Sand facies are represented by the dark yellow color and flood plain deposits by the brown color. 44

Page

Figure 18 A realization of porosity for the Gething D formation obtained through geostatistical procedures. The boxes in light purple represent UGR's lease areas. The shadowed gray box represents the section selected to extract the property maps to be used in the multi-well reservoir model for this project. 45

Figure 19 A realization of net-to-gross for the Gething D formation obtained through geostatistical procedures. The boxes in light purple represent UGR's lease areas. The shadowed gray box represents the section selected to extract the property maps to be used in the multi-well reservoir model for this project. 45

Figure 20 A realization of permeability for the Gething D formation obtained through geostatistical procedures. The boxes in light purple represent UGR's lease areas. The shadowed gray box represents the section selected to extract the property maps to be used in the multi-well reservoir model for this project. 46

Figure 21 An example realization of reservoir property maps for the section of the Gething D interval, Berland River Area, showing the properties in individual layers. 47

Figure 22 Simulation grid of the study area showing a top (**a**) and bottom (**b**) view of the three-dimensional cube of net-to-gross ratio (NTG). 48

Figure 23 Histogram and probability distribution function of depth used for modeling the initial pressure of the Berland River Field. 50

Figure 24 **a)** The multi-well reservoir model yielded a distribution of production that matches the actual distribution of Gething production and single-well reservoir model results quite well, **b)** revised production distribution for multi-well reservoir model where the lowest 10% of production values was removed from Stage-1 results. A better match with the actual distribution of Gething production and single-well reservoir model is observed. 53

Page

Figure 25 **a)** The multi-well reservoir model yielded a distribution of best-month gas production that matches the actual distribution of Gething production. **b)** Lowest 10% of production values removed from Stage 1. A better match with the actual distribution of Gething production is observed. 54

Figure 26 Cumulative distribution functions for multi-well reservoir model results for gas production for **a)** Stage 1 of 5 years and initial spacing of 640 acres and **b)** combined Stage 1 of 640-acre spacing and Stage 2 of 640, 320, 160 and 80-acre spacing. 57

Figure 27 Cumulative distribution functions for multi-well reservoir model results for gas production for **a)** Stage 1 of 5 years and initial spacing of 320 acres and **b)** combined Stage 1 of 320 acres spacing and Stage 2 of 320, 160 and 80 acres spacing. 58

Figure 28 Cumulative distribution functions for multi-well reservoir model results for gas production for **a)** Stage 1 of 5 years and initial spacing of 160 acres and **b)** combined Stage 1 of 320 acres spacing and Stage 2 of 160 and 80 acres spacing. 58

Figure 29 Cumulative distribution functions for multi-well reservoir model results for gas production for **a)** Stage 1 of 5 years and initial spacing of 80 acres and **b)** combined Stage 1 of 320 acres spacing and Stage 2 of 80 acres spacing. 59

Figure 30 Cumulative distribution functions for multi-well reservoir model results for first month gas production for Stage 1duration of 5 years and initial spacing of **a)** 640 acres, **b)** 320 acres, **c)** 160 acres and **d)** 80 acres. 59

Figure 31 Cumulative distribution functions for multi-well reservoir model results for gas production for **a)** Stage 1 of 3 years and initial spacing of 640 acres and **b)** combined Stage 1 of 640 acres spacing and Stage 2 of 640, 320, 160 and 80 acres spacing. 60

Page

Figure 32 Cumulative distribution functions for multi-well reservoir model results for gas production for **a)** Stage 1 of 3 years and initial spacing of 320 acres and **b)** combined Stage 1 of 320 acres spacing and Stage 2 of 320, 160 and 80 acres spacing. 60

Figure 33 Cumulative distribution functions for multi-well reservoir model results for gas production for **a)** Stage 1 of 3 years and initial spacing of 160 acres and **b)** combined Stage 1 of 160 acres spacing and Stage 2 of 160 and 80 acres spacing. 61

Figure 34 Cumulative distribution functions for multi-well reservoir model results for gas production for **a)** Stage 1 of 3 years and initial spacing of 80 acres and **b)** combined Stage 1 of 80 acres spacing and Stage 2 of 80 acres spacing. 61

Figure 35 Cumulative distribution functions for multi-well reservoir model results for first month gas production for Stage 1duration of 3 years and initial spacing of **a)** 640 acres, **b)** 320 acres, **c)** 160 acres and **d)** 80 acres. 62

Figure 36 Cumulative distribution functions for multi-well reservoir model results for gas production for **a)** Stage 1 of 1 year and initial spacing of 640 acres and **b)** combined Stage 1 of 640 acres spacing and Stage 2 of 640, 320, 160 and 80 acres spacing. 62

Figure 37 Cumulative distribution functions for multi-well reservoir model results for gas production for **a)** Stage 1 of 1 year and initial spacing of 320 acres and **b)** combined Stage 1 of 320 acres spacing and Stage 2 of 320, 160 and 80 acres spacing. 63

Figure 38 Cumulative Distribution functions for multi-well reservoir model results for gas production for **a)** Stage 1 of 1 year and initial spacing of 160 acres and **b)** combined Stage 1 of 160 acres spacing and Stage 2 of 160 and 80 acres spacing. 63

Page

Figure 39 Cumulative Distribution functions for multi-well reservoir model results for gas production for **a)** Stage 1 of 1 year and initial spacing of 80 acres and **b)** combined Stage 1 of 80 acres spacing and Stage 2 of 80 acres spacing. 64

Figure 40 Cumulative Distribution functions for multi-well reservoir model results for First Month gas production for Stage 1duration of 1 year and initial spacing of **a)** 640 acres, **b)** 320 acres, **c)** 160 acres and **d)** 80 acres. 64

Figure 41 Example of Cumulative distribution functions for multi-well reservoir model results for **a)** Gas Production by well for Stage 1 duration of 3 years and initial spacing of 80-acre and **b)** Gas production by well for Stage 2 of 80-acre spacing after Stage-1 of 3 years and 80-acre initial spacing. 65

Figure 42 Cumulative production and recovery efficiency versus time for Stage-1 duration of 1 year and initial spacing of 640 acres. 68

Figure 43 Cumulative production and recovery efficiency versus time for Stage-1 duration of 5 years and initial spacing of 640 acres. 68

Figure 44 Comparison of cumulative distributions for total section gas production between multi-well and single-well models **a)** Stage 1 of 3 years and initial spacing of 640 acres and **b)** Stage 1 of 640-acre spacing plus Stage 2 of 640, 320, 160 and 80-acre spacing. 71

Figure 45 Comparison of cumulative distribution for total section gas production between multi-well and single-well models **a)** Stage 1 of 3 years and initial spacing of 320 acres and **b)** Stage 1 of 320-acre spacing plus Stage 2 of 320, 160 and 80-acre spacing. 72

Page

Figure 46 Comparison of cumulative distribution for total section gas production between multi-well and single-well models **a)** Stage 1 of 3 years and initial spacing of 160 acres and **b)** Stage 1 of 160-acre spacing plus Stage 2 of 160 and 80-acre spacing. 73

Figure 47 Comparison of cumulative distribution for total section gas production between multi-well and single-well models **a)** Stage 1 of 3 years and initial spacing of 80 acres and **b)** Stage 1 of 80-acre spacing plus Stage 2 of 80-acre spacing. 73

Figure 48 Comparison of gas production for individual wells between the multi-well and single-well models for an example Monte Carlo iteration. This illustrates how extrapolating the production of the single-well model can over-predict the section production much of the time compared to the multi-well model. 74

Figure 49 Decline curve analysis performed on simulated production. The figure represents a typical gas production rate vs. time. The figure shows t_o, the transition point from hyperbolic to exponential decline.. 78

Figure 50 Schematic decision tree for an unconventional reservoir development plan. 83

Figure 51 An excerpt of the decision tree for the Berland River (Turkarslan 2010). 84

Figure 52 Influence Diagram for proposed decision model. 85

Figure 53 Integration of reservoir and decision model. The results from the reservoir simulation are used to obtain the distributions of discounted (at 10%) cumulative production. The means, standard deviations and correlation coefficients of the discounted cumulative production distribution are calculated and used as input for the decision model. The decision model processes these values along with economical considerations (NPV) and yields the optimal development strategy. ... 87

LIST OF TABLES

		Page
Table 1	Downspacing combinations evaluated in the single-section, multi-well reservoir model.	29
Table 2	Theoretical Variogram parameters.	35
Table 3	Input parameters of Berland River reservoir model.	49
Table 4	Formation depth distribution and uncertainty parameters used in modeling the Berland River Gething D reservoir.	49
Table 5	Example of results from the simulator for the Total Stage Gas Production, Total Discounted Production and Total First Month Production by a section for Stage-1 and Stage-2 for the Stage-1 of 320 acres and duration of 3 years and Stage-2 of 320, 160 and 80 acres.	65
Table 6	Example of results from the simulator for First-Month Gas Production, Stage Gas Production and Discounted Stage Gas Production for each well for Stage 1 and Stage 2 for a Stage 1 of 160 acres and duration of 3 years and Stage 2 of 160 acres.	66
Table 7	Example of Decline Parameters for Stage 1 and Stage 2 of the case for Stage 1 duration of 3 years. The results for Well 1 during Stage 1 at initial spacing of 640 acres and the results for Well 2 during Stage 2 at spacing of 320 acres are shown.	80
Table 8	Weight factors and fractiles used in the decision model.	86
Table 9	Statistical parameters for discounted stage production (MMscf) for Original and Infill wells for a Stage-1 length of 1 year.	90

Page

Table 10	Statistical parameters for discounted stage production (MMscf) for Original and Infill wells for a Stage-1 length of 3 years.	91
Table 11	Statistical parameters for discounted stage production (MMscf) for Original and Infill wells for a Stage-1 length of 5 years.	92
Table 12	Economic Assumptions for Decision Model.	93
Table 13	Optimal development strategy results for Stage-1 length of 1 year. Monetary values are per section.	96
Table 14	Optimal development strategy results for Stage-1 length of 3 years. Monetary values are per section.	97
Table 15	Optimal development strategy results for Stage-1 length of 5 year. Monetary values are per section.	98
Table 16	Optimal development strategy results for Stage-1 length of 1 year with higher gas price ($9.0/Mcf). Monetary values are per section.	99
Table 17	Optimal development strategy results for Stage-1 length of 3 years with higher gas price ($9.0/Mcf). Monetary values are per section.	100
Table 18	Optimal development strategy results for Stage-1 length of 5 years with higher gas price ($9.0/Mcf). Monetary values are per section.	101
Table 19	*PVR* evaluation for the optimal development strategy results for Stage-1 length of 1 year. Monetary values are per section.	105
Table 20	*PVR* evaluation for the optimal development strategy results for Stage-1 length of 3 years. Monetary values are per section.	106

Page

Table 21 *PVR* evaluation for the optimal development strategy results for Stage-1 length of 5 years. Monetary values are per section. 107

1. INTRODUCTION

The rapid growth in the world energy demand and the high depletion rates of existing oil and gas reserves as compared to their discoveries are a major causes of gap between supply and demand (Zahid et al. 2007). To overcome this gap and create a sustainable future energy supply, the oil industry has increased interest and investments in the exploration, production and development of unconventional resources. While this resource is large, developing it in an economic and environmentally sensitive manner is challenging.

Over the last few years, however, new technologies and expertise have greatly enhanced the accessibility of unconventional resources — so much so that this long-neglected resource is now suddenly emerging as one of the most promising complements to our energy future. Unconventional gas, long ignored as a possible contributor to the world's energy equation, suddenly looks like the next big play, mainly due to its long-term potential and its environmental cleanliness. In the United States, unconventional gas now accounts for more than half of total gas production, or some 300 billion cubic meters (bcm) in 2008 (**Fig. 1**), clearly showing the dependence on unconventional gas has increased with tight gas sands, gas shales and coalbed methane being the primary contributors. Elsewhere, the potential of unconventional gas formations is just beginning to be explored, with assessments under way in Europe, South America, India and China,

---

This thesis follows the style of *SPE Journal*.

indicating unconventional gas could soon become a major component in the global energy mix.

Unconventional gas, although plentiful, is hard to reach, locked in massive sedimentary formations; its production is not an easy task. The characterization and exploitation of these reservoirs present significant technical and engineering challenges and their productivity depends upon reservoir properties as well as completion and stimulation practices. Identifying the critical factors to enable economic development is a challenging task.

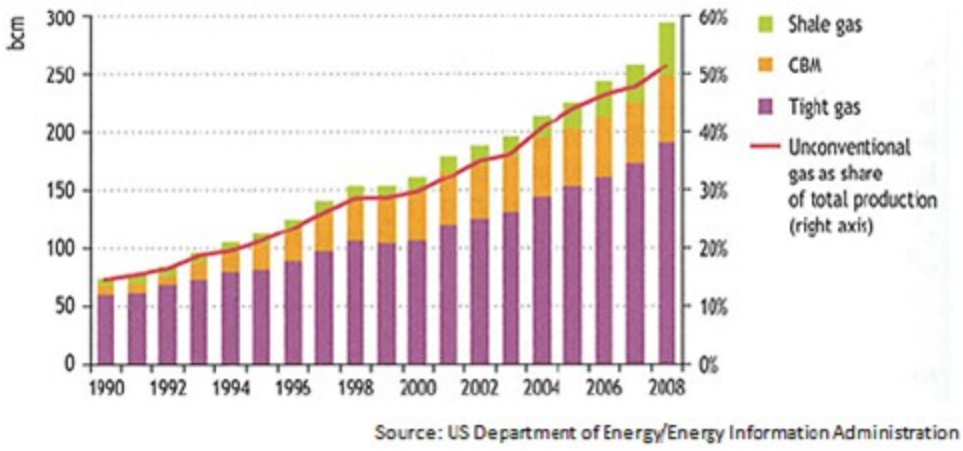

Fig. 1 — Unconventional gas production in the United States now accounts for more than half of total gas production.

Among all unconventional gas resources in North America, tight gas sands represent the major fraction, suggesting it is an important source for future reserves growth and production. Tight gas sands are often characterized by complex geological and petrophysical properties as well as heterogeneities at all scales, factors that increase

the production uncertainty. The low porosity and permeability associated with producing formations, the presence of clay minerals in pores and pore throats, and the reservoir heterogeneity in both vertical and lateral directions all contribute to the complexity of these reservoirs. Moreover, completion and stimulation efficiency are also highly uncertain. Because of the large number of uncertain variables, a deterministic approach is often incapable of capturing the impact of dependencies between parameters that are present in tight gas plays; therefore, stochastic reservoir models are often employed to quantify the uncertainty involved.

Functioning within this risky domain, operators must make sound judgments and development decisions such as determining the optimal well spacing. When making such decisions, operators must balance the need to conserve capital and protect the environment by avoiding over drilling, and maximize profitability by achieving the optimal well spacing early in the reservoir's life.

Unfortunately, development of unconventional tight gas fields, such as the Carthage Field (Panola County, Texas), follows a "series" approach where the initial development activity is followed by long periods of production performance evaluation and surveillance separated by periods of additional drilling and downspacing . Under these conditions, the optimum field spacing may not be achieved until late in the field life (McKinney et al. 2002). This type of suboptimal development can significantly reduce the value of the unconventional asset with potential losses of 50% in the asset value, which shows the importance of identifying the optimal well spacing early in the life of an unconventional gas reservoir.

Traditionally, determination of the optimal well spacing has been carried out through integrated reservoir studies or statistical comparison of the well performance for wells drilled at different spacing. In cases where sufficient data is available from several infill programs implemented over 10 to 40 years, the risk associated with over-drilling is quite low. Unfortunately, for emerging tight gas sands, lack of historical infill programs has resulted in no sufficient data to implement statistical comparison methods for evaluating optimal well spacing, and developing these fields over a 40-year time span is not desirable.

In summary, accelerating the development of unconventional gas reservoir is critical to meet the growing energy demand. Effective exploitation of these reservoirs can be achieved by developing at sufficiently dense well spacing early in the reservoir life, maximizing ultimate recovery, avoiding over drilling, minimizing capital expenditures and maximizing profits. However, the significant uncertainty associated with unconventional reservoirs makes rapid development risky and, without an effective way to manage this uncertainty, operators may under-invest in the development of these reservoirs and/or develop them too slowly.

2. BACKGROUND AND LITERATURE REVIEW

The problem of determining optimal well spacing in tight gas fields has been followed with much interest in the industry and various authors have proposed techniques to address the challenges associated with geologic complexity of these reservoirs, large numbers of wells, and limited reservoir information.

Optimizing the development of low-permeability gas reservoirs is most accurately done by conducting a full-scale reservoir evaluation involving geological, geophysical, petrophysical, and reservoir engineering analyses and interpretations. This includes developing a geological model of the field, , pore-scale characterization of the rock and fluid system, defining the rock in their basis of porosity-permeability relationships and capillary pressure characteristics, definition of the petrophysical model, building and calibrating an accurate reservoir simulation model of the study area, and using it to predict future well performance and optimize the reservoir development (Newsham and Rushing 2001; Rushing and Newsham 2001). Even though the reliability and accuracy of this approach is quite high, this method cannot always be justified given its time-consuming and expensive nature. Furthermore, including uncertainty in the predictions increase the costs and time required.

As an alternative approach to conducting integrated reservoir studies, various authors have used statistical moving-window techniques to provide rapid and cost-effective assessment of optimal well spacing in large, tight-gas basins with large data sets (Hudson et al. 2000; McCain et al. 1993; Voneiff and Cipolla 1996). These

techniques carry out statistical analyses of historical production using performance indicators, such as the best 12 consecutive months of production, maximum production rate or the monthly production rate at the time a specific cumulative production was reached, over the reservoir life. These indicators can be used as proxies for reservoir properties, production response, and reservoir pressure. Comparing performance indicators of old wells to new wells within areal windows, statistical conclusions are drawn concerning interference between existing wells, areas of depletion and undrained acreage. Based on these statistical analyses, the locations and number of infill wells can be estimated.

Guan et al. (Guan and Du 2004; Guan et al. 2002) further advanced the moving-window technology. The method consists of a multitude of local analyses, each in an areal window centered on an existing well. A model-based linear 4D regression equation is applied within each window. Once the regression equation coefficients are determined for each window, performance can be estimated for infill wells by substituting the appropriate values for candidate infill well conditions.

The technique employed by Guan et al. is based in the following assumptions. First, it assumes that reservoir properties do no vary considerable within any moving window throughout the study. Second, it assumes that completions and production technologies applied to each well are identical, regardless when the well was drilled and completed. If performance of new wells is worse than earlier wells, it will not be clear whether it is due to depletion or variation in rock properties. Last, to accurately compute drainage area and recovery per acre, the method also requires at least a few wells in each

part of the study area and that they have sufficient production history to experience boundary-dominated flow, which may take several years for a tight gas well, limiting the applicability of moving-windows for tight gas fields.

The major advantages of the moving-window technology are its speed and its reliance on only well locations and production data, which makes it a practical screening tool for large infill development projects consisting of thousands of wells. However, the estimation errors for infill well performance can be quite significant and well interference effects become complicated as reservoir heterogeneity increases (Guan et al. 2002). Regardless of these assumptions and limitations, the moving-window technique has been applied to the Ozona (Canyon) gas sands (Voneiff and Cipolla 1996), the Milk River formation in Canada (Hudson et al. 2000), the Cotton Valley in East Texas (Hudson et al. 2000; McCain et al. 1993), the Mesaverde formation in the San Juan Basin (Hudson et al. 2001) and the Morrow formation in the Permian Basin (Hudson et al. 2001) to quantify infill potential.

To improve upon moving-window methods, some authors have suggested combining reservoir simulation with automated methods for assessment of infill potential in tight gas basins. Reservoir simulation inversion techniques combine the greater accuracy of simulation-based methods with the short analysis times and low costs associated with statistical methods, to yield a method intermediate in both.

Gao and McVay (2004) introduced simulation-based regression and automated prediction methods for selecting infill candidates in gas-well fields. In this technique, well production response is calculated from the reservoir description data by using a

reservoir simulator that serves as the forward model. To estimate the permeability field, historical production data is inverted based on internally calculated sensitivity coefficients. Once the permeability field is estimated, it is used in conjunction with the forward model to help determine the expected performance of potential infill wells using automated prediction methods. The authors demonstrate that this simulation-based regression procedure results in more accurate predictions of infill performance than moving-window statistical methods. Since the model proposed by Gao and McVay (2004) regresses on permeability only while maintaining other properties fixed at their initial values, errors in the pore-volume distribution may result in large errors in infill predictions.

Cheng et al. (Cheng et al. 2008; Cheng et al. 2006) advanced the simulation-based regression approach proposed by Gao and McVay (2004) by implementing a sequential inversion of both reservoir permeability and pore volume distributions. Adding pore volume to the regression enhanced the quality of the history match, improved the resolution of reservoir characterization, and provided more reliable prediction of future performance and assessment of infill drilling potential. The simulation-based nature of the method requires all the data for initializing a reservoir simulator. Since the method aims at providing rapid and approximate estimation of infill potential, instead of conducting a detailed reservoir characterization study, average properties of any available data are used for initial applications. While the results of this approach are only approximate, they still provide a very fast way to evaluate infill performance in unconventional gas reservoirs. However, these methods are deterministic

and do not quantify the uncertainty inherent in reservoir properties and, thus, in the predictions of future performance.

Teufel et al. (2004) developed an approximate tool called the infill well locator calculator (IWLC) to assist operators in drilling infill wells in low-permeability reservoirs. The tool was used to evaluate infill potential in the San Juan Basin Mesaverde Group. While the tool is resourceful, it only provides a qualitative evaluation of infill performance since it ignores important aspects such as heterogeneity within the test area, and it provides only a deterministic assessment since it does not quantitatively consider the large uncertainty inherent in the assessment.

Turkarslan et al. (2010) implemented a probabilistic reservoir model that incorporates uncertainty in key reservoir parameters (porosity, permeability, net pay, initial pressure and reservoir size) to predict production performance in unconventional gas reservoirs. The reservoir model was integrated with a Bayesian decision model to provide the basis for determining optimal well spacing. The quantification of uncertainty in key reservoir parameters was a major extension over previous methods. In this work, input reservoir and well parameters are treated as random variables and the predictions of future performance are in the form of distributions rather than deterministic values. The reservoir model included pore volume and completion efficiency, parameters missing from previous implementations of moving-window methods.

In Turkarslan's et al. work, a single-well, one-layer, single-phase probabilistic reservoir model was built for modeling the Deep Basin (Gething D) reservoir. The reservoir grid was formulated for the analysis of a hydraulically fractured gas well

located centrally in a rectangular drainage area. The reservoir model incorporated the evaluation of two development stages, a primary development stage and a secondary downspacing stage. All possible two-stage downspacing combinations between 640, 320, 160 and 80 acres were analyzed to study the effect of downspacing and provide the basis for determining the optimal development program for the asset under evaluation. The reservoir model was built assuming the drilling of up to 8 wells in a section; however, for simplicity only 4 wells were modeled.

Simulation results quantify best-month production, stage-end average pressure, discounted stage production and 20-year discounted cumulative production for each well. These production profiles were incorporated into a flexible decision model, which allowed calculation of the expected net present value for each scenario and selection of the optimal development strategy. To facilitate the integration of the reservoir and decision models, discounted stage cumulative production values were used in the decision model. Although a single-well approach was adopted in the model, the heterogeneity was modeled by attributing different reservoir properties to each well (individually sampled from the same statistical distributions) and correlation coefficients of reservoir properties from a geostatistical study were used to account for spatial dependence of these properties between wells.

The decision model used in Turkarslan's et al. work uses decision tree-analysis. These trees are solved starting at the end (right) and "rolling-back." Thus, the optimal Stage 1 spacing decision cannot be made without first determining the optimal Stage 2 spacing, given every possible Stage 1 outcome. To simplify this procedure, the

production uncertainties were discretized using discrete probability mass functions containing five branches. This five-point approximation improves the accuracy and better illustrates the impact that learning between stages has on making decisions.

Even though the proposed model by Turkarslan incorporates uncertainty in reservoir properties not considered in previous works, the use of a single-well model and the extrapolation of the production performance of one well to obtain the performance of multiple wells in a section could produce significant errors in production predictions. For example, in a reservoir section up to 8 wells might be drilled and they could be represented by one well in the model. If the combination of sampled reservoir properties lead to a high production performance, over prediction on the performance of the section could result when the single-well results are used to represent all the wells in the section, thus misleading the production values to be used in the decision model. Due to this, it presents some limitations such as overestimation of the uncertainty that could provide errors in the prediction of production performance, its inability to capture the pressure interference and dependencies between wells, and the reservoir is reduced to a single layer with homogeneous properties. With these limitations, errors in predictions could lead to suboptimal decisions.

All these methodologies except the one proposed by Turkarslan et al. are deterministic, clearly they produce only one representation of the reservoir and do not include the quantification of uncertainty in future performance predictions that is inherent in the assessment of unconventional reservoirs and also do not quantify the risk involved in development decisions. Finally, the probabilistic reservoir model developed

by Turkarslan et al. (2010) was a single-well model where the reservoir is reduced to a single homogenous layer and potential errors in production predictions can be observed.

Based on these observations, it is clear that there is still a need to better quantify for the heterogeneity and uncertainty in reservoir properties by exploring the development of a multi-well probabilistic reservoir model using more detailed geostatistical characterization to represent the reservoir properties rather than using a constant property value. The reservoir model will be combined with a flexible decision model to evaluate multiple development scenarios and their potential economic outcomes that will allow the assessment of optimal well spacing under significance subsurface uncertainty.

3. OBJECTIVE

This research has been conducted by a group consisting of Texas A&M University, the University of Texas, and with Unconventional Gas Resources (UGR). The overall objective of this project is to develop technology to help operators determine the optimal well spacing for unconventional gas reservoirs. More specifically, it is to develop an integrated reservoir and decision model for determining the optimal well spacing early in the reservoir life in highly uncertain and risky unconventional gas reservoirs, with the goal of maximizing profitability.

My specific objectives include the development of a multi-well, single-phase probabilistic reservoir model to assess the uncertainty in key reservoir parameters and allow prediction of production performance as a function of well spacing for an unconventional gas reservoir. They also include using geostatistical characterization to model uncertainty in reservoir property distributions for a section of the reservoir to be used in the model, and integrating this reservoir model with a Bayesian decision model developed simultaneously by the Department of Industrial Engineering at Austin that will provide the basis for determining optimal well spacing. Finally, the objectives include applying the integrated model to Unconventional Gas Resources' tight gas asset in the Berland River area, Alberta, Canada, to determine the optimal well spacing and hence the optimal development strategy for this particular reservoir.

4. METHODOLOGY

The reservoir model is based on reservoir simulation techniques coupled with stochastic methods, i.e., Monte Carlo and geostatistical procedures to evaluate uncertainty in key reservoir parameters such as porosity, permeability, net pay and initial pressure. I implemented a stochastic reservoir model to predict future production performance. The quantification of uncertainty is done using 1,000 maps of reservoir properties obtained through geostatistical characterization of the area. The reservoir model was built for modeling UGR's tight gas asset in the Berland River Area, Alberta, Canada, and more specifically the Gething D formation.

I used a stochastic modeling tool, @RISK from the Palisade Corporation, coupled with CMG's (Computer Modeling Group) full-featured adaptive implicit-explicit black oil simulator, IMEX, and a VBA (Microsoft Visual Basic® for Applications) code generated in Excel® to perform thousands of simulations automatically. Future production performance was forecasted in the form of a distribution and was used as input to the decision model.

Following is a description of the methodology I used:

1. First, I built a probabilistic, multi-well reservoir simulation model for a section (640 acres) of the Gething D reservoir. The single-phase gas model includes up to 8 wells in the section and the grid is formulated to accommodate hydraulically fractured wells. The steps used to create the reservoir model are as follow:
    - A VBA code was generated in Excel® coupling CMG's IMEX simulator

with @RISK to perform thousands of simulations automatically.

- An IMEX example input file template is created in Excel® by the VBA code.
- Information regarding well locations, horizon depths, and structural maps, from an integrated reservoir study of the area provided by UGR was used to populate the simulation grid with reservoir properties.
- The integrated reservoir study built in PETREL (PETREL is a Schlumberger Windows based software for 3D visualization, 3D mapping and 3D reservoir modeling and simulation) for the area using well logs and other information was used to construct 1,000 geostatistical maps of reservoir properties (porosity, permeability and net-to gross ratio *NTG*) for the evaluation of uncertainty.
- The reservoir model was used to predict production performance of the area. Forecasted production profiles, stage gas production, average pressure, discounted cumulative gas productions and decline curve parameters for each well were determined.

2. I validated the multi-well reservoir model by comparing simulated 2-year production results to the actual first two years of production of the Berland River area and the production forecasts obtained with a single-well reservoir model previously used to evaluate the area (Turkarslan et al. 2010) .
3. The new reservoir model was evaluated with all possible 2-stage downspacing combinations that can be generated between 640, 320, 160 and 80 acres. The

proposed development scenario and decision context consisted of two stages with a varying Stage-1 time span. The reservoir model was run with Stage-1 durations of 1-, 3- and 5-year and Stage-1 plus Stage-2 duration combine a total of 20 years. I used the reservoir model results to determine the effect of downspacing and later coupled the results with a flexible decision model to determine the optimal infill drilling program.

4. I fitted the production profiles with decline curves to facilitate the integration of the reservoir model with the decision model. The decline curve model was calibrated against the reservoir simulation results and could be directly integrated into the decision model if required. The decline model used a hyperbolic decline for initial production (accounting for the long transient decline period in unconventional reservoirs) and terminates in an exponential decline to avoid unrealistically high reserves estimations that would be obtained if a hyperbolic decline is used alone. Although we experimented with use of the decline curve model for integration of reservoir modeling results into the decision model, ultimately we decided not to use it.
5. A decision model developed simultaneously with this research by the Department of Industrial Engineering at the University of Texas at Austin was used. The forecasted probabilistic production from the reservoir model was used as input in the decision model with all possible combinations of stages and well spacing. The decision model uses decision tree analysis to assess the uncertainty in production performance from the reservoir model and determine the optimal

well spacing.

6. Applying these integrated tools and working with the operating company, specific development decisions (optimal development policies) in the UGR's Deep Basin (Gething) tight gas sands in the Berland River area, Alberta were modeled.

5. BERLAND RIVER FIELD

5.1. Geological Background

The Deep Basin of western Alberta and northeastern British Columbia encompasses one of the North America's largest gas fields with recoverable reserves ranging between 50 to 150 Tcf (Masters 1979). However, development of these big fields continues to be a major challenge for the industry. Most of the gas in this basin is found in low-porosity, low-permeability reservoir rocks, which combined with recent economics makes commercial development of many of the gas zones extremely difficult (Smith et al. 1984). **Fig. 2** shows the approximate location of the Berland River area, located on the edge of the Deep Basin of Western Alberta. As it happens with most tight gas fields, its successful exploitation depends on the ability to identify areas of good porosity and associated permeability. In western Alberta, higher permeability is normally associated with coarse-grained sandstones and chert pebble conglomerates. The Berland River area for this study includes approximately 236 million square meters (58,240 acres, 91 sections), which includes about 120 wells, involving about 46 wells operated by Unconventional Gas Resources (UGR).

A review of the literature of the area allowed us a better understanding of the regional structural and stratigraphic characteristics of the Gething sands. Stratigraphically, the Gething sands are overlain by the Bluesky formation and underlain by the Cadomin sands (**Fig. 3).** Geologically, the Cadomin formation was deposited in

Barremian time, the Gething sands and carbonaceous strata were deposited in Aptian time, and the Bluesky was deposited in Albian time.

Fig. 2 — Location map showing the position of the study (Berland River) area relative to the Deep Basin of Alberta (Smith et al. 1984).

During the early Cretaceous, the Cordillera of Western North America was continuous from Mexico to Alaska. Periodic uplifts within the Cordillera resulted in the shedding of clastics into the Pacific Ocean (westward) and the North American interior (eastward). The physiography of the interior during this time varied between a low-relief, near-sea-level plain to a shallow epicratonic sea in which sedimentation kept pace with basin subsidence. At this time, the relationship between land and sea in the interior

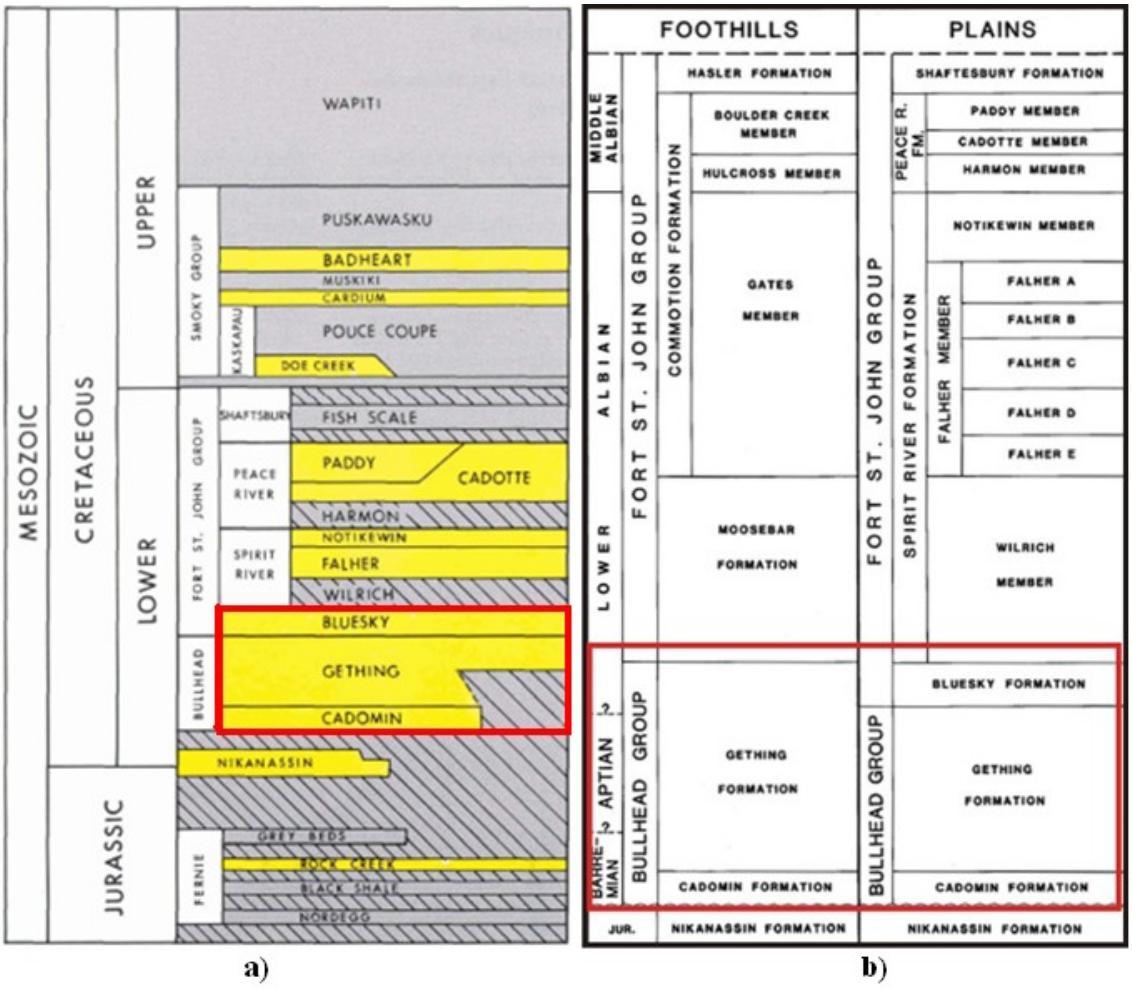

Fig. 3 — a) Stratigraphic correlation chart of Lower Cretaceous indicating the formation under study (Hietala and Connolly 1984) **b)** Stratigraphic column of the Lower Cretaceous in the Deep Basin are. (Smith et al. 1984).

is defined by evaluation of the environments of deposition. A strong Cordilleran uplift during Barremian time caused more shedding of clastics, represented by the alluvial fan and braid-plain conglomerates of the Cadomin Formation that were deposited in a belt flanking the eastern of the Cordillera. In Aptian time, the developing trough continued to deepen resulting in the accumulation of the fluvial and delta plain sediments of the

Gething Formation. An advance of the Boreal Sea into northeastern British Columbia and northern Alberta during Aptian time is represented by the coastal and shallow marine sandstones of the Bluesky member.

Tectonic elements affecting the Lower Cretaceous deposition within the Alberta basin were minimal. Apart from the Cordilleran uplift, the only tectonic feature that affected the depositional environment was the Peace River Arch (**Fig. 4)** located to the north of the study area. However, it had limited effect on the Lower Cretaceous with only a gentle thickening of the strata along the arch axis.

The various depositional environments for the study area are:

1- Cadomin - Alluvial fan and plain environment

2- Gething - Fluvial deposits and flood plain

3- Bluesky - Shore face sand and shales

Since the formation of interest in this study is the Gething formation, below is a more detailed description of this formation.

5.2. Gething Formation

Sediments of the Gething formation consist primarily of inter-bedded fine- to medium-grained sandstones, siltstones, mudstones and coaly formations. The sequence is terrestrial and is described as a low-relief interior drainage plain on the eastern flank of the Lower Cretaceous Cordillera. Sandstones are fining upward or thin-bedded. Trough and planar cross-bedded, ripple-bedded and parallel-laminated sandstones are

common. Plant material including fossil leaves, stems, logs, stumps, and other carbonaceous debris are also common. Coal beds occur throughout the Gething formation and dinosaur foot prints have been discovered in Peace River canyon (**Fig. 5**).

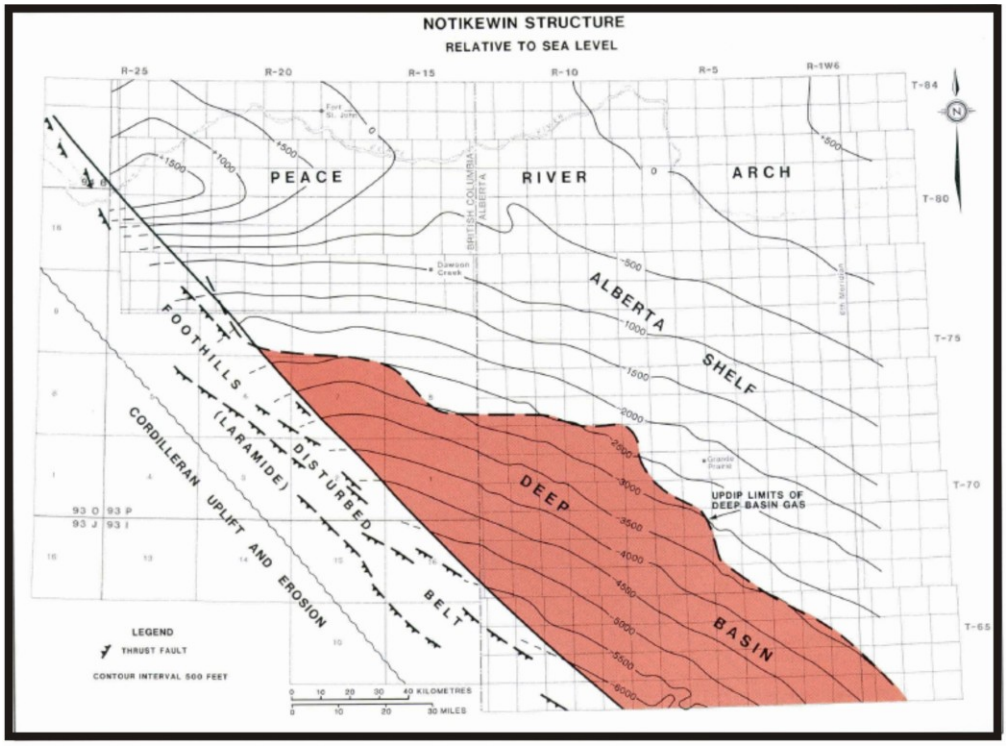

Fig. 4 — Structure map of the study area at the Lower Cretaceous showing the configuration of the Deep Basin and the adjacent Peace River Arch (Smith et al. 1984).

The sandstones of the Spirit River system are primarily restricted to the lower Gething, this is illustrated in **Fig. 5** that shows the type logs of the various facies of the Gething formation, being D the lower section. During the late Gething the drainage pattern changed significantly. The Fox Creek Escarpment was buried by Gething sediments and the drainage plain expanded eastward. Since there was no constraint, the

river system meandered across a considerably larger drainage plain. The physiography of this larger drainage system was a low-lying swampy plain with numerous shallow lakes. There were braided streams to the west and meandering streams to the east. No evidence of marine sedimentation was observed in the study area although the coastline was not far away.

During early Aptian time, rivers flowed northeast from the Cordillera then northwest along a main river channel (Spirit River Channel). **Fig. 6,** an isopach of net Gething sandstone, displays the drainage pattern. Belts of active tributary channels clearly show a northeast drainage pattern. The Spirit River Channel system has narrowed from Cadomin time but is still a major trunk system.

In conclusion, Gething sediments represent channel and overbank deposition across a wide, low-relief plain located on the eastern flank of the Cordilleran uplift. Rivers flowed east from the Cordillera across the plain to join a major north-flowing trunk system, the Spirit River Channel. Sediments include fining-upward fluvial channel sandstones, siltstones, shales and coal. Reservoir rock is restricted primarily to channel sandstones.. The Gething formation in the Berland River area exhibits average porosity of 6% and permeability ranges from 0.001 to 2.3 md, reflecting the “tight” nature of this formation.

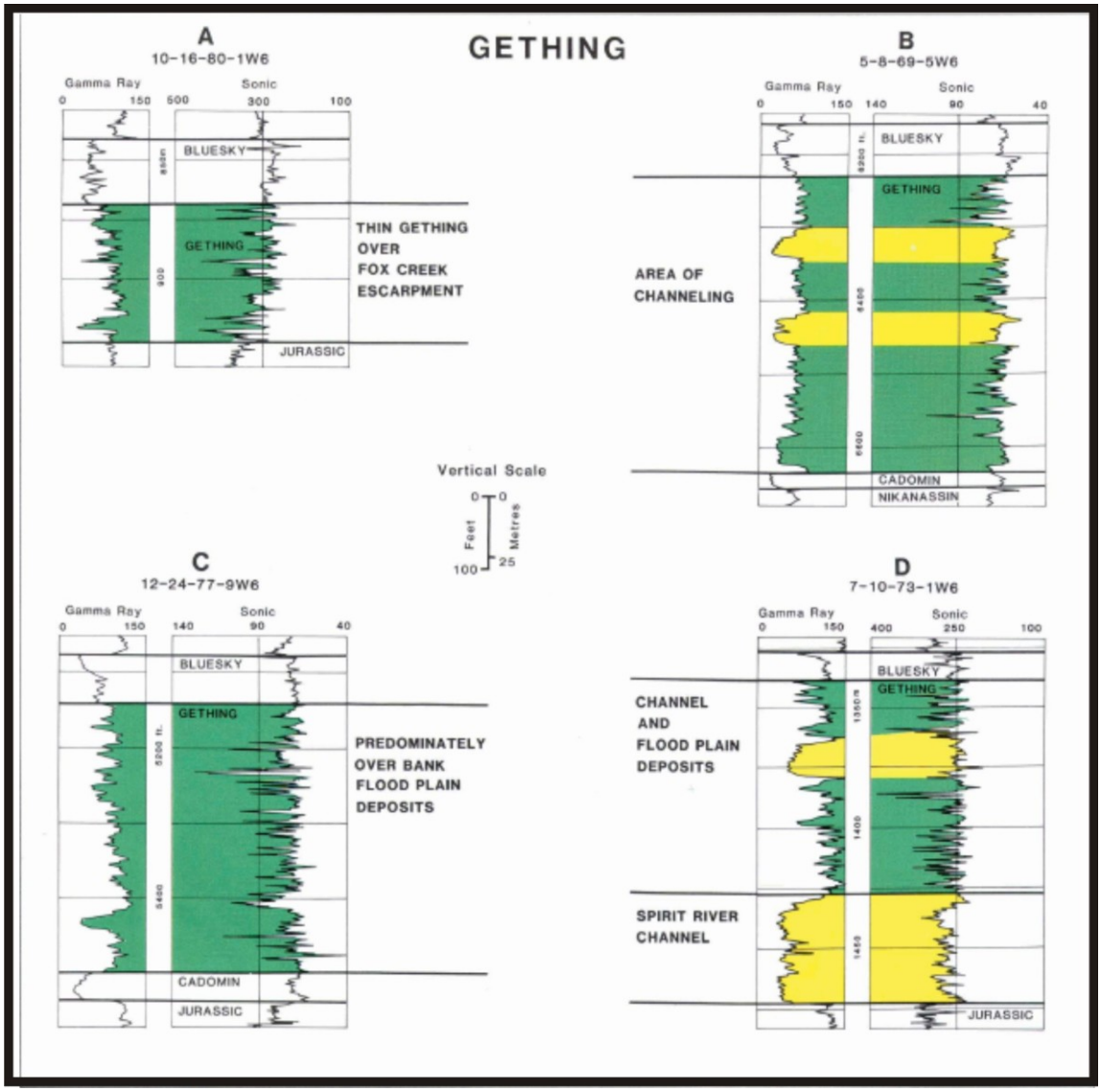

Fig. 5 — Type logs of the various facies of the Gething Formation (Smith et al. 1984).

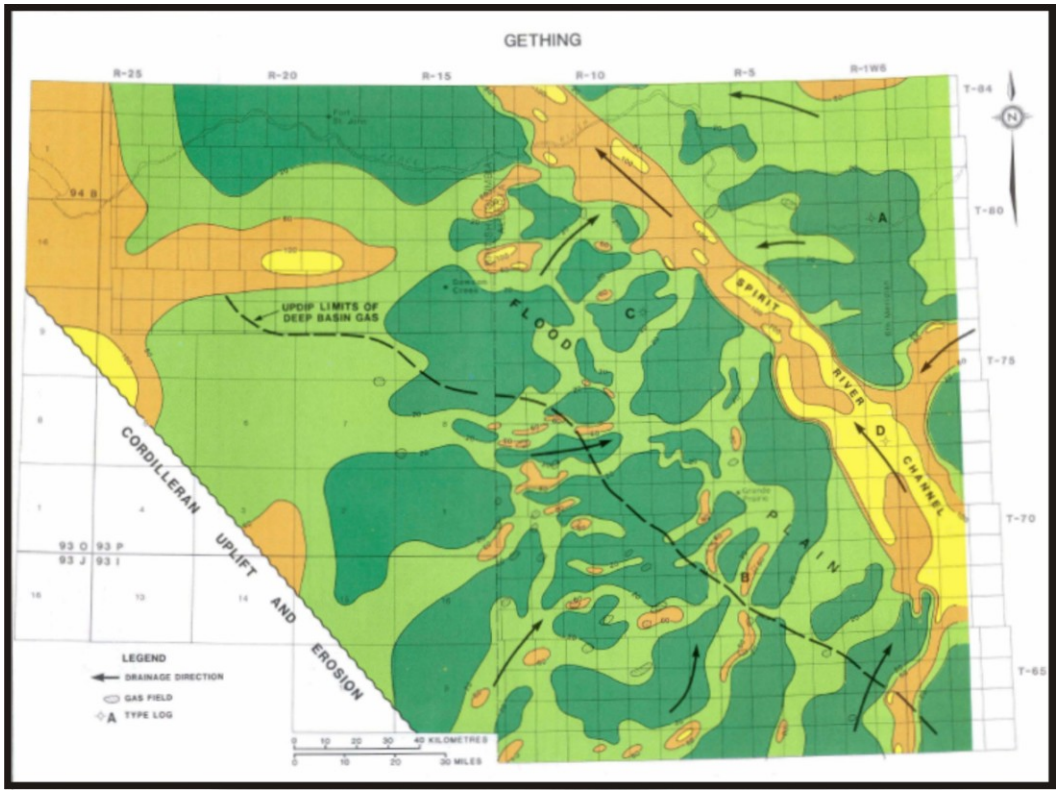

Fig. 6 — Net sand isopach map and paleography map of the Gething formation (Smith et al. 1984).

6. RESERVOIR MODEL

6.1. Multi-Well Reservoir Model Specifications

Monte Carlo (MC), or stochastic, simulation has been used to explore the impact of uncertainty on oil and gas project performance worldwide. It is also widely used to propagate uncertainty in input parameters through a reservoir performance model (Oudinot et al. 2005; Schepers et al. 2009; Turkarslan 2010; Turkarslan et al. 2010; White et al. 2000). The uncertainty is addressed by generating a large number of simulations, sampling distributions for geologic, engineering and other important parameters. The MC simulation employees a mathematical model that introduces randomness between limits to determine a probabilistic outcome. Typically this result is in the form of a distribution, the shape of which provides insights into what is likely to occur if the modeled course of action is pursued (Oudinot et al. 2005).

Thus, stochastic modeling is helpful in dealing with reservoir heterogeneity (Acosta and Mata 2005). Sampling for uncertainty assessment requires a sufficiently large number of model runs with randomly sampled inputs. Stochastic analysis could need thousands of simulations runs, especially if there are many uncertain variables present and an accurate performance response is required (Kalla and White 2005). Geostatistical algorithms are normally used to obtain possible realizations of a reservoir parameter honoring its geological spatial behavior and considering the rock intrinsic heterogeneity. Coupling a Monte Carlo simulation procedure with geostatistical

characterization of reservoir parameters can be found in literature mostly for conventional reservoirs, (Schepers et al. 2009; White et al. 2000). However, only recently geostatistical characterization coupled with MC procedure has been applied for reservoir simulation of unconventional plays (Gonzalez et al. 2006; Schepers et al. 2009; Turkarslan et al. 2010).

I implemented in this research a probabilistic, multi-well reservoir model based on reservoir simulation techniques coupled with stochastic methods and geostatistical characterization. Two major extensions over a previous probabilistic single-well model developed by (Turkarslan et al. 2010) are: (1) key reservoir parameters are incorporated in the form of areal reservoir property maps obtained through geostatistical procedures and (2) it incorporates multiple wells in the model rather than using just one well.

The reservoir model simulates one section of the reservoir (640 acres). A data input file for CMG's IMEX simulator is created by the VBA code. Key reservoir parameters (porosity, permeability and *NTG*) are included as geostatistical maps and initial pressure is defined by a @RISK distribution function. The single-section multi-well reservoir model includes up to 8 wells in the section. The wells are numbered consistent with the order in which they would be drilled if spacing was progressively reduced from 640-ac spacing to 320-ac, 160-ac, and then 80-ac spacing. The reservoir model is formulated for the analysis of hydraulic fractured gas wells.

Fig. 7 shows a map of net-to-gross ratio in the Gething D formation, the simulation grid, and the locations of the wells in the section. The simulation study included all possible combinations of two-stage downspacing between 640, 320, 160 and

80 different acres (**Table 1**) for Stage-1 durations. The proposed development scenario consisted of two stages with varying time spans. Stage-1 was evaluated at time durations of 1, 3 and 5 years. Stage-2 was evaluated for time duration of 19, 17 and 15 years respectively. The total simulated time between both stages was 20 years. Forecasted production profiles, stage gas production, average pressure, discounted cumulative gas productions and decline curve parameters for each well are determined.

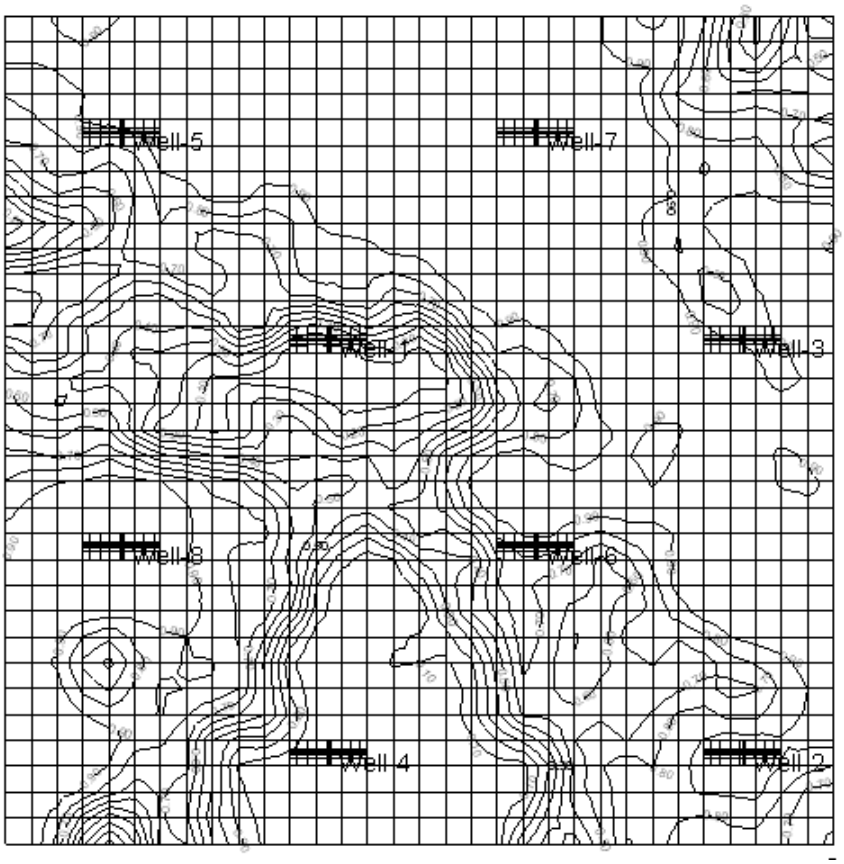

Fig. 7 — Top section of a net-to-gross ratio map showing the location of the individual wells to be simulated.

Table 1 — Downspacing combinations evaluated in the single-section, multi-well reservoir model

Stage-1 \ Stage-2	640	320	160	80
640	X	-	-	-
320	X	X	-	-
160	X	X	X	-
80	X	X	X	X

6.2. Reservoir Simulation Grid

One of the steps in building the reservoir model was to determine the simulation grid. An integrated reservoir study of the area provided by UGR was used as basis for this reservoir model. The study used around 120 wells within the area to build the structural model. The other wells are located mostly one location outside UGR's leases.

Fig. 8 shows the distribution of wells completed in the area, 46 wells are operated by UGR. The integrated study was done in PETREL. On the study, a structural map was constructed for the area by correlating sands tops through a grid of cross-sections, connecting every well with log curves. From the cross-sections, structure maps were made for the Cadomin, Gething and Bluesky formations. **Fig. 9** shows one of the structure maps built, in this case for the Gething D formation interval. The structure maps were used for the framework of the 3-D static model developed in their study.

The simulation grid was selected for a section (640 acres) of the modeled area in the integrated study. The section was selected to include an area where the main perforated interval was the Gething D formation, the main producer sand from the area. The Gething D formation in the integrated study was subdivided vertically into three

layers to capture the vertical layering seen on the logs (**Fig. 10**), and replicate the high degree of vertical and lateral heterogeneity seen in the distribution of gas through the reservoir. Fig. 9 shows the North-South section presented in Fig. 10. The final grid selected for the model was a 32x32x3 grid with a total of 3072 cells. The model includes a hydraulic fracture in each well, along the x-axis. To accurately model gas flow in the hydraulically fractured wells, the hydraulic fracture is explicitly modeled by refined grids along the fracture and around the well bore.

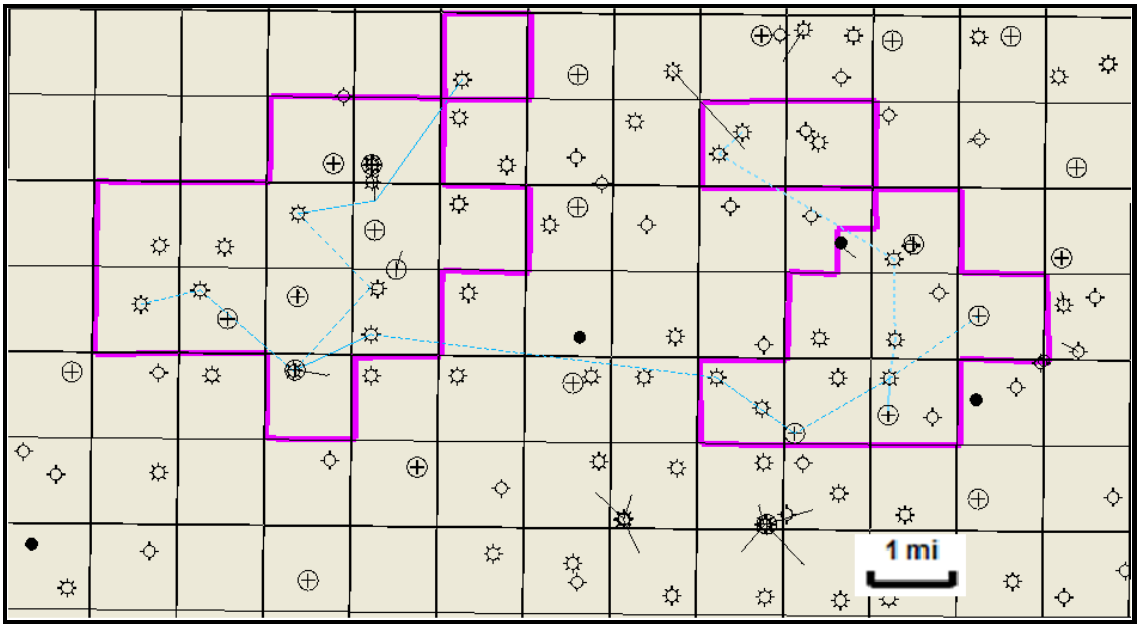

Fig. 8 — Top view of the simulated area by Schlumberger showing the wells used in their study. The regions enclosed in light purple represent the UGR asset.

6.3. Reservoir Properties Maps

Geostatistics is generally applied to obtain more realistic reservoir characterization, which honors geological spatial behavior and considers rock heterogeneity. The use of multiple geological scenarios and realizations has been discussed in the context of brown fields' development (Acosta and Mata 2005; Manceau et al. 2001; Mishra et al. 2002; Twartz et al. 1998). In these studies, multiple geological scenarios or multiple realizations within one geological scenario were generated to identify P_{10}, P_{50}, and P_{90} geological models to be used in history matching and forward predictions.

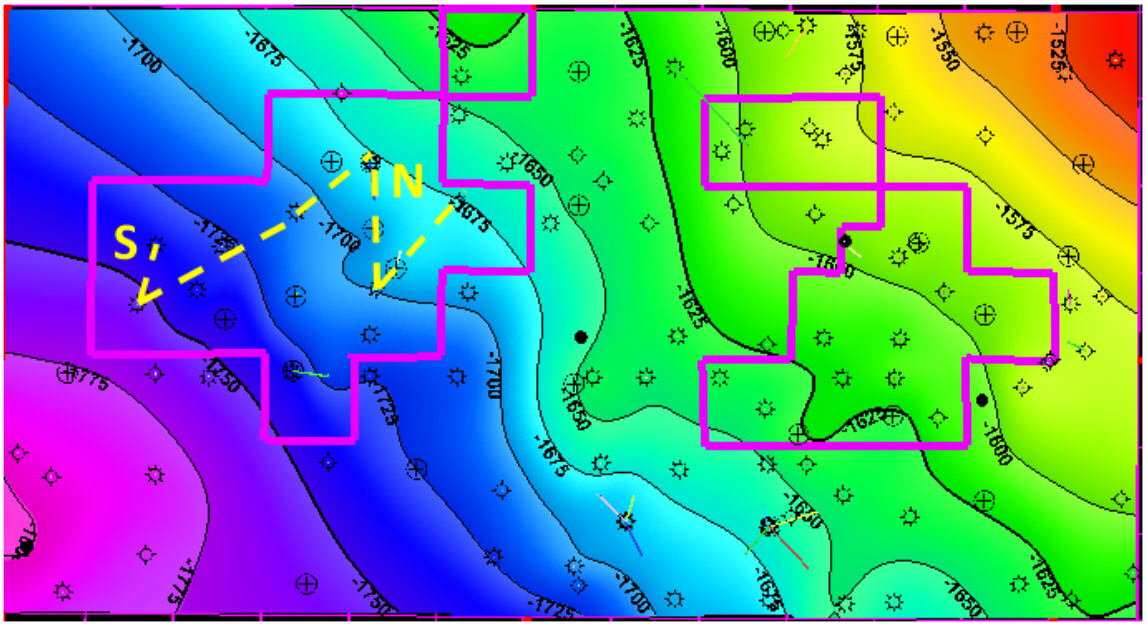

Fig. 9 — An example of structure map, top of Gething D Formation for the study area in UGR's integrated reservoir study, meters sstvd (subsea true vertical depth). N – S yellow dashed line indicates a section in the North to South direction shown on Fig. 10.

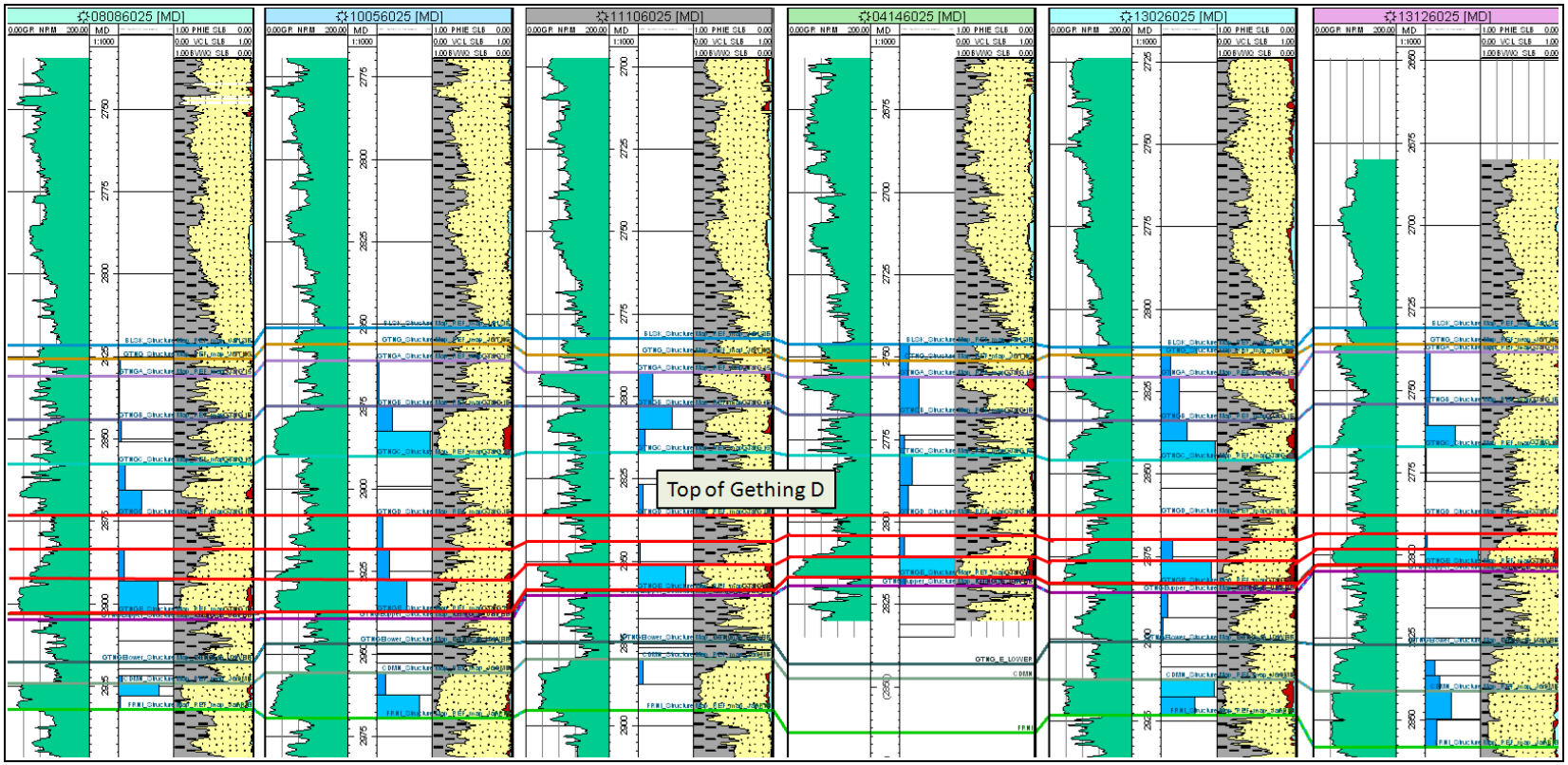

Fig. 10 — Example North-South section indicated by the N-S dashed yellow line on map shown on Fig. 9 for UGR's Berland River area showing the vertical layering of Gething D formation interval. The three vertical layers of Gething D formation are indicated by red color lines.

The procedure developed in this research includes the use of geostatistical characterization to generate multiple possible representations of the primary reservoir parameters to populate the reservoir model. To evaluate the uncertainty in the reservoir model, 1,000 maps of key reservoir parameters, including net-to-gross ratio (*NTG*), gas porosity (ϕ_{gas}) and gas permeability (k_{gas}), were obtained. The wells with available log data that can be used for interpretation from the UGR's integrated field study of the Berland River area were used as input to generate the maps.

The property modeling workflow used for the integrated field study of Berland River Area was done in PETREL. It includes data analysis which is a process of quality controlling the data, exploring the data to identify key geological features and prepare the input for petrophysical modeling, it also includes data transformation, correlation between properties and variograms, followed by vertical up-scaling and finally horizontal population of the main properties (*NTG*, ϕ_{gas}, k_{gas}) to describe rock quality. In total, log data from 109 wells that have been in production at some time during the field life were used.

Basic reservoir parameters were upscaled. As the simulation grid cells often are much larger than the sample density for well logs, well log data must be scaled up before they can be entered into the grid. When scaling up the well logs, PETREL will first find the 3D grid cells that the wells penetrate. For each grid cell, all log values that fall within the cell will be averaged according to the selected algorithm to produce one log value for that cell. For discrete well logs (e.g. facies or zone logs), the average method "Most of" is recommended. For this method, the upscaled value will then correspond to the value

that is most represented in the log for that particular cell. The result of the scale up well logs process is placed as a property model icon in the Properties folder for the 3D grid. It only holds values for the 3D grid cells the wells have penetrated. All other cells have an undefined value. Property modeling is then used to assign values to all the other grid cells, based on the scaled up well logs and optional trend data.

Normalized Gamma Ray logs were used to generate volume of shale logs (*Vsh* logs) that were used to obtain net-to-gross ratio logs (*NTG=1-Vsh*), since *Vsh* logs can be upscaled and populated as a continuous property; normalized density and neutron logs were used as porosity inputs; and the permeability model is based on a porosity-permeability relationship conditioned to core data from the field and validated by pressure build-up. I used the upscaled logs already available in the integrated field study to generate the reservoir property maps using PETREL's property modeling process.

Using the available upscaled logs at the wells location I first constructed variogram maps of the main properties to evaluate the direction of anisotropy and determine in which direction there is enough stable data to construct empirical variograms to be used for the property modeling. The variogram map is obtained by calculating variograms in all possible azimuths and plotting them in a Cartesian plane. This gives the appearance of a contour map, where the contour maps are lines connecting points of equal variance. If the data have any anisotropy, it will be reflected in this variogram map in the form of elliptical contours. The direction of the elliptical closure will indicate the anisotropy direction. Once the anisotropy is identified, then the variograms are obtained. PETREL's data analysis module was used to obtain the

variogram maps and then the empirical variograms for the main properties in the major and minor directions of anisotropy. The major direction defines the direction in which the sample points have the strongest correlation (the main angle is specified as the clockwise angle from the north for the main search directions), the minimum direction is perpendicular to the major direction. **Fig. 11** is the variogram map for gas porosity; from this map we observed the major direction of anisotropy for gas porosity to be 68 degrees. Similarly, **Fig. 12** and **Fig. 13** show the variogram maps for *NTG* and permeability. The major directions of anisotropy are 297 degrees for *NTG* and 264 degrees for permeability. The empirical variograms were fitted by variogram models to obtain the theoretical variograms. **Table 2** shows the type of variograms models used and the variogram parameters. **Fig. 14** to **Fig. 16** show the fitted variograms for each property in both the major and minor directions.

Table 2 — Theoretical Variogram parameters

Property	Variogram Model	Angle of Major Direction	Range Major Direction (m)	Range Minor Direction (m)	Sill	Nugget
Gas Porosity	Exponential	68	3910	2015	1.054	0.034
NTG	Gaussian	247	2570	2470	0.952	0.116
Permeability	Spherical	264	2520	2430	0.997	0.050

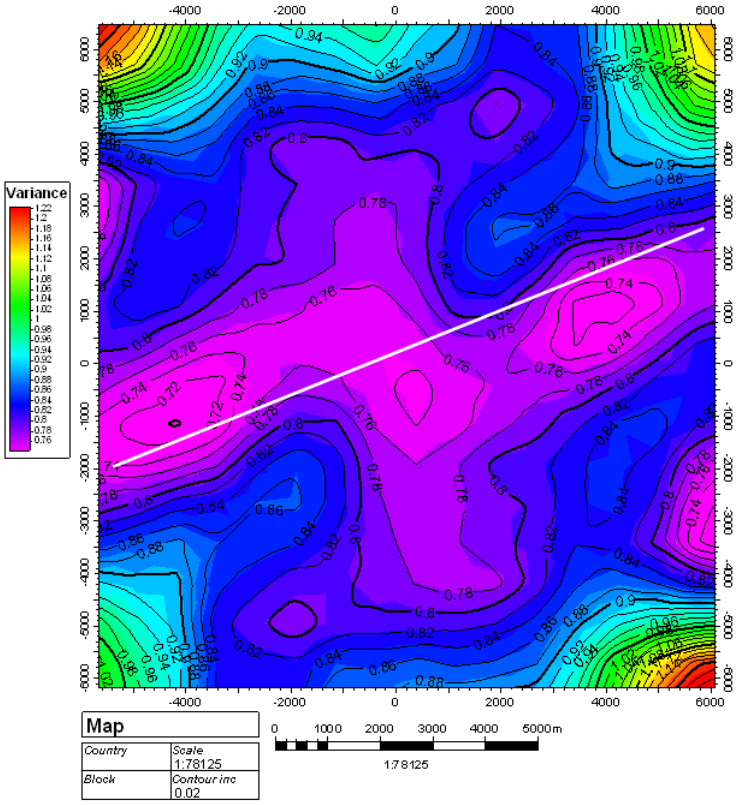

Fig. 11 — Variogram map for gas porosity. The white line shows the major direction of anisotropy.

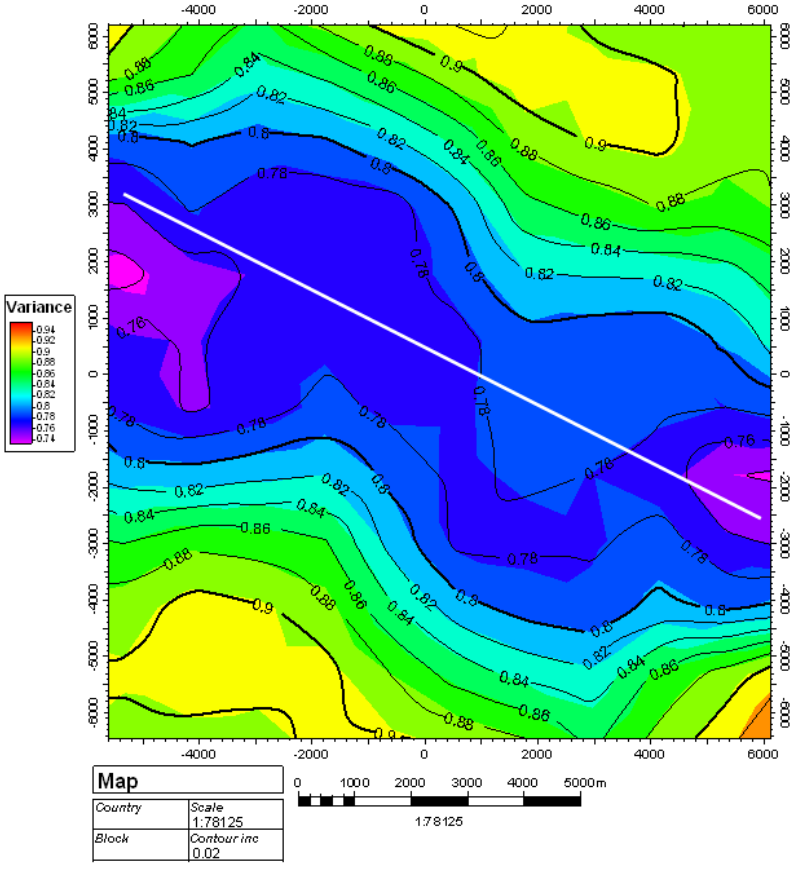

Fig. 12 — Variogram map for net-to-gross ratio. The white line shows the major direction of anisotropy.

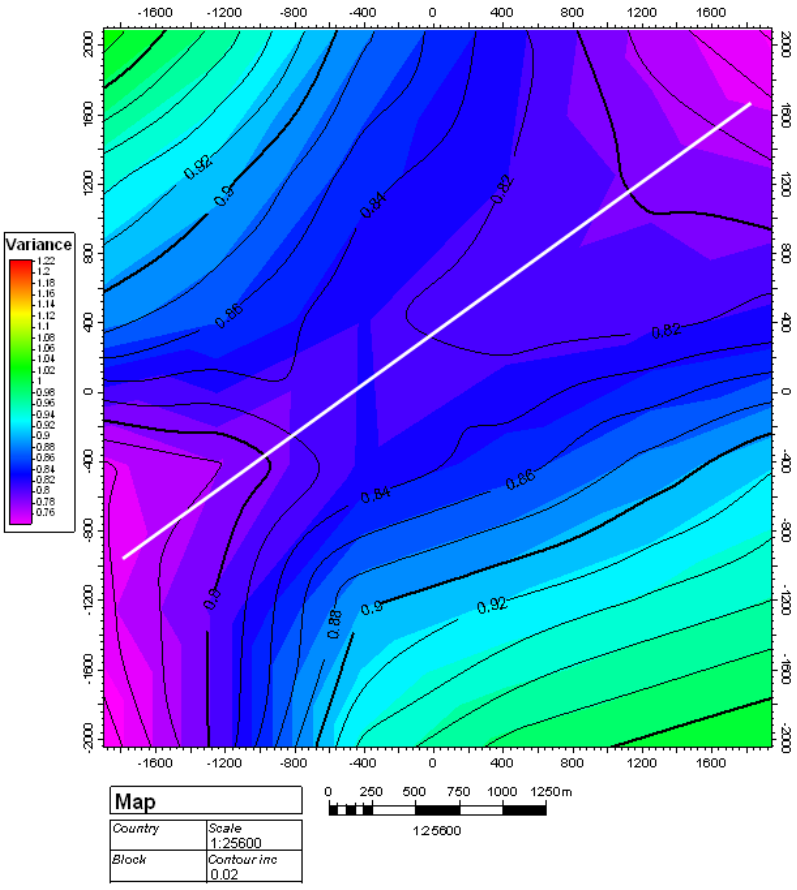

Fig. 13 — Variogram map for permeability. The white line shows the major direction of anisotropy.

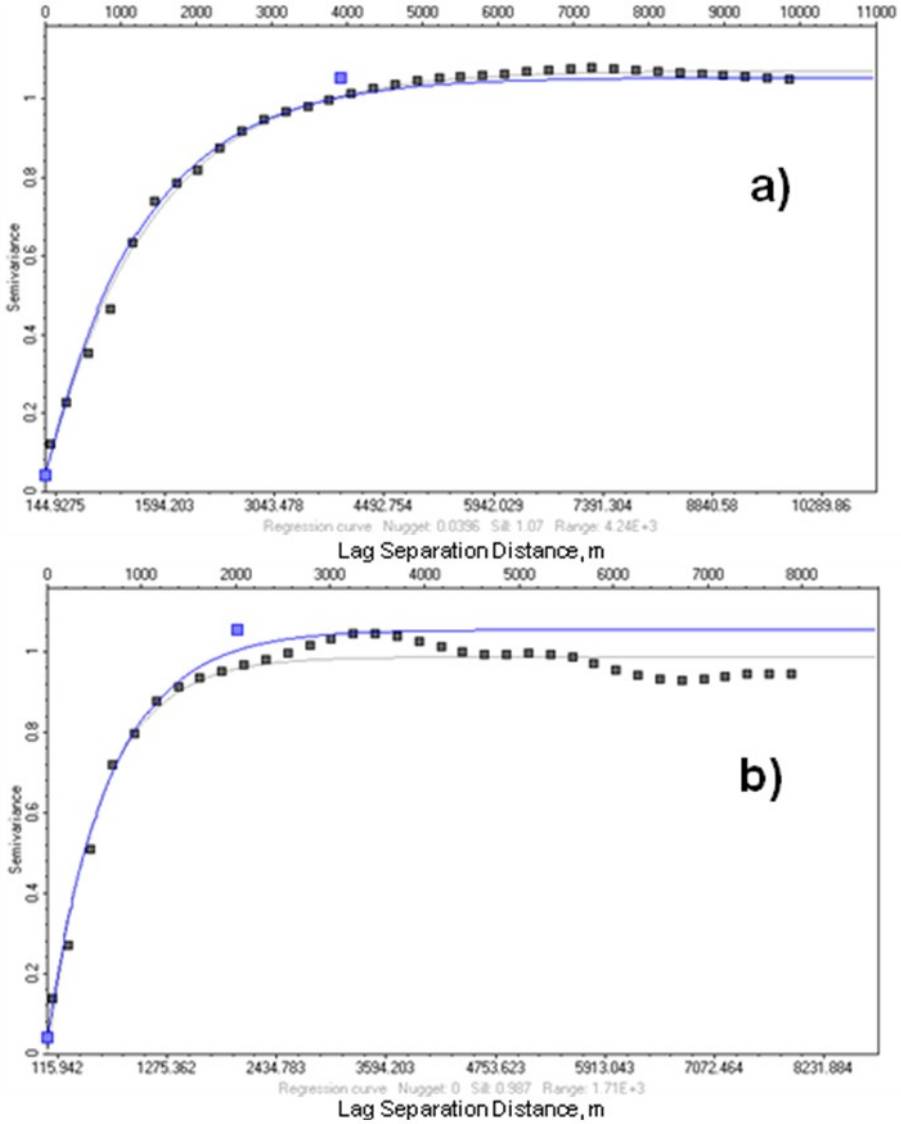

Fig. 14 — An exponential variogram model for gas porosity. **a)** is the variogram in the major direction of anisotropy and **b)** is the variogram in the minor direction.

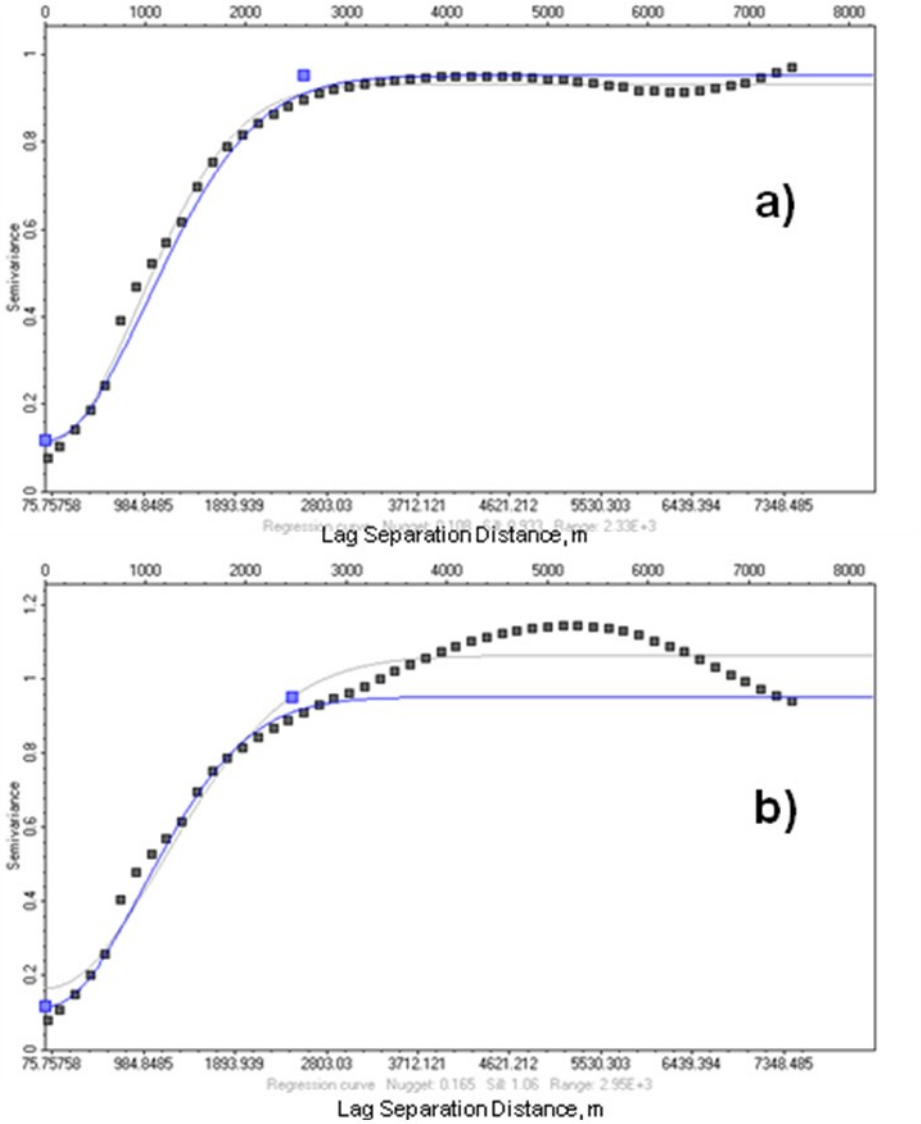

Fig. 15 — A Gaussian variogram model for NTG. **a)** is the variogram in the major direction of anisotropy and **b)** is the variogram in the minor direction.

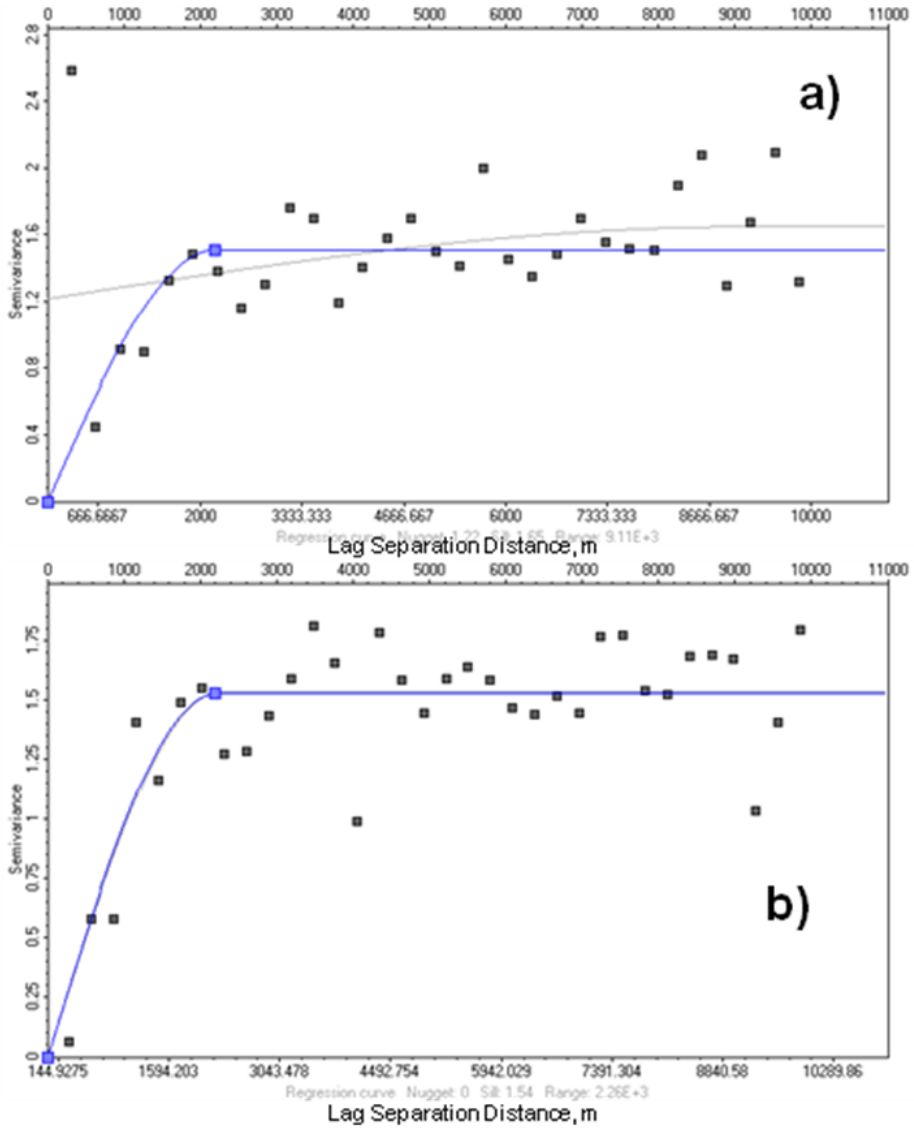

Fig. 16 — A spherical variogram model for permeability. **a)** is the variogram in the major direction of anisotropy and **b)** is the variogram in the minor direction.

I used a Sequential Gaussian Simulation (SGS) algorithm from PETREL's petrophysical modeling process which is a stochastic method of interpolation based on kriging, which honors the well data, input distributions, variograms and trends, to generate the 1,000 property maps. Upscaled logs, variograms and input distributions were used during the petrophysical modeling. All cells in the simulation grid were given values. The upscaled parameters are fixed at the wellbore of existing wells and are honored by the algorithm; the model then was populated with the three pertinent parameters away from wellbores. Ordinary kriging was used as part of the SGS process to generate 1,000 reservoir properties maps. Facies were defined, one to represent sands and one to represent the flood plain deposits. Logs of these facies were generated for the available wells and the facies modeling was done in conjunction with property modeling. **Fig. 17** shows an example of a facies log for one of the wells in the area.

For permeability, a co-kriging option was used to steer the simulation using the spatial distribution of a second variable together with a correlation coefficient to calculate the contribution of the secondary variable at each point. The pore volume normalized by the arithmetic mean was used as the secondary variable and a correlation coefficient of 0.68 determined by PETREL was used. The correlation coefficient was estimated based on the upscaled log values and it is given for the normal score transformed data of both primary and secondary variables. The correlation coefficient is obtained from a cross-plot of the two variables in the normal score space and basically summarizes the relationship between the two variables.

Fig. 18 to **Fig. 20** show one of the individual realizations of the porosity, net-to-gross ratio and permeability maps of the Gething D formation for the entire Berland River Area obtained through the geostatistical procedure described above. Gas porosity ranges from 0 to 0.1, net-to-gross ratio ranges from 0 to 1, and gas permeability ranges from 0.001 to 2.3 md. These property maps show the heterogeneous nature of the reservoir. The gray area on these figures represents the section from where the 1,000 property maps were obtained for the multi-well reservoir model for this project.

An example of one realization of reservoir properties map for the selected section of the Berland River Area is presented in **Fig. 21**. **Fig. 22** also shows one realization of the property *NTG* on a 3-D display of the simulation grid. Note the high degree of heterogeneity seen through the model both laterally and vertically in the study area. The high degree of heterogeneity both vertically and laterally displayed on Figs. 21and 22 highlights the need for using a multi-well model to simulate the tight gas reservoir.

After the reservoir simulation using the 1,000 realizations of properties maps was initiated, some issues were found with the maps that needed correction before the simulation could be continued. The most significant was related to adjustment required to the NTG value for certain cells that need to change its value from 0% to 0.5% to avoid undesired stops in the simulation.

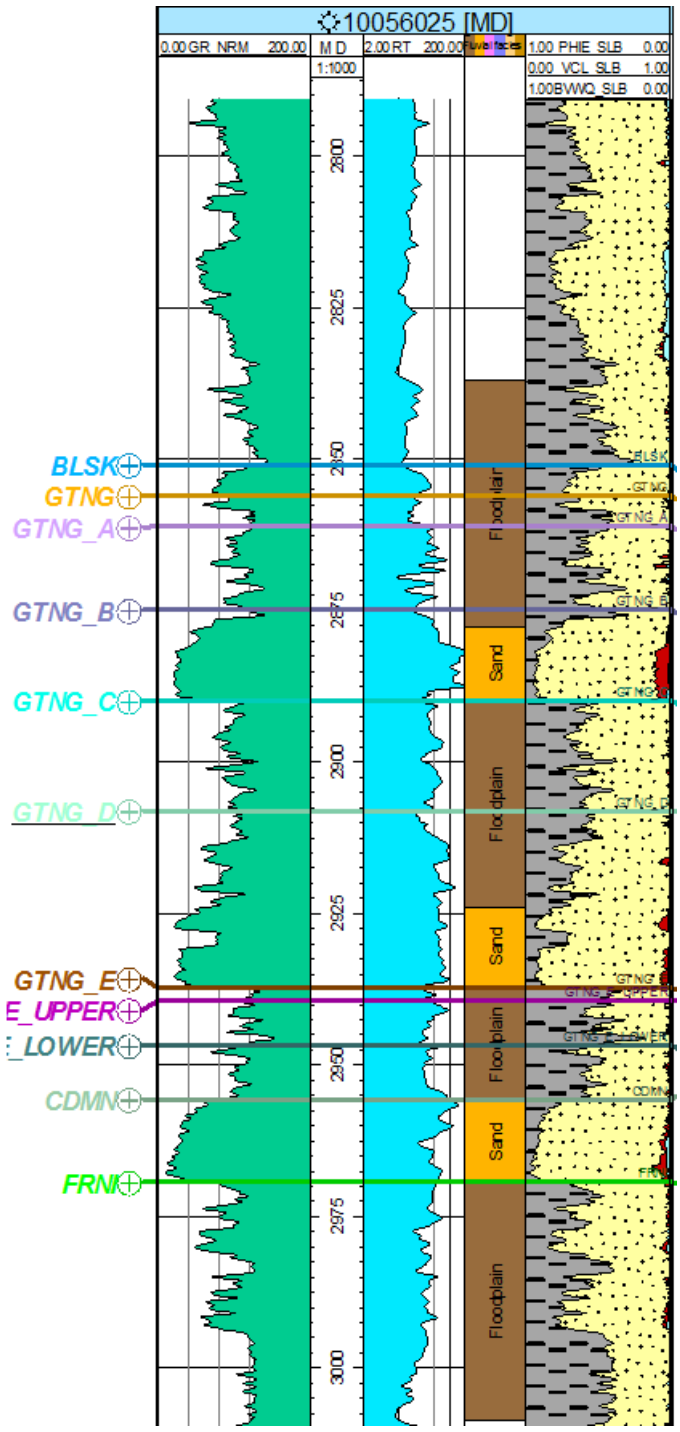

Fig. 17 — An example of a log including facies for a well of the area under study. The facies log is presented on Track 4. Sand facies are represented by the dark yellow color and flood plain deposits by the brown color.

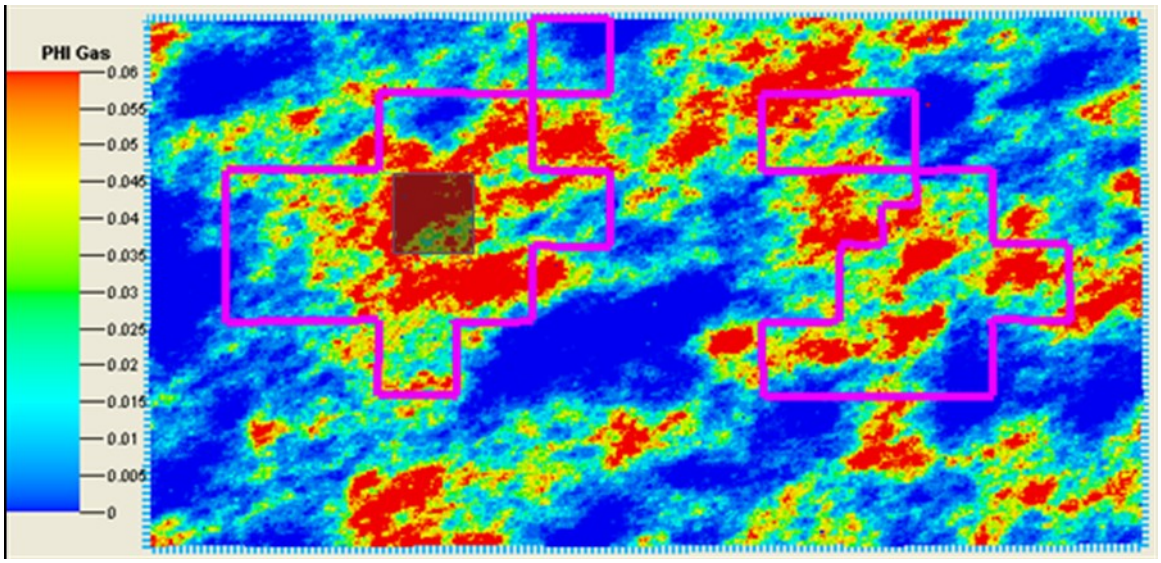

Fig. 18 — A realization of porosity for the Gething D formation obtained through geostatistical procedures. The boxes in light purple represent UGR's lease areas. The shadowed gray box represents the section selected to extract the property maps to be used in the multi-well reservoir model for this project.

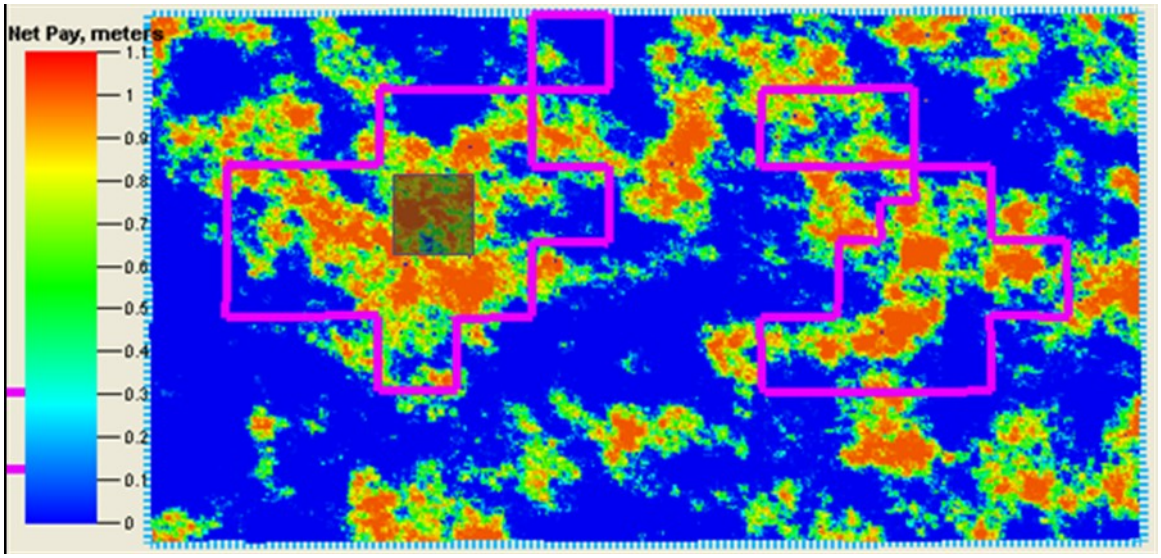

Fig. 19 — A realization of net-to-gross for the Gething D formation obtained through geostatistical procedures. The boxes in light purple represent UGR's lease areas. The shadowed gray box represents the section selected to extract the property maps to be used in the multi-well reservoir model for this project.

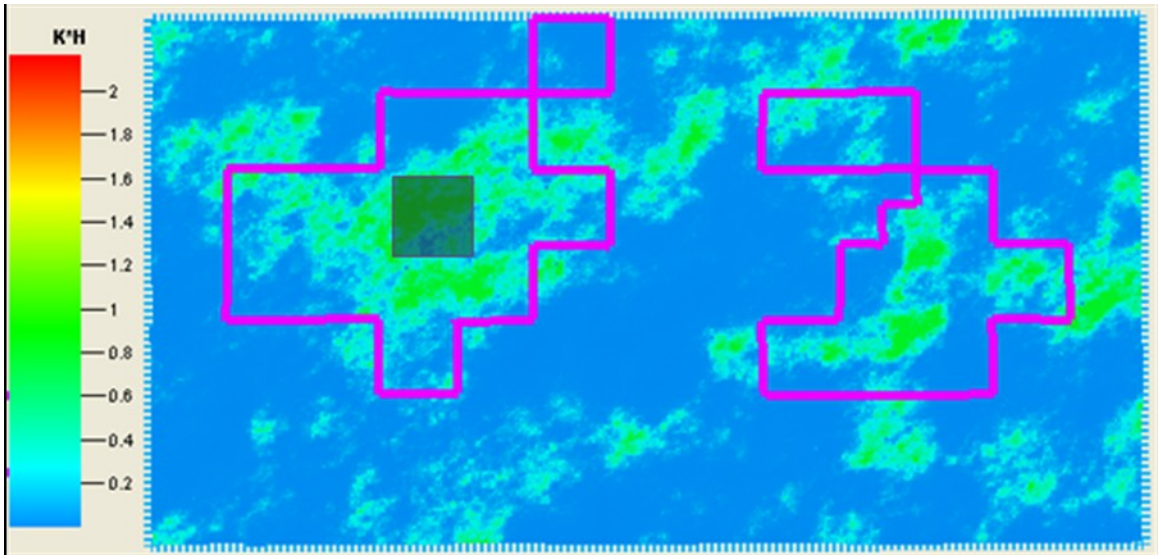

Fig. 20 — A realization of permeability for the Gething D formation obtained through geostatistical procedures. The boxes in light purple represent UGR's lease areas. The shadowed gray box represents the section selected to extract the property maps to be used in the multi-well reservoir model for this project.

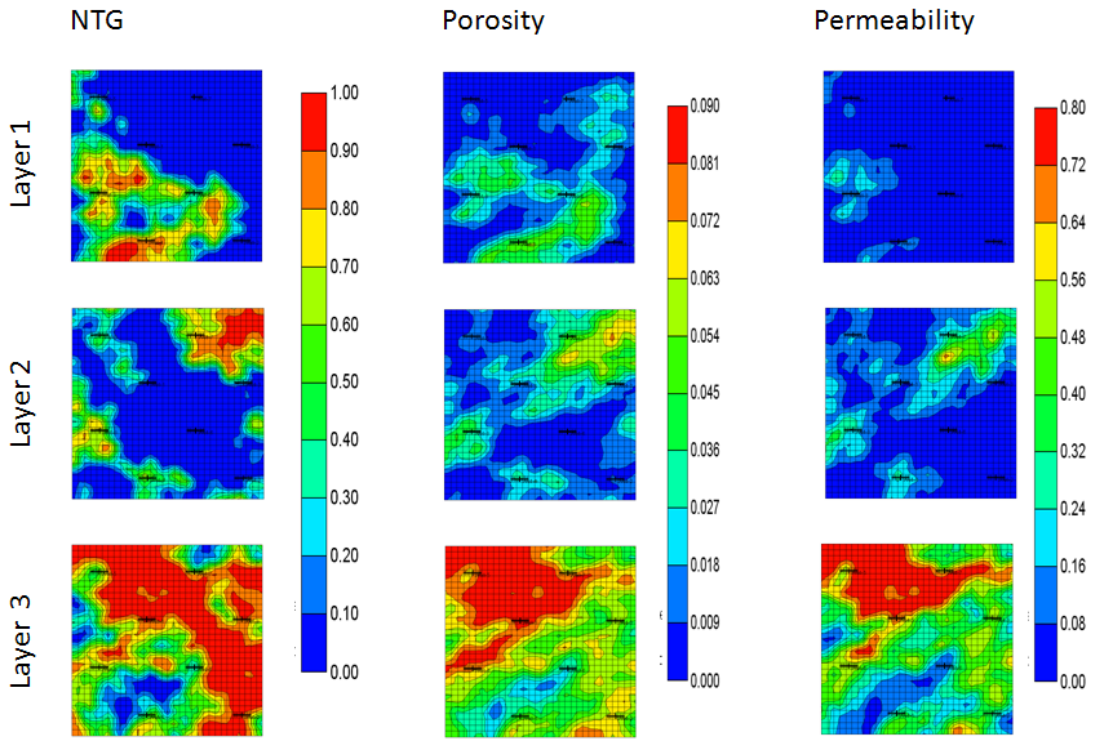

Fig. 21 — An example realization of reservoir property maps for the section of the Gething D interval, Berland River Area, showing the properties in individual layers.

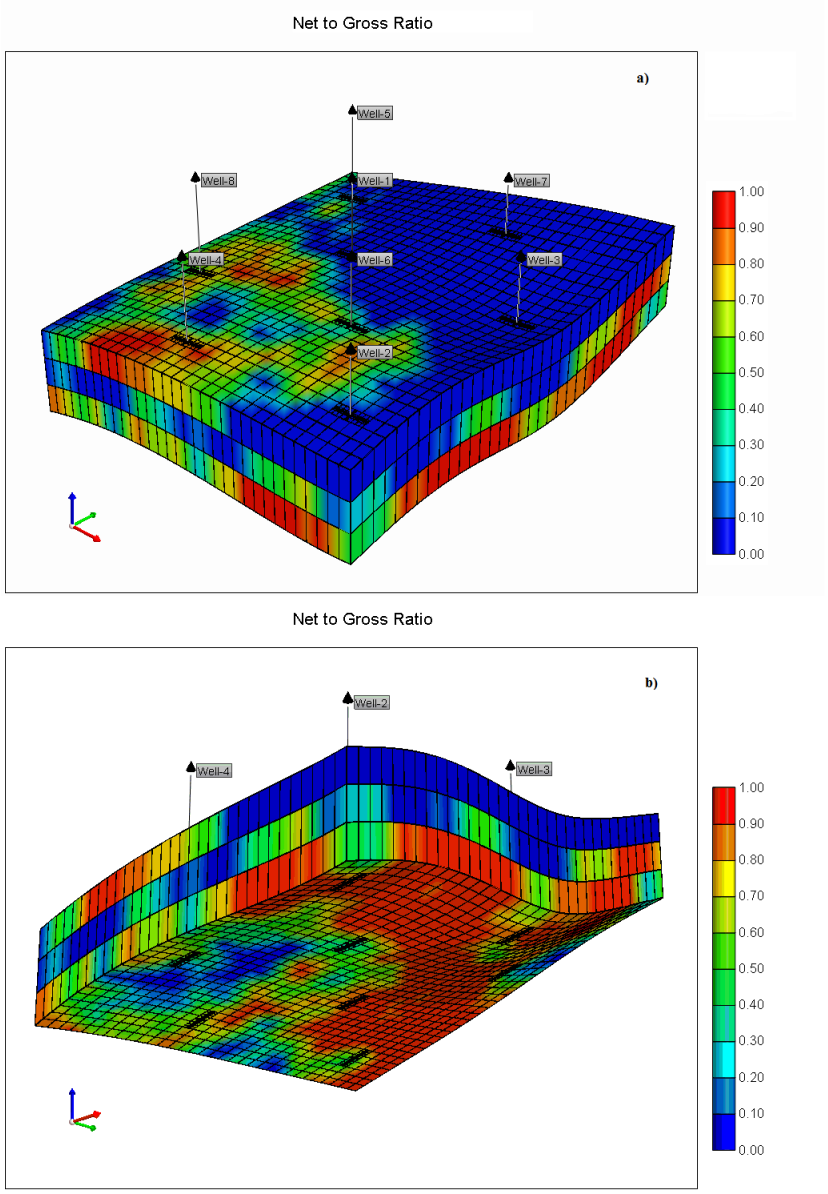

Fig. 22 — Simulation grid of the study area showing a top (**a**) and bottom (**b**) view of the three-dimensional cube of net-to-gross ratio (NTG).

6.4. Other Parameters

Other input parameters in the Berland River reservoir model are presented in **Table 3**. The model includes a hydraulic fracture with half length of 200 ft and with an approximate fracture width of 0.04 ft. The dimensionless fracture conductivity (F_{cD}) used in the model is 1.3. A formation depth distribution was used to model the initial pressure for the multi-well model by multiplying a constant pressure gradient by the formation depth, (**Table 4**). The histogram and corresponding probability distribution function of formation depth are shown in **Fig. 23**.

Table 3 — Input parameters of Berland River reservoir model

Parameter	Units	Value
Pressure Gradient	**psi/ft**	**0.28**
Reservoir Temperature	**°C**	**90**
Gas Gravity	**-**	**0.71**
Water Saturation	**%**	**30**
Fracture Length	**ft**	**200**
Fracture width	**ft**	**0.04**
Dimensionless Fracture Conductivity	**-**	**1.3**

Table 4 — Formation depth distribution and uncertainty parameters used in modeling the Berland River Gething D reservoir

Parameter	Units	Distribution Type	Minimum	Maximum	Mean	Standard Deviation	Shift
Formation Depth	m	Normal	2,600	3,100	2,780	91	-

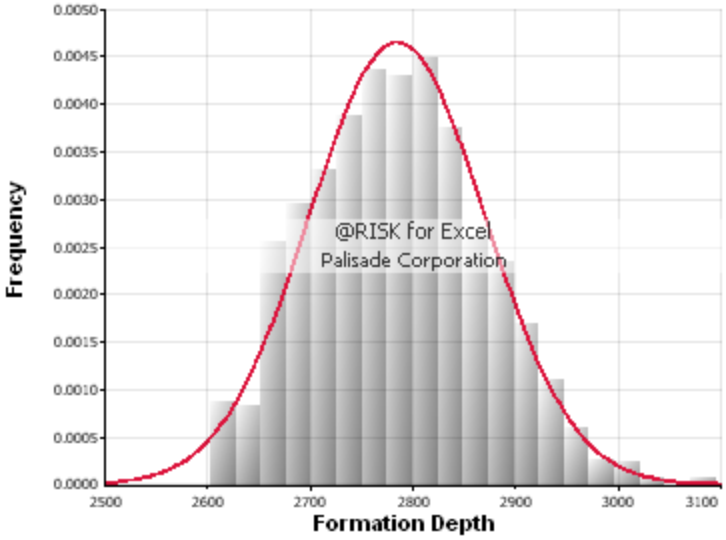

Fig. 23 — Histogram and probability distribution function of depth used for modeling the initial pressure of the Berland River Field.

The hydraulic fracture permeability is computed using the following equation:

$$k_f(d) = \frac{F_{cD} L_f k}{w} \quad \text{..... (1)}$$

where k_f is the fracture permeability, k is the formation permeability, L_f is the fracture length, and w is the fracture width. Because using an F_{cD} of 1.3 could result in extremely high fracture conductivities for the higher permeability wells, wk_f was limited to a maximum value of 150 md-ft, which means that the fracture permeability, k_f, cannot be larger than 3750 md.

6.5. Validation of Reservoir Model

Validation of the probabilistic reservoir model was conducted against the distribution of actual production data from the wells operated by UGR. The information provided by UGR and the base map of the Berland River area (**Fig. 8**) suggest that the study area is developed predominately on 640 and 320-acre spacing; therefore, up to two wells are already in production in almost each section of the field. Because of this, the simulation results from Wells 1 and 2 were selected for the validation of the reservoir model. One thousand iterations of the multi-well reservoir model were run for stage duration of 2 years for both Stage 1 and Stage 2 to obtain the cumulative production for wells on 640- and 320-acre spacing (Wells 1 and 2). Since 24-month production is being compared, for Stage 1 the production results for Well 1 at 640-acre spacing and Wells 1 and 2 at 320-acre spacing were used, and for Stage 2 only the production results of Well 2 at 320-acre spacing after downspace from 640 was included since it is only the new well in production in Stage 2. The results were used to compare the production response from the multi-well model to actual production from the Berland River Area. The results were also compared to the single-well model results developed by Turkarslan (2010).

The new reservoir model yielded a distribution of production that matches the actual distribution of Gething production and the single-well reservoir model production results quite well (**Fig. 24 a)**). Since around 10% of the maps had problems with wells in zones of very low pay, the lowest 10% of production values were removed from the

Stage-1 production results for 640- and 320-acre spacing for Wells 1 & 2 and the Cumulative distribution functions (CDF) was constructed again (**Fig. 24 b)**). A better comparison between actual data, single-well model results and multi-well model results is obtained in this case.

Similarly, comparison was done for best-month production on individual wells (Wells 1 & 2). The multi-well model produced a distribution that matches much better the actual production results from the Berland River area than the single-well model (**Fig. 25 a)**. Similarly, 10% of the lowest production values were removed and the cumulative distribution plot was constructed again and a better comparison between the multi-well reservoir results and the actual production data is observed (**Fig. 25 b).**

6.6. Multi-well Reservoir Results

Once the model was validated against actual reservoir performance and the single-well reservoir model, the multi-well reservoir model was used to forecast production for different combinations of well spacing and Stage-1 and Stage-2 durations. The first-month production, stage production, and stage production discounted to time 0 for both Stage 1 and Stage 2 were obtained. Even though Stage 2 could start 1 to 5 years after Stage 1, the production of Stage 2 was also discounted to time zero to allow calculation of economic value at the time the decision is being made. CDF of first-month production, stage production, total production (Stage 1 plus Stage 2), and individual well production were obtained.

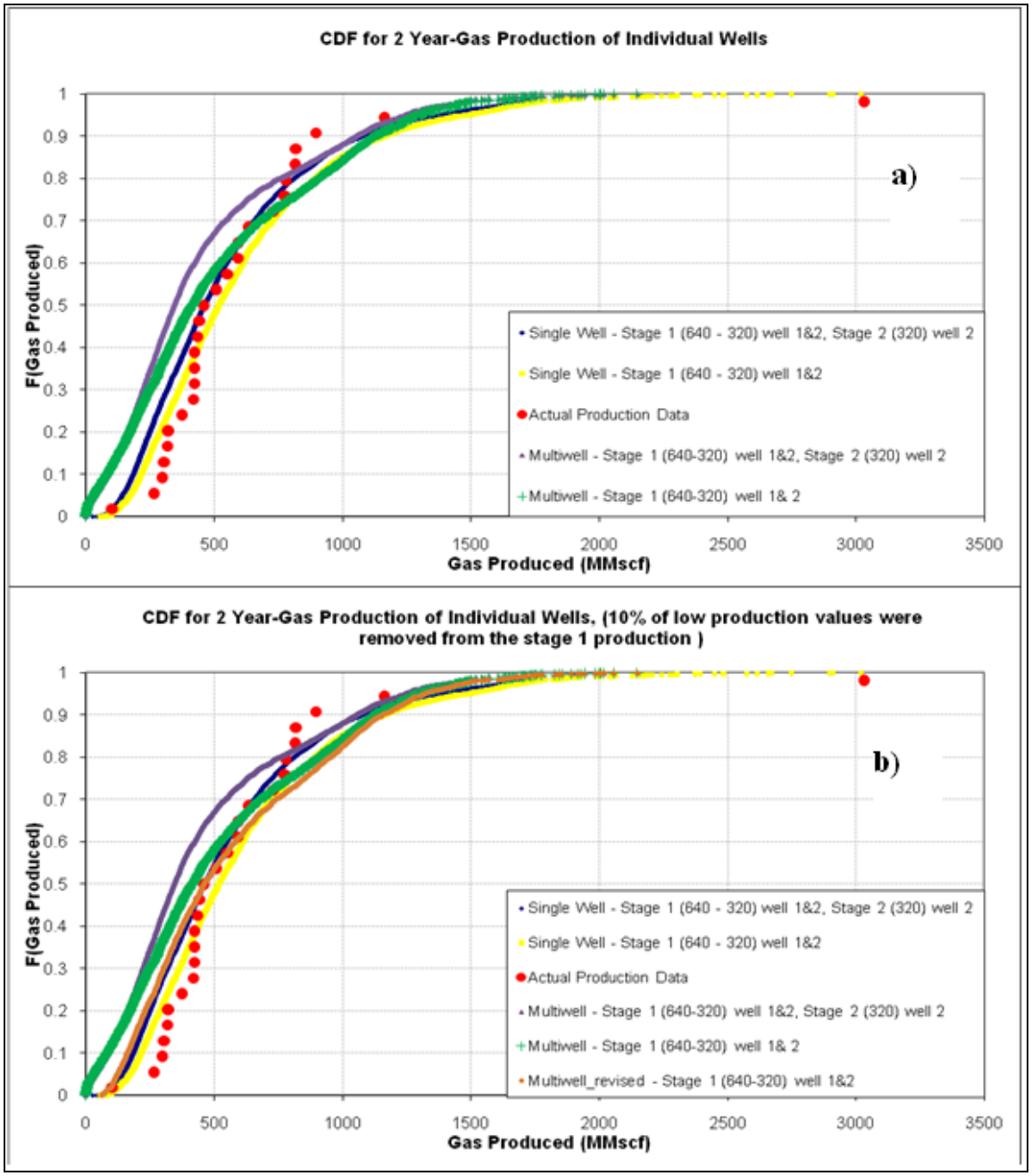

Fig. 24 — a) The multi-well reservoir model yielded a distribution of production that matches the actual distribution of Gething production and single-well reservoir model results quite well, **b)** revised production distribution for multi-well reservoir model where the lowest 10% of production values was removed from Stage-1 results. A better match with the actual distribution of Gething production and single-well reservoir model is observed.

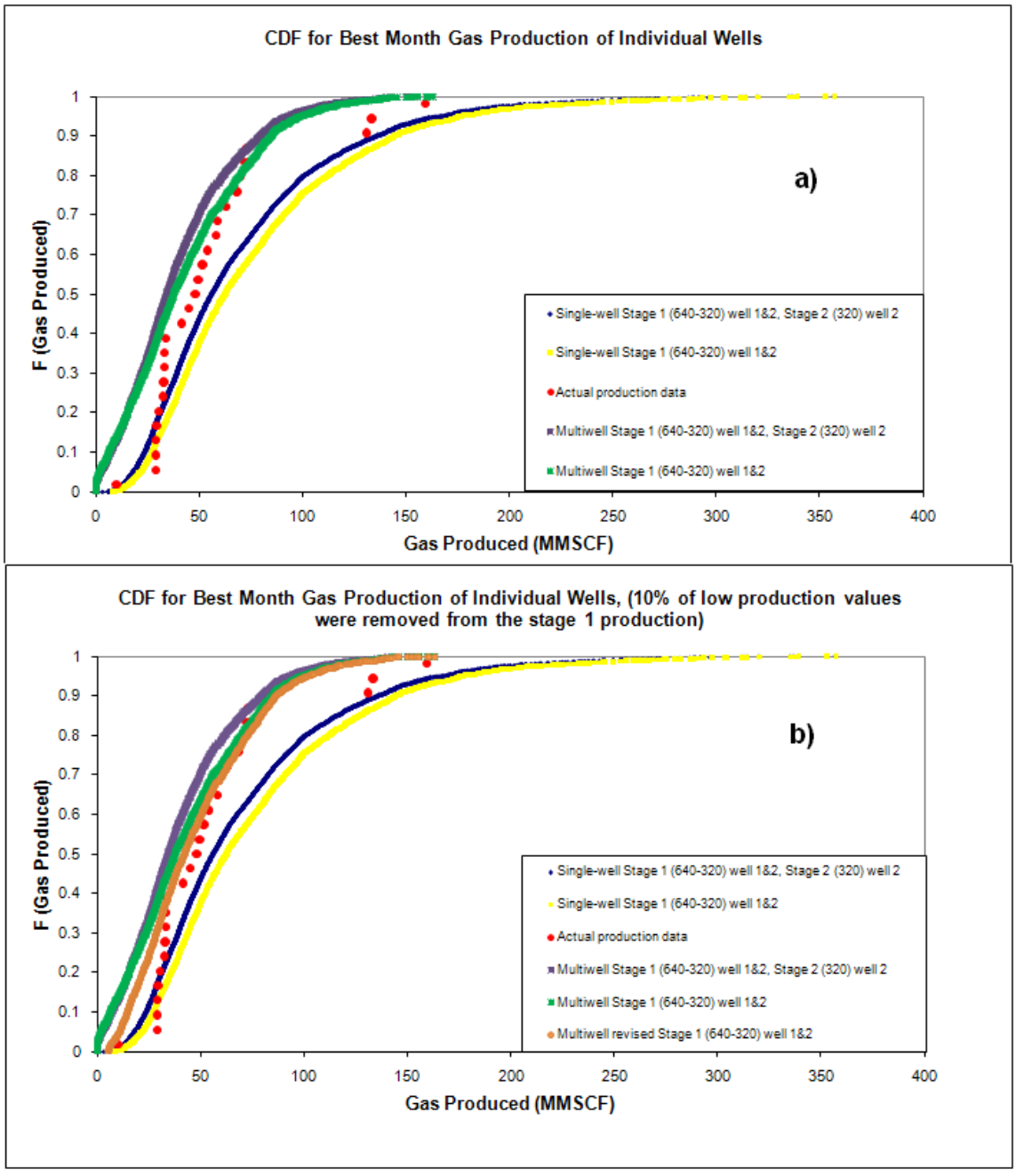

Fig. 25 — a) The multi-well reservoir model yielded a distribution of best-month gas production that matches the actual distribution of Gething production. **b)** Lowest 10% of production values removed from Stage 1. A better match with the actual distribution of Gething production is observed.

Fig. 26 a) shows the CDF of gas production for Stage 1 of 5 years and initial spacing of 640 acres. The average stage production is 1,279.39 MMscf with a maximum production of 4,321.4 MMscf and a minimum of 0.649 MMscf. The large variability in gas production indicates significant uncertainty is being modeled with the 1,000 reservoir properties maps used in the reservoir model. **Fig. 26 b)** shows the CDF of total gas production for the section for Stage 1 of 640-acre plus Stage 2 of 640, 320, 160 and 80-acre spacing. In this figure we observe how the combined stages production gradually increases as the spacing decreases (i.e., as more wells are added to the section). For example, the average total gas production for Stage 1 and Stage 2 of 640-acre spacing, (i.e., no wells are added after Stage 1) is 2,339.25 MMscf with a maximum production of 7,258 MMscf and a minimum production of 2.739 MMscf, while the average total gas production for Stage 1 of 640-acre spacing and Stage 2 of 80-acre spacing (i.e., 7 infill wells are added to the section) is 3,934.38 MMscf with a maximum production of 8,449.69 MMscf and a minimum of 1,046.91 MMscf. Similar CDF plots were obtained for Stage 1 duration of 5 years and initial spacing of 320, 160 and 80 acres (**Fig. 27** to **Fig. 29**). **Fig. 30 a)** shows the CDF for first-month gas production for Stage 1 duration of 5 years for initial spacing of 640 acres. In this case only results for Well 1 are presented since only one well is simulated in this case. Similarly, **Fig. 30 b)** shows the CDF for first-month gas production for Stage 1 duration of 5 years when the initial spacing is 320-acre; in this case Wells 1 and 2 results are presented. **Fig. 30 c)** is a similar CDF plot when the initial spacing is 160-acre (Wells 1 to 4) and **Fig. 30 d)** shows a similar CDF plot when the initial spacing is 80-acre (in which case the results

for Wells 1 to 8 are presented). A significant variation in the distribution of first-month gas production between wells is observed, which is consistent with the heterogeneity observed in the reservoir property maps.

Similarly, **Fig. 31** to **Fig. 35** show the CDF plots for gas production for Stage-1 duration of 3 years, and **Fig. 36** to **Fig. 40** show CDF plots for gas production for Stage-1 duration of 1 year. **Table 5** shows an example of Monte Carlo results from the simulator for best month production, gas production and discounted gas production by section for Stage 1 and the combined Stage 1 plus Stage 2 gas production and discounted gas production for a Stage-1 duration of 3 years, initial spacing of 320-acre and different downspacing combinations. **Table 6** shows an example of Monte Carlo results from the simulator for first-month gas production, stage gas production and stage discounted gas production for each well simulated in the section for Stage1 and Stage 2 for a Stage-1 duration of 160 acres and duration of 3 years and Stage 2 of 160 acre.

Fig. 41 a) shows the CDF plot for gas production by well in the section for Stage 1 duration of 3 years and initial spacing of 80 acres (Wells 1 to 8). **Fig. 41 b)** shows the CDF plot for gas production by well for Stage 2 of 80 acres after Stage-1 duration of 3 years and initial spacing of 80 acres. The significant variation in individual-well production distributions results from the heterogeneity inherent in the reservoir property maps.

The results of the combined Monte Carlo and reservoir simulation modeling provided production forecast distributions under different development scenarios accounting for the uncertainty in reservoir properties. Distributions for discounted stage

cumulative production were incorporated into the decision model as the basis to obtain an economic evaluation of each development scenario. More specifically, the expected net present value was determined and these results provided the basis for the selection of the optimal development strategy. By including the simulated relationship between Stage-1 and Stage-2 production response, the decision model can assess the value of learning from the initial development spacing to determine the optimal overall development strategy. This evaluation is described in Section 8.

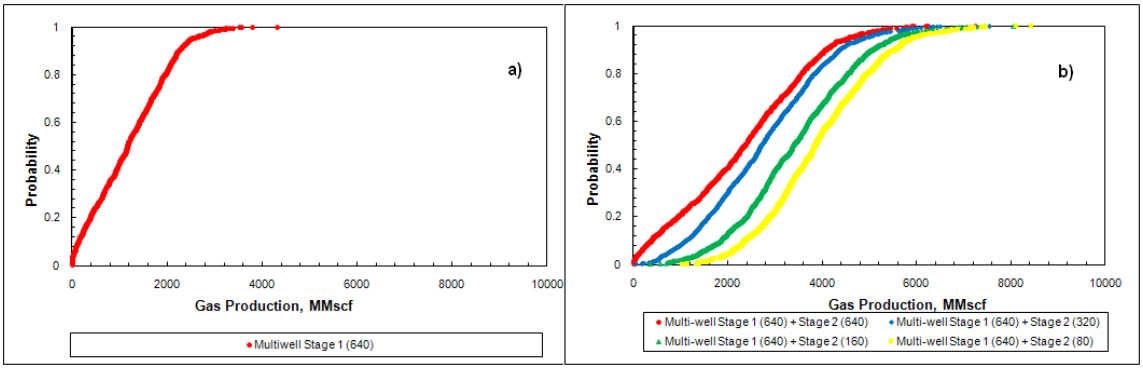

Fig. 26 — Cumulative distribution functions for multi-well reservoir model results for gas production for **a)** Stage 1 of 5 years and initial spacing of 640 acres and **b)** combined Stage 1 of 640-acre spacing and Stage 2 of 640, 320, 160 and 80-acre spacing.

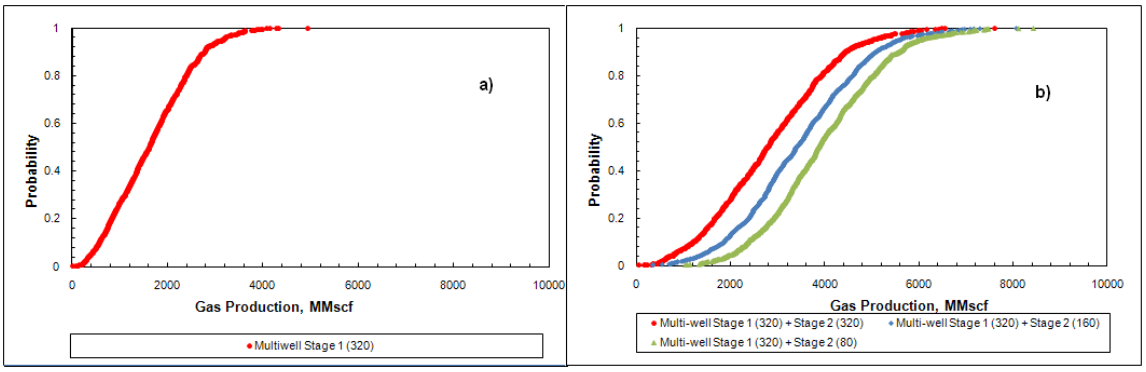

Fig. 27 — Cumulative distribution functions for multi-well reservoir model results for gas production for **a)** Stage 1 of 5 years and initial spacing of 320 acres and **b)** combined Stage 1 of 320 acres spacing and Stage 2 of 320, 160 and 80 acres spacing.

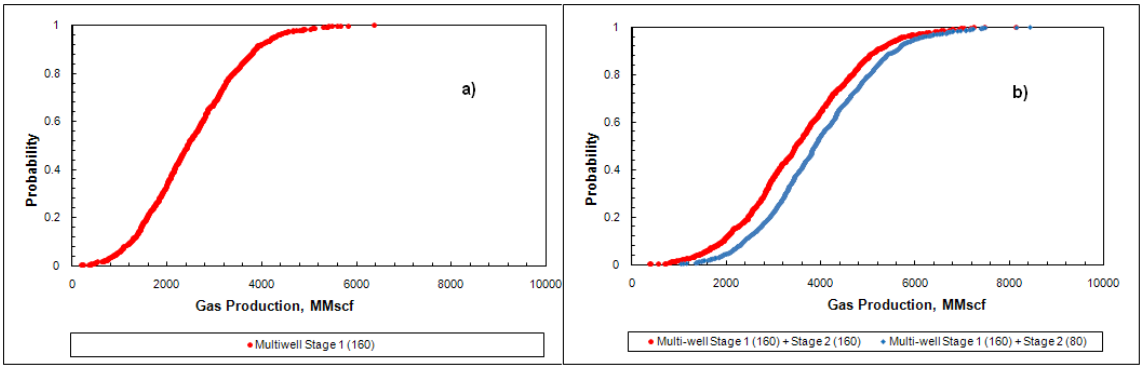

Fig. 28 — Cumulative distribution functions for multi-well reservoir model results for gas production for **a)** Stage 1 of 5 years and initial spacing of 160 acres and **b)** combined Stage 1 of 320 acres spacing and Stage 2 of 160 and 80 acres spacing.

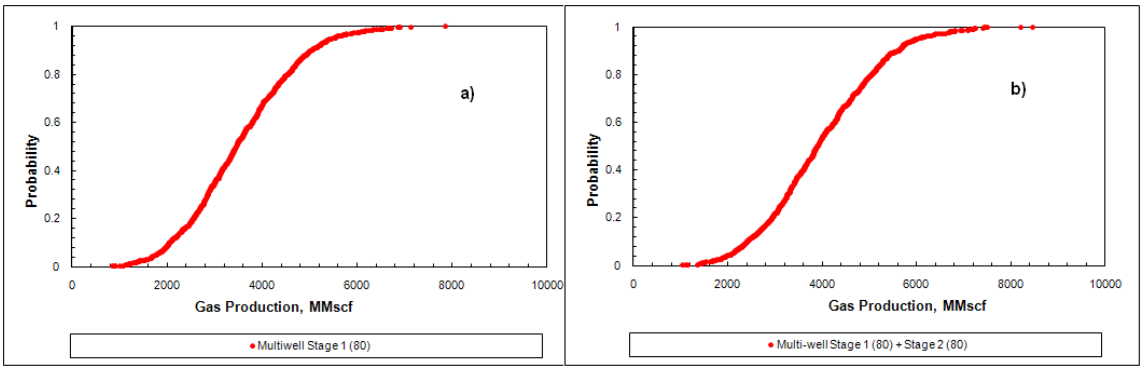

Fig. 29 — Cumulative distribution functions for multi-well reservoir model results for gas production for **a)** Stage 1 of 5 years and initial spacing of 80 acres and **b)** combined Stage 1 of 320 acres spacing and Stage 2 of 80 acres spacing.

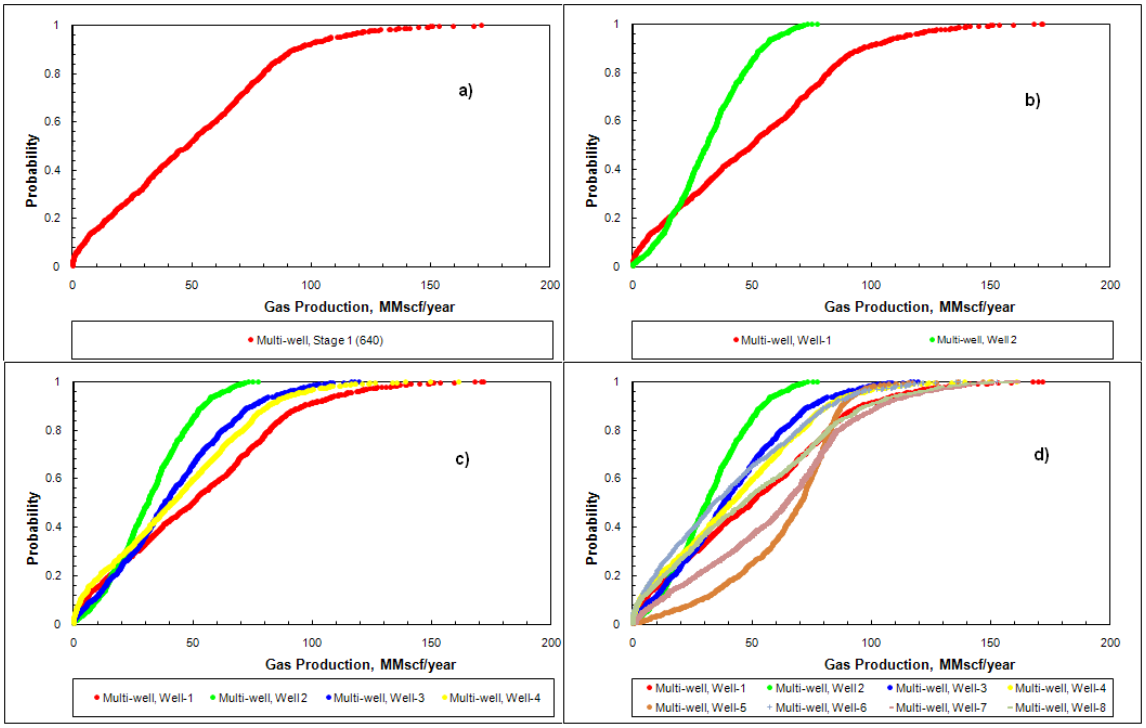

Fig. 30 — Cumulative distribution functions for multi-well reservoir model results for first month gas production for Stage 1duration of 5 years and initial spacing of **a)** 640 acres, **b)** 320 acres, **c)** 160 acres and **d)** 80 acres.

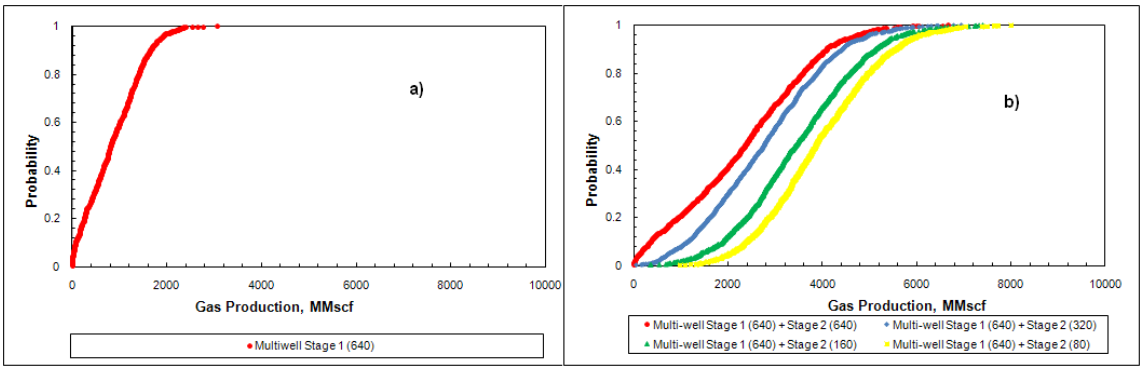

Fig. 31 — Cumulative distribution functions for multi-well reservoir model results for gas production for **a)** Stage 1 of 3 years and initial spacing of 640 acres and **b)** combined Stage 1 of 640 acres spacing and Stage 2 of 640, 320, 160 and 80 acres spacing.

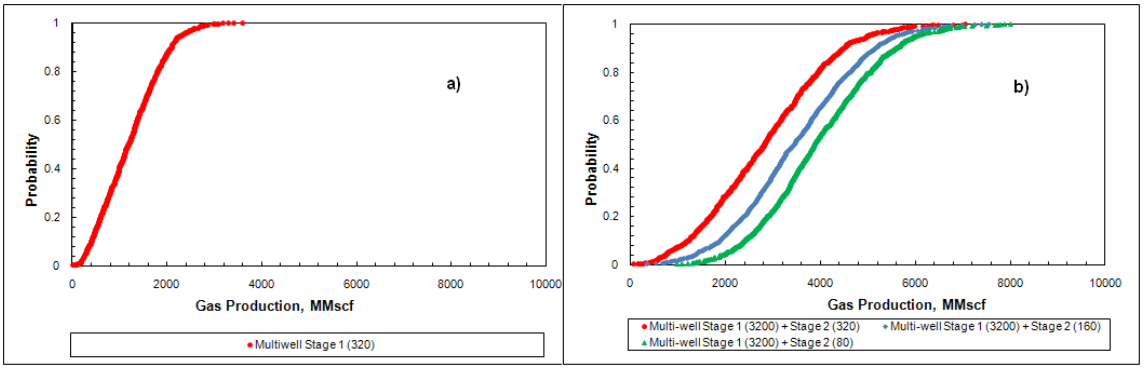

Fig. 32 — Cumulative distribution functions for multi-well reservoir model results for gas production for **a)** Stage 1 of 3 years and initial spacing of 320 acres and **b)** combined Stage 1 of 320 acres spacing and Stage 2 of 320, 160 and 80 acres spacing.

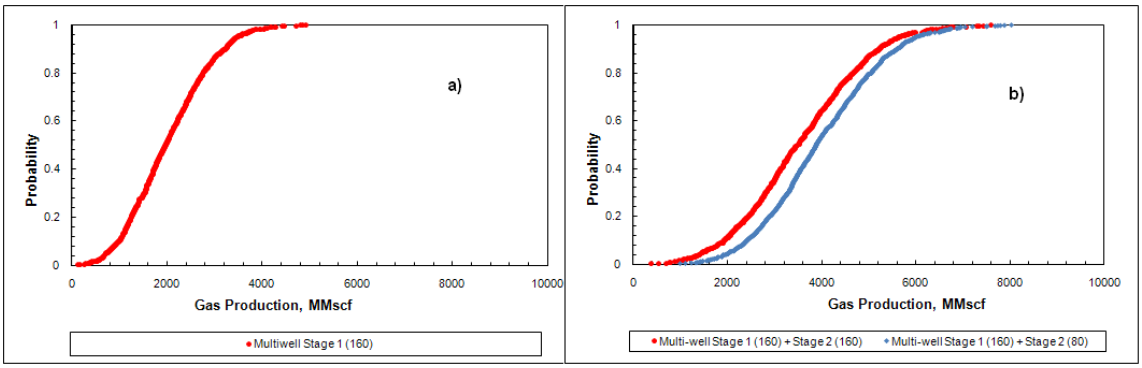

Fig. 33 — Cumulative distribution functions for multi-well reservoir model results for gas production for **a)** Stage 1 of 3 years and initial spacing of 160 acres and **b)** combined Stage 1 of 160 acres spacing and Stage 2 of 160 and 80 acres spacing.

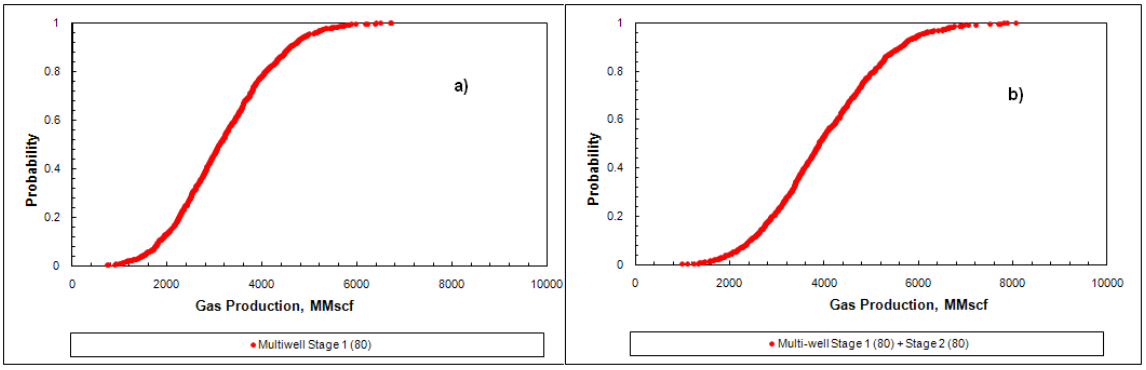

Fig. 34 — Cumulative distribution functions for multi-well reservoir model results for gas production for **a)** Stage 1 of 3 years and initial spacing of 80 acres and **b)** combined Stage 1 of 80 acres spacing and Stage 2 of 80 acres spacing.

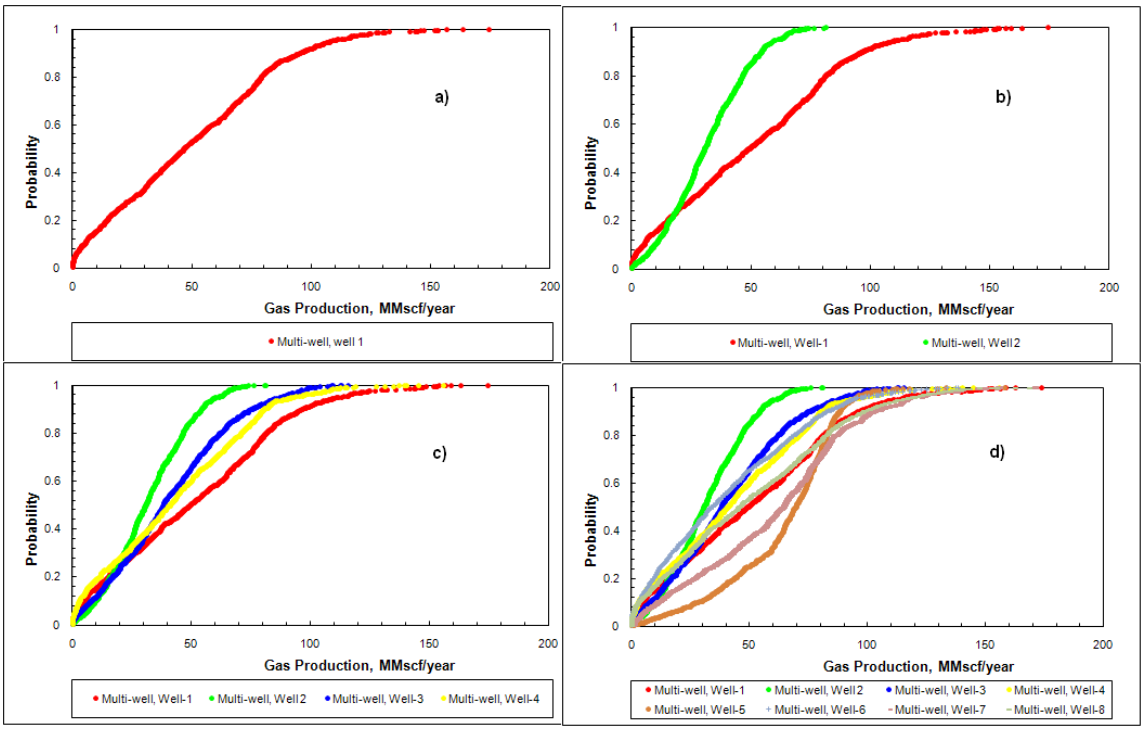

Fig. 35 — Cumulative distribution functions for multi-well reservoir model results for first month gas production for Stage 1duration of 3 years and initial spacing of **a)** 640 acres, **b)** 320 acres, **c)** 160 acres and **d)** 80 acres.

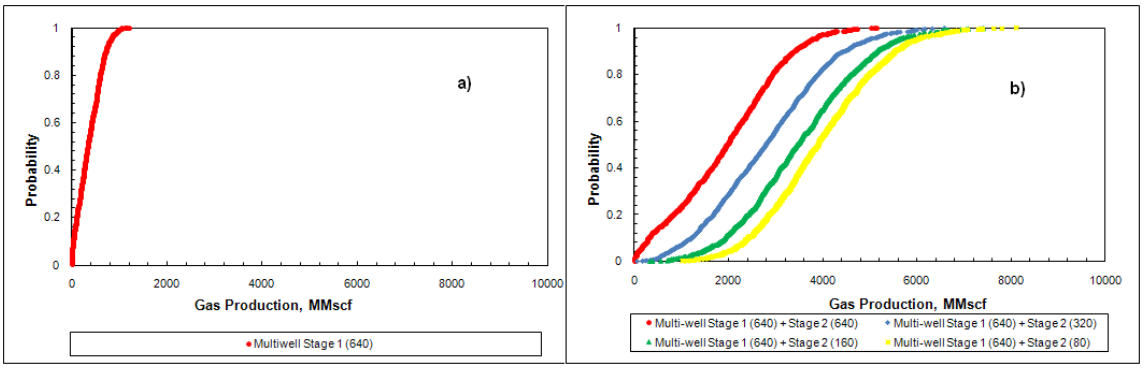

Fig. 36 — Cumulative distribution functions for multi-well reservoir model results for gas production for **a)** Stage 1 of 1 year and initial spacing of 640 acres and **b)** combined Stage 1 of 640 acres spacing and Stage 2 of 640, 320, 160 and 80 acres spacing.

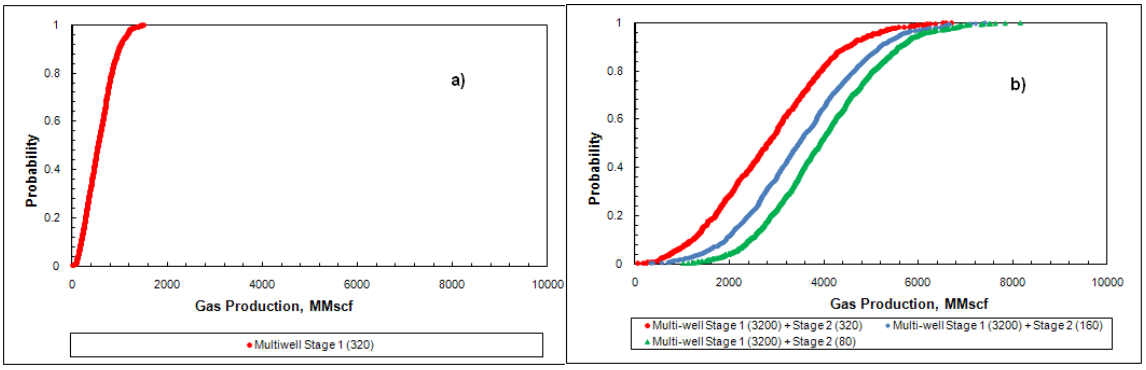

Fig. 37 — Cumulative distribution functions for multi-well reservoir model results for gas production for **a)** Stage 1 of 1 year and initial spacing of 320 acres and **b)** combined Stage 1 of 320 acres spacing and Stage 2 of 320, 160 and 80 acres spacing.

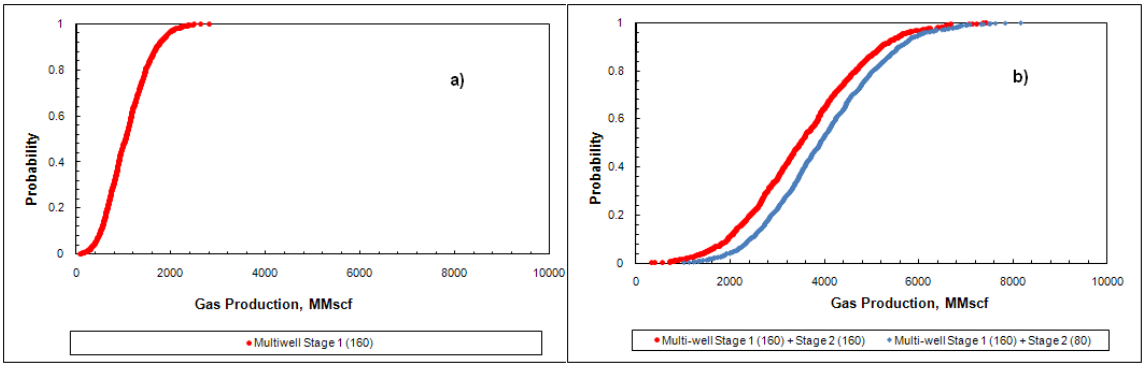

Fig. 38 — Cumulative Distribution functions for multi-well reservoir model results for gas production for **a)** Stage 1 of 1 year and initial spacing of 160 acres and **b)** combined Stage 1 of 160 acres spacing and Stage 2 of 160 and 80 acres spacing.

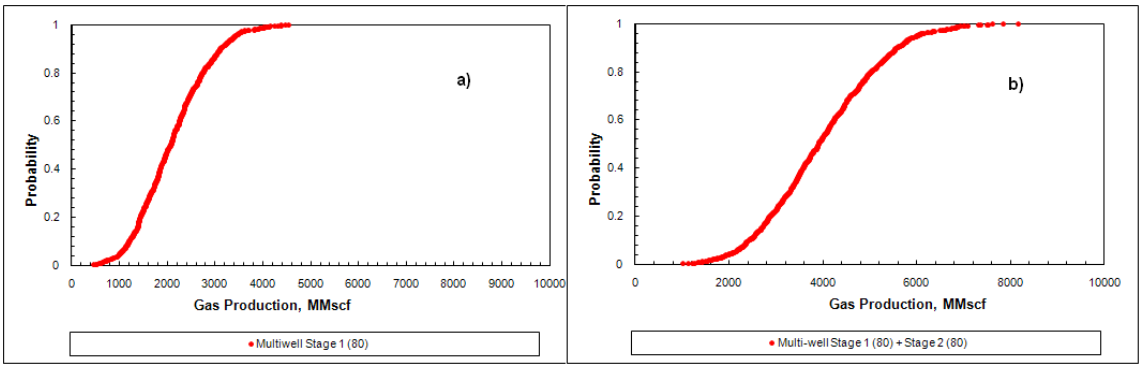

Fig. 39 — Cumulative Distribution functions for multi-well reservoir model results for gas production for **a)** Stage 1 of 1 year and initial spacing of 80 acres and **b)** combined Stage 1 of 80 acres spacing and Stage 2 of 80 acres spacing.

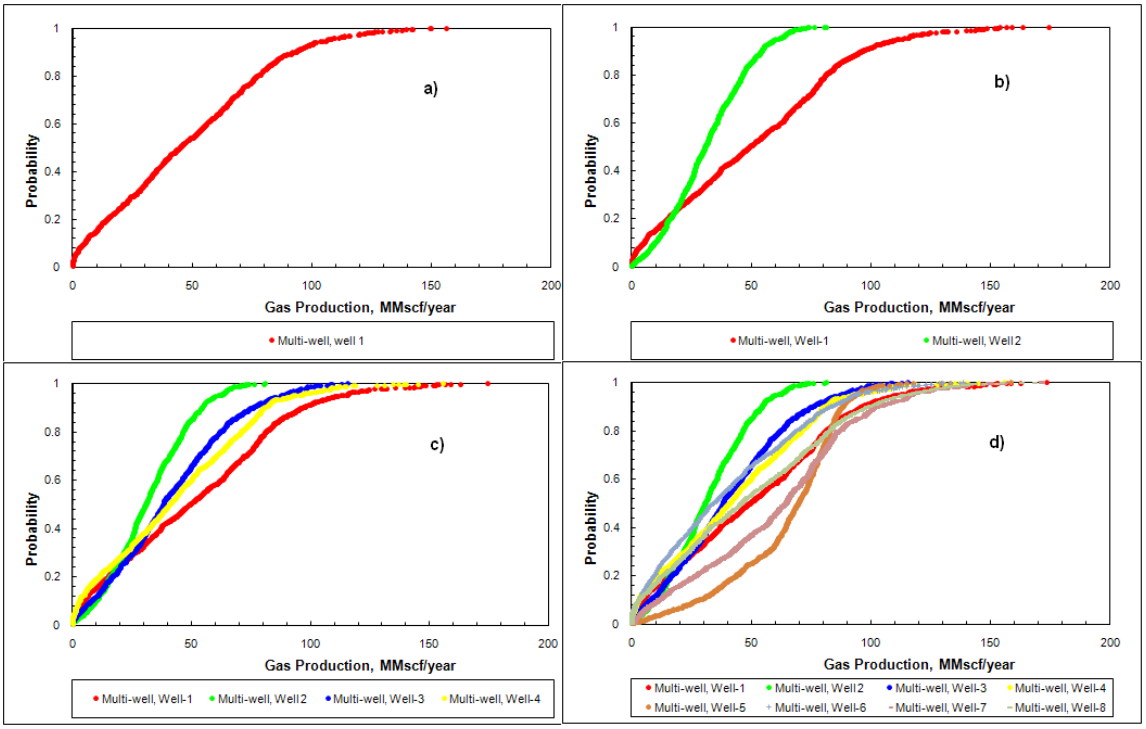

Fig. 40 — Cumulative Distribution functions for multi-well reservoir model results for First Month gas production for Stage 1duration of 1 year and initial spacing of **a)** 640 acres, **b)** 320 acres, **c)** 160 acres and **d)** 80 acres.

Table 5 — Example of results from the simulator for the Total Stage Gas Production, Total Discounted Production and Total First Month Production by a section for Stage-1 and Stage-2 for the Stage-1 of 320 acres and duration of 3 years and Stage-2 of 320, 160 and 80 acres

Run #	Total Stage 1, 320 acres			Total Stage 1+2 (320-320)		Total Stage 1+2 (320-160)		Total Stage 1+2 (320-80)	
	Stage 1 1st Month Gas Prod (MMscf)	Stage 1 Gas Production (MMscf)	Stage1 Discounted Production (MMscf)	Stage 1+2 Gas Production (MMscf)	Stage 1+2 Discounted Production (MMscf)	Stage 1+2 Gas Production (MMscf)	Stage 1+2 Discounted Production (MMscf)	Stage 1-2 Gas Production (MMscf)	Stage 1+2 Discounted Production (MMscf)
1	85.14	1555.80	1378.91	3469.84	2303.33	4000.34	2641.25	4394.27	3144.88
2	113.89	1912.61	1698.63	4248.29	2824.99	4663.15	3167.47	4943.71	3579.35
3	86.78	1422.13	1262.43	3508.80	2226.89	4224.07	2680.47	4773.15	3335.42
4	59.49	965.63	853.85	2908.04	1709.42	3845.62	2365.84	4248.25	2879.42
5	92.07	1101.58	981.62	2752.40	1735.34	3110.65	1985.88	3992.21	2756.44
6	66.54	898.01	800.13	1995.19	1323.70	2423.52	1586.11	2711.54	1923.21
7	48.75	514.61	463.31	1210.95	766.47	1348.85	841.34	2134.22	1437.51
8	57.94	784.91	699.77	1698.38	1136.99	2148.92	1428.73	2381.21	1681.11
9	59.35	507.37	457.00	1166.06	744.12	1723.30	1029.64	2562.35	1679.74
10	124.82	1613.11	1437.24	3794.28	2454.85	4287.19	2829.37	4665.44	3284.94
11	72.67	902.88	806.37	2137.09	1365.60	2618.65	1639.61	3194.74	2166.87
12	37.28	497.35	441.46	1465.65	863.87	2552.99	1513.08	3124.88	2027.95
13	91.93	1309.23	1163.06	3087.18	1998.75	4215.74	2752.57	4515.13	3214.08
14	30.36	292.69	263.19	769.69	466.02	1117.57	685.15	2223.12	1432.42
15	44.78	726.43	643.77	1957.09	1194.26	3025.23	1858.46	3428.09	2309.03
16	95.34	1329.23	1187.03	2546.08	1792.57	2596.91	1830.94	3160.63	2330.28
17	92.13	1422.07	1263.22	3027.60	2049.25	4023.58	2748.06	4333.49	3116.76
18	23.35	345.42	304.12	1358.08	724.96	2204.28	1238.43	3012.74	1932.18
19	31.43	403.68	358.98	1093.90	667.75	1420.38	939.62	1671.58	1148.37
20	71.02	1418.11	1252.01	3569.41	2268.48	4129.74	2687.69	4548.60	3207.81

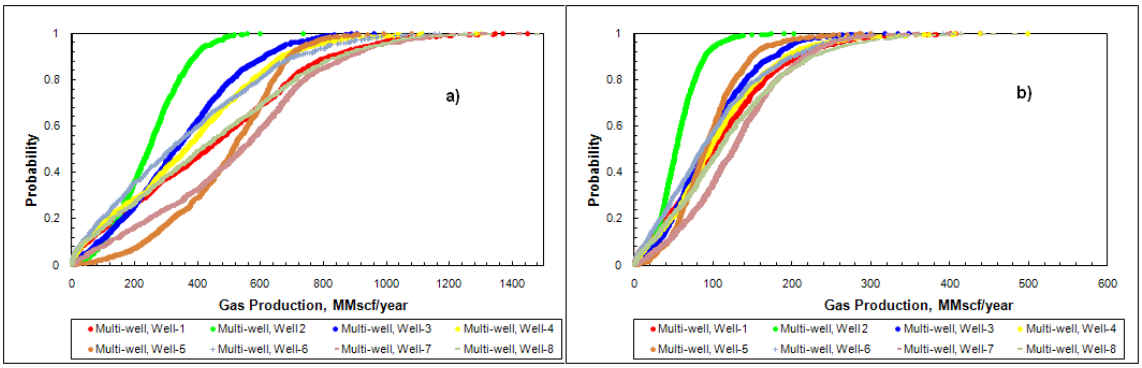

Fig. 41 — Example of Cumulative distribution functions for multi-well reservoir model results for **a)** Gas Production by well for Stage 1 duration of 3 years and initial spacing of 80-acre and **b)** Gas production by well for Stage 2 of 80-acre spacing after Stage-1 of 3 years and 80-acre initial spacing.

Table 6 — Example of results from the simulator for First-Month Gas Production, Stage Gas Production and Discounted Stage Gas Production for each well for Stage 1 and Stage 2 for a Stage 1 of 160 acres and duration of 3 years and Stage 2 of 160 acres

Run #	Stage 1, Well 1, 160 acres			Stage 2, Well 1, 160 acres			Stage 1, Well 2, 160 acres			Stage 2, Well 2, 160 acres			Stage 1, Well3, 160 acres			Stage 2, Well3, 160 acres			Stage 1, Well 4, 160 acres			Stage 2, Well 4, 160 acres		
	Stage 1 1st Month Gas Prod (MMscf)	Stage 1 Gas Production (MMscf)	Stage1 Discounted Production (MMscf)	Stage 2 1st Month Gas Prod (MMscf)	Stage 2 Gas Production (MMscf)	Stage 2 Discounted Production (MMscf)	Stage 1 1st Month Gas Prod (MMscf)	Stage 1 Gas Production (MMscf)	Stage1 Discounted Production (MMscf)	Stage 2 1st Month Gas Prod (MMscf)	Stage 2 Gas Production (MMscf)	Stage 2 Discounted Production (MMscf)	Stage 1 1st Month Gas Prod (MMscf)	Stage 1 Gas Production (MMscf)	Stage1 Discounted Production (MMscf)	Stage 2 1st Month Gas Prod (MMscf)	Stage 2 Gas Production (MMscf)	Stage 2 Discounted Production (MMscf)	Stage 1 1st Month Gas Prod (MMscf)	Stage 1 Gas Production (MMscf)	Stage1 Discounted Production (MMscf)	Stage 2 1st Month Gas Prod (MMscf)	Stage 2 Gas Production (MMscf)	Stage 2 Discounted Production (MMscf)
1	61.65	1093.20	972.65	18.14	956.00	486.49	23.49	301.51	270.84	4.04	207.61	105.81	27.51	399.24	356.12	6.52	356.59	178.51	24.26	355.82	317.16	5.95	372.76	181.01
2	88.00	1328.50	1188.70	19.29	935.70	484.67	25.86	298.95	270.11	3.39	169.23	86.83	31.21	541.43	482.64	8.48	437.43	223.24	41.37	592.77	531.05	8.36	397.24	206.35
3	58.33	903.68	805.04	15.16	861.72	429.91	28.44	370.32	333.18	4.72	287.66	140.56	30.39	473.41	420.53	8.65	562.59	271.91	24.88	401.37	357.18	6.91	422.39	207.73
4	51.04	726.16	646.97	12.40	821.34	392.82	8.45	99.16	89.63	1.08	57.02	28.65	20.60	250.94	224.40	3.98	231.92	115.16	82.40	972.67	873.99	13.31	739.83	369.28
5	24.75	504.60	446.11	9.92	743.90	346.62	67.31	433.31	397.07	3.48	189.69	95.01	10.96	200.64	177.49	3.99	284.01	133.48	44.82	464.04	418.53	5.79	329.44	162.73
6	41.85	687.20	611.57	11.71	672.80	335.54	24.71	142.19	131.22	0.83	33.08	17.52	38.68	426.73	382.13	6.60	360.96	180.37	2.73	45.38	40.19	0.89	83.29	36.53
7	12.25	201.62	177.89	4.33	440.72	192.14	36.49	304.30	278.19	2.38	150.80	70.81	0.68	14.02	12.27	0.34	54.87	21.72	6.37	85.65	76.26	1.52	113.34	52.64
8	25.13	426.06	379.44	6.99	370.50	188.49	32.79	263.48	240.27	2.37	115.90	58.87	22.46	305.34	273.80	4.28	226.70	114.58	24.37	266.90	240.31	3.51	196.06	98.17
9	18.96	167.75	150.83	2.43	162.19	76.53	40.40	271.55	248.90	2.09	159.96	70.65	6.84	142.86	125.70	3.22	367.86	156.62	33.70	268.17	243.49	2.83	243.89	105.91
10	82.63	1048.50	936.05	17.24	984.40	488.98	42.15	385.40	351.10	3.45	151.32	80.11	32.89	322.50	288.54	5.28	306.82	151.74	45.38	632.52	566.07	9.38	499.98	251.92
11	27.91	381.45	338.38	7.46	544.11	255.83	44.76	420.10	382.05	3.92	201.45	100.96	15.80	203.73	182.27	3.13	210.77	99.89	20.85	275.24	244.94	4.98	429.59	195.30
12	0.09	2.63	2.30	0.06	6.74	2.94	37.19	394.45	355.16	5.18	293.25	143.10	10.67	185.59	163.69	4.04	392.64	172.98	70.80	795.89	715.81	10.62	549.11	274.03
13	49.19	776.53	692.30	12.56	648.67	330.77	42.72	296.38	271.45	2.31	105.92	55.33	64.35	807.27	723.72	11.66	588.13	300.28	70.80	663.70	601.44	7.20	375.30	190.72
14	0.13	3.89	3.41	0.08	8.45	3.76	30.24	221.19	202.84	1.59	98.10	46.11	20.45	113.36	103.64	1.06	91.15	41.22	32.69	299.45	270.32	3.81	317.14	141.76
15	34.28	580.45	514.01	11.38	719.25	349.96	10.50	108.03	98.22	0.98	50.96	25.66	66.22	802.29	718.92	11.81	599.21	302.63	6.73	90.54	80.51	1.66	113.59	54.35
16	81.36	1218.90	1086.91	19.97	1069.20	540.05	13.97	95.33	87.72	0.57	18.37	10.34	5.70	98.61	87.59	1.76	97.14	48.90	0.04	1.02	0.89	0.03	5.06	1.91
17	56.12	655.35	591.13	7.68	309.83	166.40	35.96	371.70	337.27	3.63	143.15	77.36	40.23	481.54	434.38	5.61	236.11	125.76	107.95	1241.80	1120.97	14.30	616.40	325.40
18	6.82	148.30	129.84	3.64	399.06	172.91	16.53	143.97	129.83	1.89	129.44	59.94	30.86	260.80	236.11	3.07	200.32	95.96	35.97	468.60	420.40	6.63	509.12	232.40
19	10.73	125.77	113.00	1.69	77.80	40.10	20.71	167.10	152.94	1.24	54.91	28.19	53.15	474.17	430.58	4.81	220.75	114.63	19.33	197.83	179.23	2.10	117.53	58.37
20	60.20	1056.20	939.47	17.74	931.70	474.16	10.83	156.03	139.98	2.12	115.32	58.31	7.61	110.76	98.51	1.97	99.88	50.76	80.94	960.36	861.30	13.94	744.14	374.14

6.7. Recovery Efficiency

Recovery efficiency was calculated for one of the reservoir property maps that provide a production performance close to the P_{50} of production distribution (medium production value). The results are shown in **Fig. 42** and **Fig. 43** where cumulative production and recovery efficiency as functions of time for Stage-1 durations of 1 year and 5 years, respectively, when the initial spacing is 640 acres are shown. The overall recovery efficiency when no downspacing in Stage 2 is around 48%, when downspacing to 320-acre is around 58%, when downspacing to 160acre is around 72% and when downspacing to 80-acre is around 85%. It is observed in both cases that similar recovery efficiencies are reached after 20 years of production; however, for Stage-1 duration of 1 year, when additional wells are added, recovery is accelerated earlier in the reservoir life, which leads to a higher net present value (NPV), than for the 5-year Stage 1.

6.8. Comparison of Multi-Well Reservoir Model and Single-Well Model

The results from the multi-well model described herein were compared to the single-well model developed by Turkarslan (2010) for the same field **Fig. 44** to **Fig. 47** show a comparison of cumulative distribution for total gas production for Stage-1 duration of 3 years at different initial spacing between the two models. A narrower uncertainty range for the multi-well reservoir model is observed when compared to the single-well model.

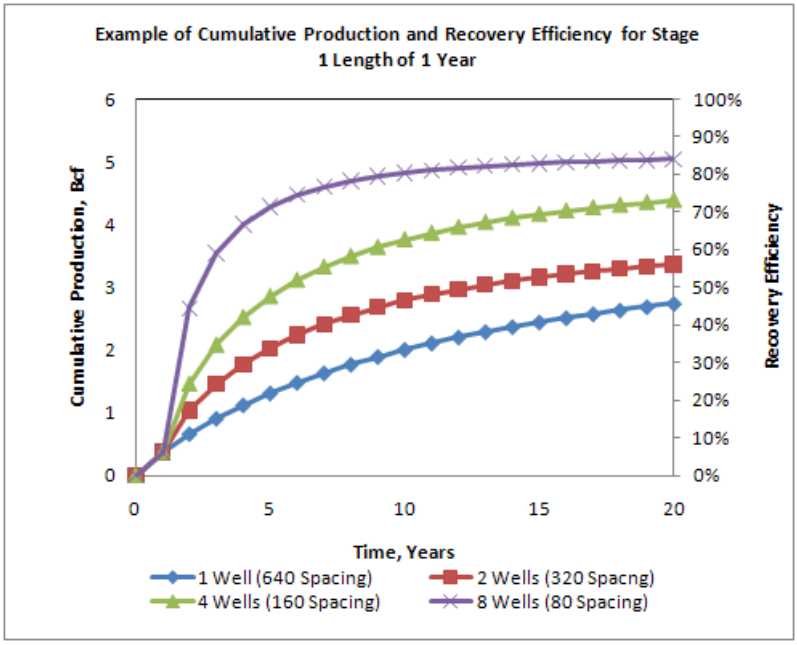

Fig. 42 — Cumulative production and recovery efficiency versus time for Stage-1 duration of 1 year and initial spacing of 640 acres.

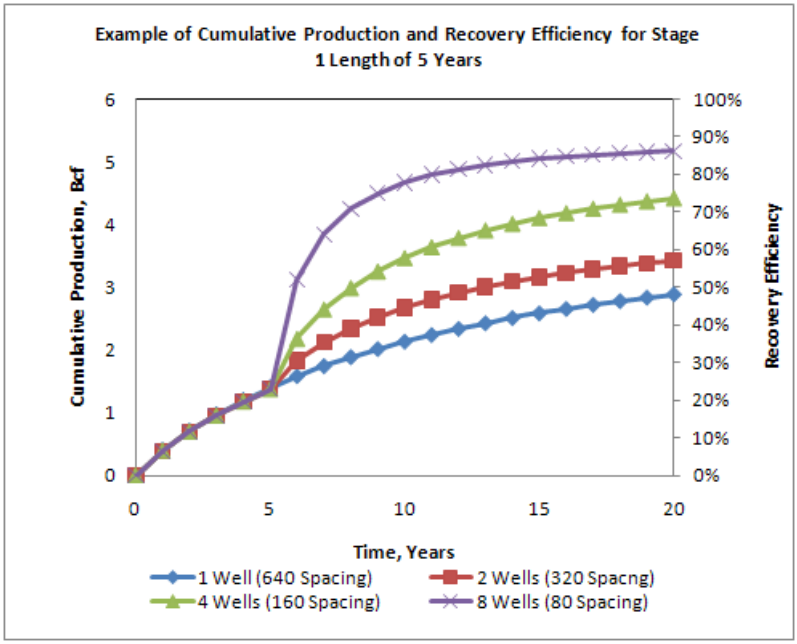

Fig. 43 — Cumulative production and recovery efficiency versus time for Stage-1 duration of 5 years and initial spacing of 640 acres.

With the single-well model, since the results of one well are extrapolated to obtain the performance of multiple wells in a section, this feature could produce errors in the production distributions. For example, in a reservoir section up to 8 wells might be drilled and represented by one well. If the combination of sampled reservoir properties leads to a very high value in the production performance, this could result in over-prediction of the performance of the section when the single-well production is multiplied by 8. **Fig. 48** shows production by well in the multi-well model and the single-well model. In this figure, which shows production for Stage 2 of 160-acre spacing after Stage 1 of 160-acre spacing, 4 wells in the multi-well model are represented by the color lines and the well for the single-well model is represented by the black line. For this particular case, the single-well model presents a production distribution that is very similar to the production distribution for the well with highest production in the multi-well model. When the production of the well in the single-well model is multiplied by 4 to obtain the section production, the production for the section could be much higher than the combination of 4 wells from the multi-well model (**Fig. 46 b)**). Over many Monte Carlo samples, this will tend to assign too much probability to the extreme values and widen the distributions for the single-well model.

I consider the multi-well modeling to be more realistic, since each well's performance is simulated in the model and aspects such as pressure interference and heterogeneities are better reproduced. Geostatistical maps are used to model heterogeneity in the multi-well reservoir model, which better models the uncertainty in reservoir properties. The single-well model overestimates the uncertainly because the

reservoir representation for individual wells is reduced to a single layer with homogeneous properties.

In summary, the production results obtained using the single-well reservoir model proposed by Turkarslan et al. (2010) could provide errors in the production predictions leading to suboptimal decisions. The multi-well reservoir model and the use of properties reservoir maps obtained through geostatistical characterization can provide a better basis for the decision model.

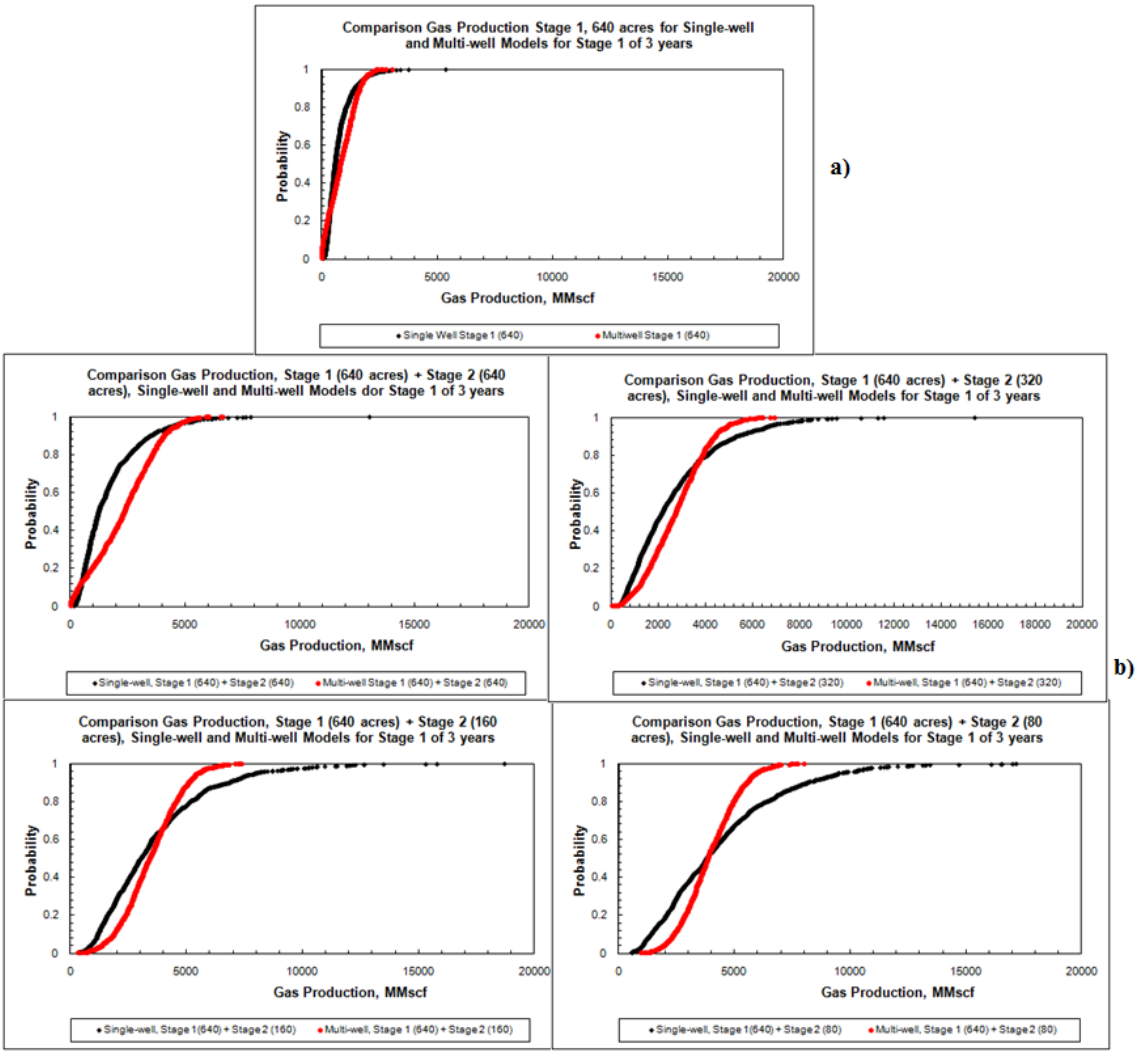

Fig. 44 — Comparison of cumulative distributions for total section gas production between multi-well and single-well models **a)** Stage 1 of 3 years and initial spacing of 640 acres and **b)** Stage 1 of 640-acre spacing plus Stage 2 of 640, 320, 160 and 80-acre spacing.

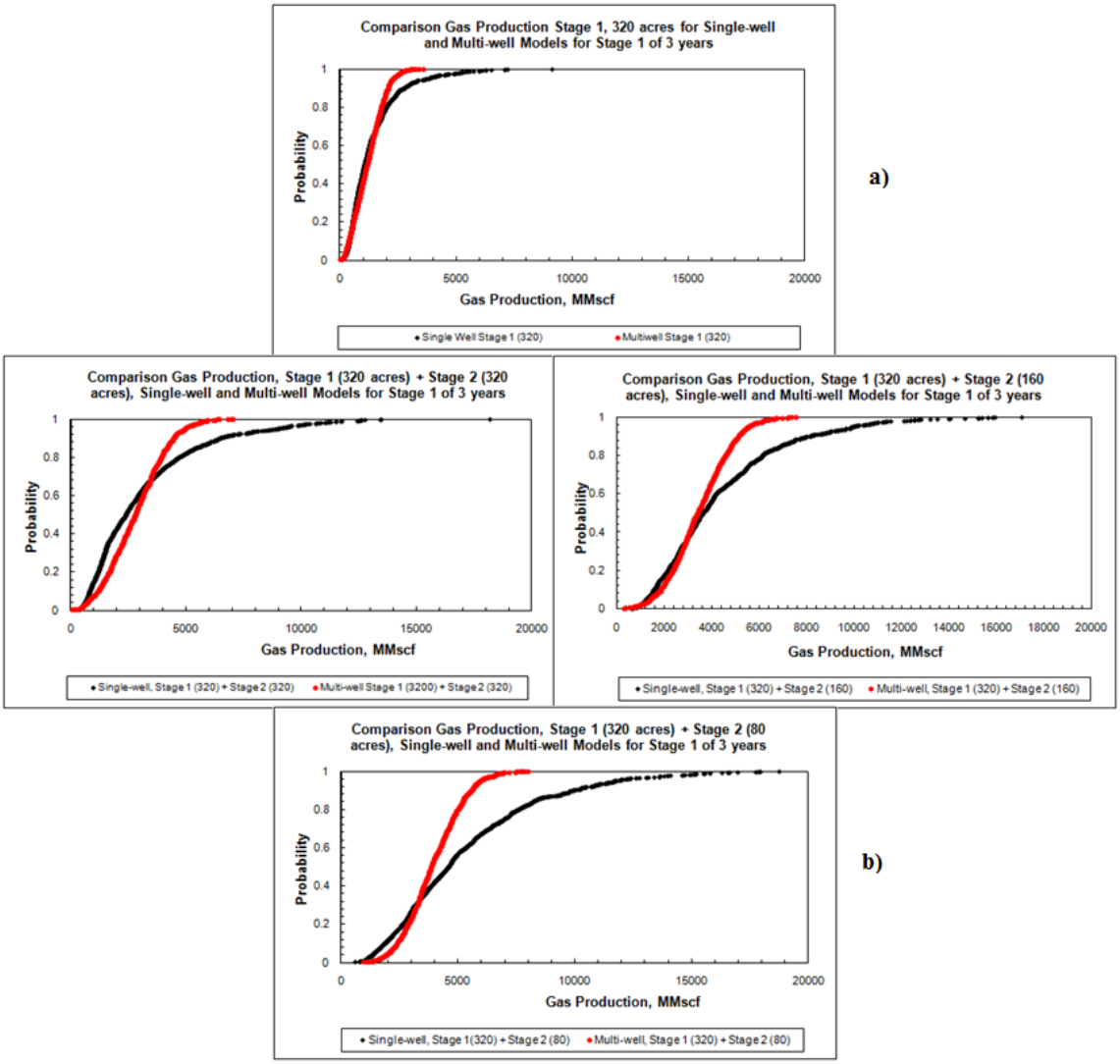

Fig. 45 — Comparison of cumulative distribution for total section gas production between multi-well and single-well models **a)** Stage 1 of 3 years and initial spacing of 320 acres and **b)** Stage 1 of 320-acre spacing plus Stage 2 of 320, 160 and 80-acre spacing.

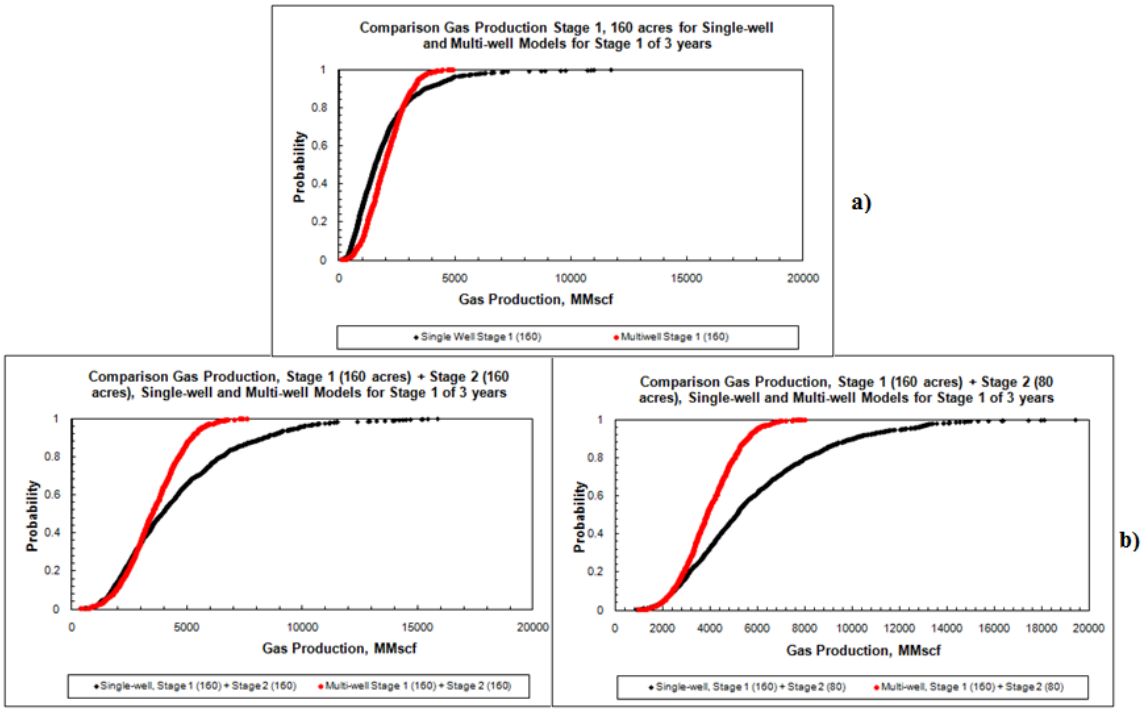

Fig. 46 — Comparison of cumulative distribution for total section gas production between multi-well and single-well models **a)** Stage 1 of 3 years and initial spacing of 160 acres and **b)** Stage 1 of 160-acre spacing plus Stage 2 of 160 and 80-acre spacing.

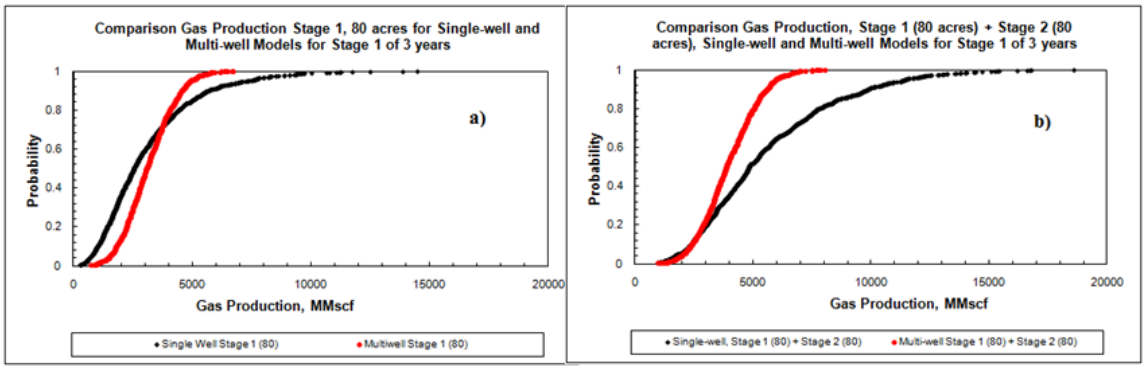

Fig. 47 — Comparison of cumulative distribution for total section gas production between multi-well and single-well models **a)** Stage 1 of 3 years and initial spacing of 80 acres and **b)** Stage 1 of 80-acre spacing plus Stage 2 of 80-acre spacing.

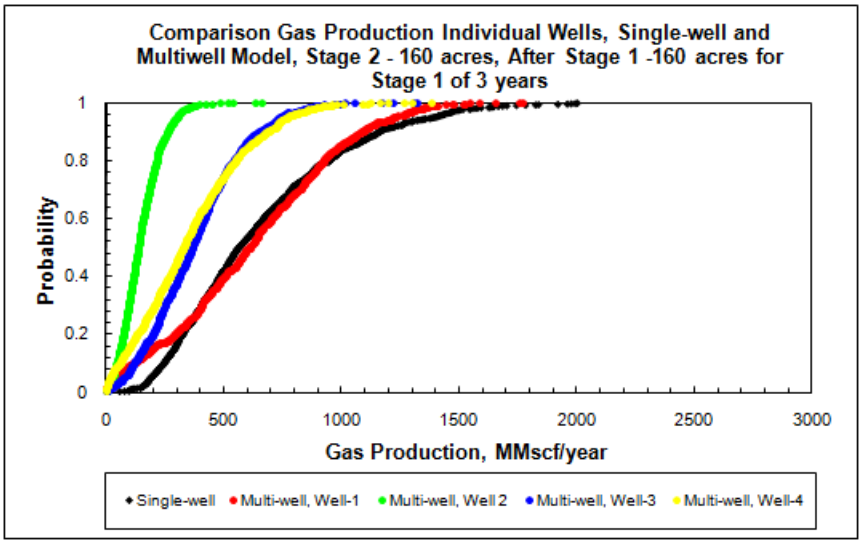

Fig. 48 — Comparison of gas production for individual wells between the multi-well and single-well models for an example Monte Carlo iteration. This illustrates how extrapolating the production of the single-well model can over-predict the section production much of the time compared to the multi-well model.

7. DECLINE CURVE MODEL

During this research, I studied the option to use decline curve analysis (DCA) as a means to integrate the reservoir and the decision model, since DCA can be used to predict production performance. The production profiles from the reservoir simulation can be fit with a decline curve. Then, the decline parameters obtained can be incorporated and used in the decision model to predict the expected net present value for the different development scenarios and the results can be used as a mean to decide on the optimal development strategy. Ultimately, the use of DCA parameters to integrate the reservoir and decision model was not used in this project. Nonetheless, I present in this section the proposed methodology and results for a decline model that was developed during the project to represent the Gething formation.

7.1. Overview

Decline curve analysis is one of the most common reservoir engineering tools used to forecast production performance. Among its advantages over others techniques are that it requires minimal data and is simple to use. It is widely used in the industry (Kupchenko et al. 2008). Due to its nature, it can be used as a method of production forecasting for tight gas reservoirs without the need of a more complex technique. However, care must be taken when using this method in unconventional reservoirs because inaccurate forecasts may be predicted (Cheng et al. 2008 a); Cheng et al. 2008

b); Kupchenko et al. 2008; Mattar 2008). Since DCA can predict production performance, it might be possible to use it for determining the optimal well spacing.

The production performance from tight gas reservoirs can often be described by a steep initial decline rate and a long period of transient flow, which then transitions into conventional boundary-dominated flow (BDF) model after a certain time. Conventional decline curve analysis applies to cases where the transient flow has finished and the well is producing at constant bottom hole pressure and stabilized flow conditions. Accordingly, it is very important that DCA is applied only after boundary-dominated flow is reached. Since DCA assumes boundary-dominated flow, if decline analysis is done using the transient production data (thus violating DCA assumptions), errors in production forecasts and reserves estimates will result since the effective drainage area of the well increases during transient flow (Kupchenko et al. 2008). Since transient flow can last a long time in unconventional reservoirs (months or years), a method to predict the production performance over both the transient and BDF regimes is required.

7.2. Decline Curve Model

Arps (1945) introduced the empirical exponential and hyperbolic rate decline relations, which are still widely used relations for production forecasting of gas and oil wells. The general hyperbolic form of the Arps decline equation is given by:

$$q = q_i(1 + bD_i t)^{(-1/b)} \quad \text{..... (2)}$$

This equation is used to predict the gas flow rate q as a function of time t. The hyperbolic decline exponent b, initial production rate q_i, and initial decline rate D_i can be determined by matching the production performance. When b approaches 0, the decline becomes exponential and is given by:

$$q = q_i \cdot exp(-Dt) \quad \text{..... (3)}$$

where D is the constant exponential decline rate.

In this research I used the model proposed by Fattah, (Fattah 2006) where a hyperbolic decline is used for early production (accounting for the long transient period in unconventional reservoirs) and an exponential decline is used for later, boundary-dominated production. The 20-year production profiles of the simulated wells were matched to a DCA model with early hyperbolic decline terminating in an exponential decline at time t_o as boundary-dominated flow is reached (Eqs. 4-5). An example fit of this DCA model to simulated production is shown in **Fig. 49**.

Hyperbolic decline segment

$$q = q_i(1 + D_i bt)^{(-1/b)} \quad 0 \le t \le t_0 \quad \text{..... (4)}$$

Exponential Decline segment

$$q = q_i(1 + D_i bt_0)^{(-1/b)} exp\left(\frac{-D_i(t - t_0)}{(1 + bD_i t_0)}\right) \quad t \ge t_0 \quad \text{..... (5)}$$

A VBA code utilizing the Solver add-in of Excel was written to perform decline curve analysis on the simulated production data and was incorporated into the reservoir model VBA code. For each simulation run, the four best fit decline parameters, q_i, D_i, b, and t_o, have been determined.

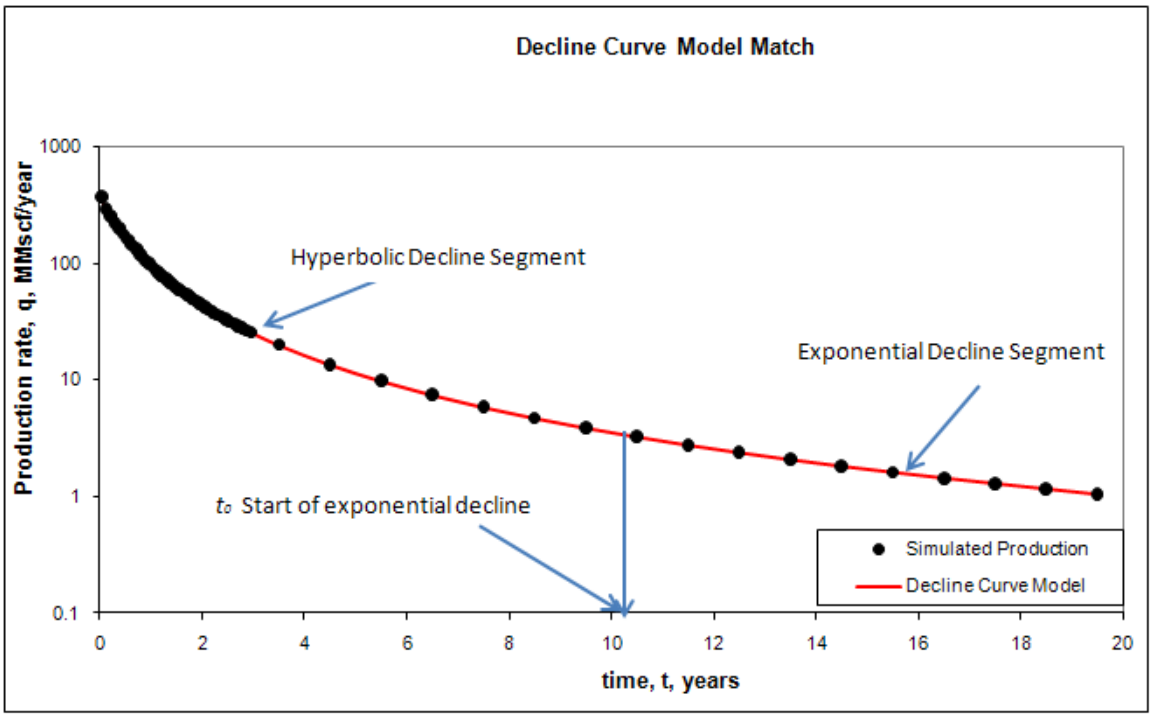

Fig. 49 — Decline curve analysis performed on simulated production. The figure represents a typical gas production rate vs. time. The figure shows t_o, the transition point from hyperbolic to exponential decline.

The production data during Stage 1 was acquired on a monthly basis and matched with the model. Since most of the production from Stage 1 was still in transient flow, the match of Stage 1 produced mainly hyperbolic declines. For Stage 2, which varies from 15 to 19 years depending on the length of Stage 1 (1 to 5 years), the early production (1 year) was acquired on a monthly basis to help the Solver algorithm obtain a better match, while the rest of the performance history was acquired on a yearly basis and matched using the combined hyperbolic-exponential decline model. The value

obtained for t_0 was used to compute the minimum decline during exponential decline D using the equation below.

$$D = \left(\frac{-D_i}{(1 + bD_i t_0}\right) \quad t \geq t_0 \qquad \text{..... (6)}$$

Decline parameters of Stage 1 (q_i, D_i, , b) and Stage 2 (q_i, D_i, b, t_0) were determined along with their statistics (mean, standard deviation and pair-wise correlation) to serve as inputs to the decision model. The cumulative distribution functions of decline parameters were obtained. **Table 7** shows an example of calculated decline parameters for Stage 1 and Stage 2 for the case of Stage 1 duration of 3 years. The table specifically shows the results for Well 1 at Stage 1 spacing of 640 acres (3 year decline parameters) and results for Well 2 at Stage 2 spacing of 320 acres (17 years declines parameters).

Table 7 — Example of Decline Parameters for Stage 1 and Stage 2 of the case for Stage 1 duration of 3 years. The results for Well 1 during Stage 1 at initial spacing of 640 acres and the results for Well 2 during Stage 2 at spacing of 320 acres are shown

Run #	Stage 1, Well 1, 640 acres				Stage 2, Well 2, 320 acres					
	3 Year Decline Parameters				Stage 2 (17 Years) Decline Parameters					
	Qi MMscf/year	Di 1/year	b	Residuals	Qi MMscf/year	Di 1/year	b	Residuals	to year	Dmin 1/year
1	740.21	1.25	2.71	0.03	209.69	2.00	1.46	0.08	5.04	0.13
2	937.32	1.30	2.58	0.02	246.94	2.28	1.29	0.03	6.19	0.12
3	796.02	2.46	2.88	0.02	300.14	1.79	1.43	0.02	7.12	0.09
4	2457.90	3052.65	4.26	0.01	105.40	4.51	2.28	0.00	7.20	0.06
5	313.17	2.19	6.70	0.02	1027.91	12.77	1.48	0.02	6.22	0.11
6	475.09	1.73	2.78	0.03	352.16	5.93	0.72	0.12	16.5	0.08
7	460.83	7090.59	5.36	0.01	511.85	4.07	0.93	0.10	16.5	0.06
8	244.46	1.24	3.30	0.02	400.83	4.51	1.15	0.03	9.06	0.09
9	120.54	3.53	2.24	0.02	811.04	19.52	1.71	0.00	16.4	0.04
10	1217.50	39.80	3.89	0.01	482.12	3.52	1.25	0.03	6.07	0.13
11	2639.34	27813.7	4.05	0.05	486.10	2.51	1.15	0.04	8.36	0.10
12	1.98	87.98	56.91	0.00	651.01	17.63	2.75	0.03	4.42	0.08
13	281.82	1.11	4.71	0.01	642.64	14.91	1.87	0.05	4.19	0.13
14	2.29	30.61	139.7	0.00	546.68	14.51	1.86	0.01	10.0	0.05
15	407.15	5.41	4.31	0.04	132.68	2.70	0.95	0.08	16.5	0.06
16	875.89	1.64	1.82	0.04	164.03	2.84	0.50	0.11	9.96	0.19
17	879.91	14.22	4.16	0.03	303.23	2.57	1.69	0.08	4.28	0.13
18	197.25	15177.9	9.58	0.06	2151.16	31134.	3.23	0.06	5.52	0.06
19	455.85	16801.1	5.77	0.07	290.19	5.77	1.59	0.02	6.50	0.10
20	722.84	1.56	3.42	0.03	99.52	1.51	1.99	0.04	4.18	0.11

8. INTEGRATED RESERVOIR AND DECISION MODEL

8.1. Overview

Decision Analysis (DA), in the form of decision tree analysis has been used in the past for brown-field development (Guyaguler and Horne 2001; King et al. 2005) and assessing uncertainty in well placement optimization. Wongnapapisan et al. (2004) also described the use of decision tree analysis to optimize field performance for a wide range of reservoir management decisions; however, the integration of geological uncertainties into this decision analysis was not discussed. Turkarslan et al. (2010) used DA coupled with a reservoir model assessing uncertainty in key reservoir parameters to determine the optimal well spacing in a tight gas reservoir. The decision tree is used to evaluate all possible combination of outcomes with associated probabilities (Wongnapapisan et al. 2004). In decision tree analysis, three branch descriptions (high, mean and low) are often used as substitutes for an entire continuous distribution.

8.2. Decision Model

A practical and flexible decision model was developed and validated simultaneously with this research by researchers in the Department of Industrial Engineering at University of Texas at Austin. The decision model developed evaluates the dependence between two-stage development scenarios with the goal to determine the

optimal development policy (primary and secondary development plans) in an unconventional gas reservoir in the face of significant subsurface uncertainty. The procedure takes economic considerations into account and quantifies the associated revenues and costs with the objective of maximizing the profitability and selecting the optimal development policy.

The sequential development decision requires capturing the dependence between stages and using the primary stage production results to make decisions for the next stage. The decision model employs decision trees to determine the optimal development program (Bickel and Smith 2006). **Fig. 50** shows a schematic decision tree illustrating the decision context. The operator first chooses the primary spacing and then observes the uncertain production results after some fixed amount of time, such as one, three or five years. Then, based on these results, the operator makes the downspacing decision for Stage 2 and production results for the second stage are observed. The ultimate objective of this sequential plan is to maximize the expected net present value.

Fig. 51 shows an excerpt of the decision tree used in the Berland River area, which demonstrates the structure of the sequential development program. This part of the tree shows initial development at 160-acre spacing, and then at a later date, as influenced by the primary production results, the downspacing decision between 160-acre and 80-acre spacing for Stage 2 is made.

The influence diagram for the decision of the development plan for the Berland River area is presented in **Fig. 52**. The Net Present Value (NPV) is the variable to be maximized. In other words, the decision model selects the optimal development policy

with the objective of maximizing profitability. The optimal policy consists of primary and secondary well spacing which are decision variables. Discounted cumulative production distributions are the uncertain variables used in the calculation of the expected NPV.

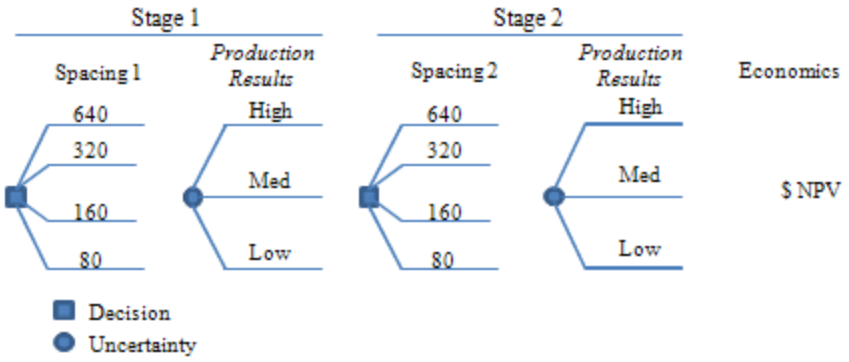

Fig. 50 — Schematic decision tree for an unconventional reservoir development plan.

The primary production results will provide information to the operator that he/she will be able to use to make a more informed downspacing decision. The value of a primary development plan is then the value of the primary production *plus* the value of the information it provides that can be used to develop the optimal secondary spacing. Distribution functions for discounted cumulative production by stage obtained from the reservoir modeling are the input to the decision model. The discounted cumulative production distribution for each stage and downspacing scenario is summarized by its mean, standard deviation and correlation coefficients.

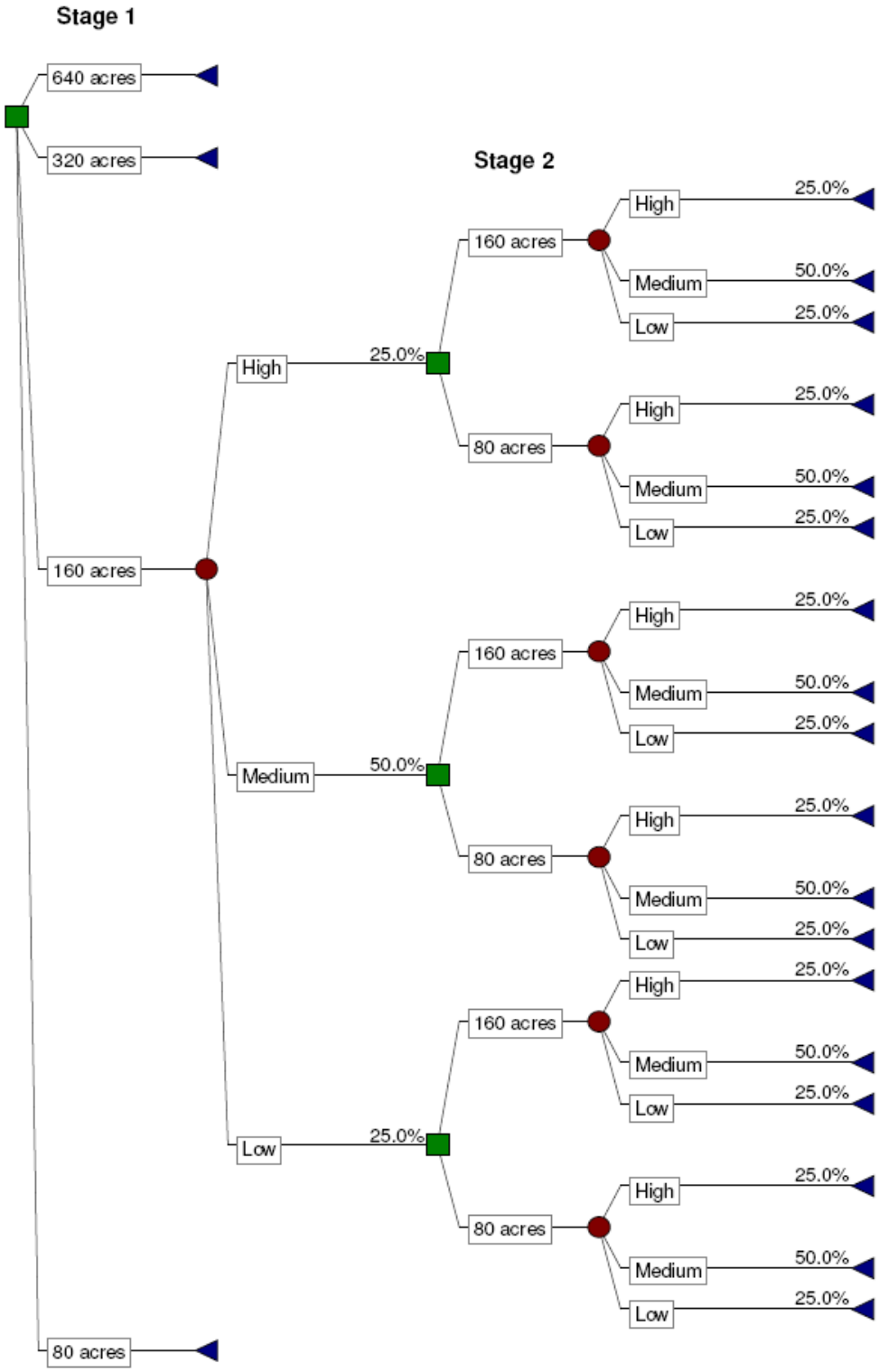

Fig. 51 — An excerpt of the decision tree for the Berland River (Turkarslan 2010).

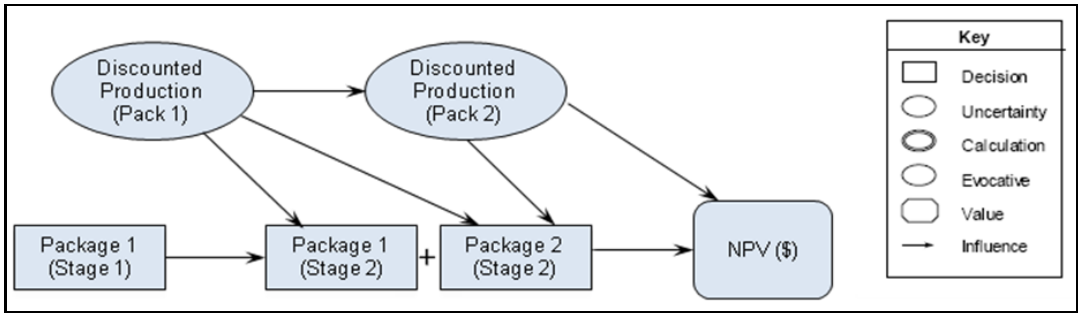

Fig. 52 — Influence Diagram for proposed decision model.

To model the dependence between primary and secondary development plans, joint probability distributions of the discounted cumulative production based on the statistical parameters are constructed. These distributions are then used to calculate the expected net present values that form the basis of the decision. The conditional distribution of production between stages is defined by the following equation:

$$\mu_{2/1}(a) = \mu_2 + \rho_{1,2}\frac{\sigma_2}{\sigma_1}(a - \mu_1) \quad \text{..... (7)}$$

where $\mu_{2/1}(a)$ is the expected discounted cumulative production at Stage 2 given the discounted cumulative production of Stage 1 (a), $\rho_{1,2}$ is the correlation coefficient between stages, $\frac{\sigma_2}{\sigma_1}$ is the ratio between standard deviation at each Stage, μ_2 is the expected value for discounted cumulative production for Stage 2, and μ_1 is the expected value for discounted cumulative production for Stage 1.

The production uncertainties are discretized by using three branch descriptions, P_{90}, P_{50} and P_{10}. Specifically, these percentiles are weighted to approximate the expected value using the Swanson's Mean of Extended-Swanson-Megill (ESM) (Hurst et al.

2000; Megill 1984), which weight these branches by 0.25, 0.5 and 0.25 respectively. This method is commonly applied directly to the percentiles of log-normal distributions The P_{90}, P_{50}, and P_{10} percentiles are computed, which represent the high, medium and low production values that are associated with probabilities of 25%, 50% and 25%, respectively (**Table 8**). These percentiles along with the statistical parameters are used in Equation 7 to determine the conditional means of Stage 2 given Stage 1 and ultimately allow the estimation of the combined net present value of Stages 1 and 2.

Table 8 — Weight factors and fractiles used in the decision model

Discretization	
Weights	**fractiles**
0.25	0.90
0.50	0.50
0.25	0.10

8.3. Integration of Reservoir with the Decision Model

A key feature of the decision model is its integration with the reservoir model (**Fig. 53**). The forecasted production profiles of the reservoir model were used as input to the decision model and then the decision model calculated the expected net present value for each scenario that allows the selection of the optimal development strategy. In this research the discounted cumulative production at a discount rate of 10% for two separate stages were used to facilitate the integration of the reservoir and decision models.

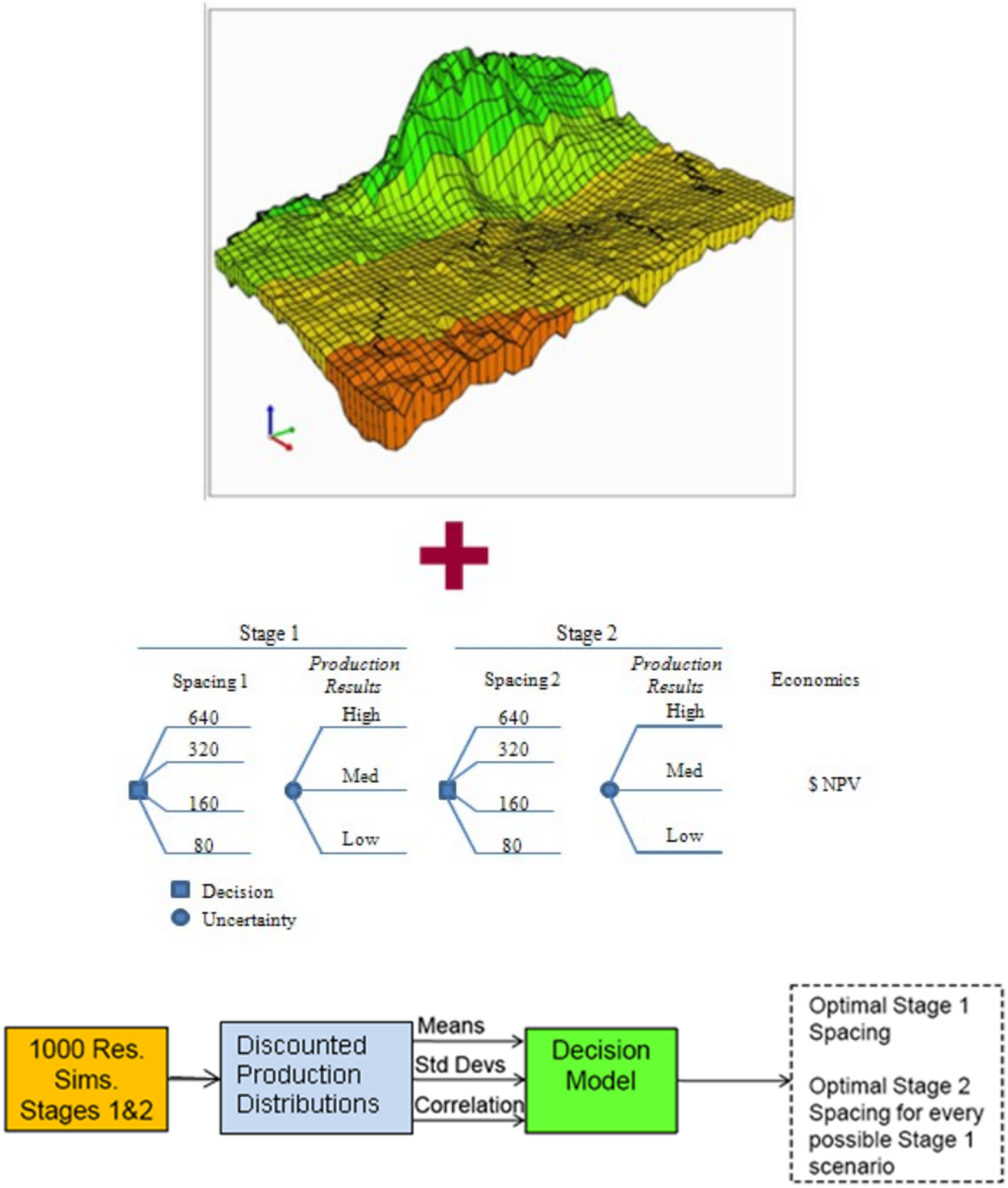

Fig. 53 — Integration of reservoir and decision model. The results from the reservoir simulation are used to obtain the distributions of discounted (at 10%) cumulative production. The means, standard deviations and correlation coefficients of the discounted cumulative production distribution are calculated and used as input for the decision model. The decision model processes these values along with economical considerations (NPV) and yields the optimal development strategy.

The reservoir model was run with Stage-1 durations of 1, 3 and 5 years to understand the trade-off between Stage 1 duration and well spacing. The package of wells drilled during Stage 1 is referred as Original Wells and the package of wells drilled during Stage 2 are referred as the Infill Wells. The wells in each stage will be drilled at 640, 320, 160 and 80-acre spacing. The production results were evaluated during both stages for each set of wells. Since gas production is commonly represented by a lognormal distribution, the natural logarithm of discounted cumulative production for the two packages of wells previously defined was computed. Means, standard deviations and correlation coefficients were obtained considering all possible downspacing combinations. The statistical parameters described before for Stage-1 lengths of 1, 3 and 5 years are presented in **Table 9** to **Table 11**. For ease in understanding of these tables, the values presented are transformed back from the natural logarithm; however, during the application of the integrated model, the natural-log transformed values were used. The tables show the outputs from the reservoir model that were used in the decision model.

The correlations coefficients between Stages 1 and 2 for stage length of 1 year (Table 9) are 0.96 for the Original Wells and 0.47 for the Infill Wells when going from 640 to 80-acre spacing. Because a correlation is observed, we can use the Original Wells production during Stage 1 to forecast the mean production of Infill Wells during Stage 2 and the accompanying uncertainty, assuming that the uncertainty between stages is jointly log-normally distributed. The statistical parameters for the natural log of the discounted production of each set of wells for each stage are used in Equation 7 (in this

case, the variable *a* is the natural logarithm of discounted cumulative production of Stage 1) as the basis for the decision tree analysis, enabling the determination of the optimal development policy for the field.

In Tables 9-11 we observe that correlation coefficients between Stage 1 and Stage 2 Original Wells are much higher than correlation coefficients between Stage 1 and Stage 2 Infill Wells. This shows that Original Wells' production in Stage 1 tells us more about how these wells will perform in Stage 2 than how the Infill Wells will perform. This is expected as Infill Wells are a new set of wells. We also observe that correlation coefficients for Original Wells increase as spacing is decreased; this might have directly relation with the reservoir area being drain by each well as the spacing is decreased. It is also observed that correlation coefficients for Infill Wells decrease as the Stage-1 duration is increased, indicating that our ability to learn about the production of the Infill Wells decreases as the initial stage duration increases, particularly for a Stage-1 duration of 5 years where the correlation coefficients are close to zero. One explanation of this could be related to the onset of depletion effects for longer Stage-1 durations. Permeabilities in the Gething formation are relatively high for a tight gas reservoir, which can explain why boundary-dominated flow could be reached within a couple of years in many cases.

Table 9 — Statistical parameters for discounted stage production (MMscf) for Original and Infill wells for a Stage-1 length of 1 year

1-Year Pilot Phase									
	Discounted Cumulative Production (MMscf)								
	Original Wells	Original Wells				Infill Wells			
	Stage 1	Stage 2				Stage 2			
spacing	**640**	**640**	**320**	**160**	**80**	**640**	**320**	**160**	**80**
mean	354.40	1066.92	965.32	716.15	324.43	-	465.32	1347.16	2406.80
standard deviation	247.16	646.95	594.55	442.41	208.00	-	243.59	524.36	690.66
correlation	1.00	0.95	0.95	0.95	0.96	-	-0.02	0.22	0.47
spacing	**320**	**640**	**320**	**160**	**80**	**640**	**320**	**160**	**80**
mean	551.00	-	1301.37	914.42	467.37	-	-	1001.40	2108.51
standard deviation	288.66	-	609.89	454.48	220.78	-	-	453.78	647.47
correlation	1.00	-	0.93	0.95	0.96	-	-	0.26	0.49
spacing	**160**	**640**	**320**	**160**	**80**	**640**	**320**	**160**	**80**
mean	1029.50	-	-	1549.87	835.17	-	-	-	1335.54
standard deviation	442.57	-	-	573.66	305.38	-	-	-	427.41
correlation	1.00	-	-	0.91	0.94	-	-	-	0.49
						-	-	-	
spacing	**80**	**640**	**320**	**160**	**80**	**640**	**320**	**160**	**80**
mean	2019.42	-	-	-	1336.83	-	-	-	-
standard deviation	706.89	-	-	-	391.36	-	-	-	-
correlation	1.00	-	-	-	0.89	-	-	-	-

Table 10 — Statistical parameters for discounted stage production (MMscf) for Original and Infill wells for a Stage-1 length of 3 years

3-Year Pilot Phase									
	Discounted Cumulative Production (MMscf)								
	Original Wells	Original Wells				Infill Wells			
	Stage 1	Stage 2				Stage 2			
spacing	**640**	**640**	**320**	**160**	**80**	**640**	**320**	**160**	**80**
mean	770.24	666.55	598.28	444.86	204.68	--	335.74	972.39	719.64
standard deviation	526.06	386.58	349.55	258.70	124.55	--	181.85	381.02	481.91
correlation	1.00	0.94	0.94	0.95	0.96	--	-0.15	0.06	0.24
spacing	**320**	**640**	**320**	**1160**	**80**	**640**	**320**	**160**	**80**
mean	1,098.77	--	757.06	536.98	277.64	--	--	666.72	1,413.62
standard deviation	577.56	--	329.77	247.10	123.57	--	--	310.22	430.58
correlation	1.00	--	0.91	0.93	0.95	--	--	0.14	0.28
spacing	**160**	**640**	**320**	**1160**	**80**	**640**	**320**	**160**	**80**
mean	1,825.55	--	--	757.85	410.27	--	--	--	763.37
standard deviation	769.30	--	--	256.37	139.49	--	--	--	247.97
correlation	1.00	--	--	0.85	0.90	--	--	--	0.21
spacing	**80**	**640**	**320**	**160**	**80**	**640**	**320**	**160**	**80**
mean	2,916.96	--	--	-	443.41	--	--	--	-
standard deviation	975.39	--	--	-	124.76	--	--	--	-
correlation	1.00	--	--	-	0.74	--	--	--	-

Table 11 — Statistical parameters for discounted stage production (MMscf) for Original and Infill wells for a Stage-1 length of 5 years

5-Year Pilot Phase									
	Discounted Cumulative Production (MMscf)								
	Original Wells	Original Wells				Infill Wells			
	Stage 1	Stage 2				Stage 2			
spacing	**640**	**640**	**320**	**160**	**80**	**640**	**320**	**160**	**80**
mean	1,008.50	429.58	386.65	290.74	136.61	--	243.98	713.42	1,261.43
standard deviation	675.3	239.8	217.1	161.7	79.8	--	139.9	293.4	371.6
correlation	1.00	0.92	0.93	0.94	0.95	--	-0.27	-0.09	0.03
spacing	**320**	**640**	**320**	**160**	**80**	**640**	**320**	**160**	**80**
mean	1,388.18	--	465.27	335.65	177.66	--	--	461.31	988.26
standard deviation	717.34	--	190.52	144.24	74.09	--	--	227.42	320.51
correlation	1.00	--	0.87	0.91	0.93	--	--	0.04	0.09
spacing	**160**	**640**	**320**	**160**	**80**	**640**	**320**	**160**	**80**
mean	2,161.83	--	--	419.78	232.78	--	--	--	478.90
standard deviation	890.82	--	--	134.16	74.56	--	--	--	174.41
correlation	1.00	--	--	0.77	0.85	--	--	--	-0.01
spacing	**80**	**640**	**320**	**160**	**80**	**640**	**320**	**160**	**80**
mean	3,161.04	--	--	-	198.01	--	--	--	-
standard deviation	1,038.40	--	--	-	57.40	--	--	--	-
correlation	1.00	--	--	-	0.60	--	--	--	-

8.4. Optimal Well Spacing Determination

Applying the integrated tools described above, I modeled specific development decisions for the Gething formation in the Berland River Area. The decision model determines the spacing development policy that maximizes net present value (NPV) and selects the one with the highest output as our objective is to maximize the expected NPV. I used the economic assumptions presented in **Table 12** and the weights and percentiles presented in Table 8. The economics are computed on a section basis. For simplicity, the calculations to obtain the NPV for each stage are not presented here and only the optimal policy results for the three Stage-1 durations evaluated in this study are presented **Table 13** to **Table 15**. Based on these results, the decision model calculates the expected NPV for each scenario.

Table 12 — Economic Assumptions for Decision Model

Gas Price	$/Mcf	5.50
Marginal Cost	$/Mcf	1.00
Field Cost	MM$/yr/well	0.05
Drilling Cost	MM$/well	1.00
Discount Rate	-	0.10
No Royalty		

On Tables 13 to 15 the initial spacing and then based on the decision tree analysis the recommended downspacing for Stage-2 are determined. The results for Stage-1 length of 1 year (Table 13) shows that if we start with a 640-acre spacing and

the initial production is high (P90), the downspace alternative that maximizes the NPV is to continue on 640-acre spacing; in this case no additional wells will be drilled in Stage 2. The total NPV of this scenario, including Stage 1, is $15.88 MM. If we observe low production (P_{10}), the optimal Stage-2 decision is to downspace to 160 acres, in which case the NPV is $2.21 MM. We also downspace to 160 acres if P_{50} production is observed; for this case the NPV is $4.45 MM. Weighting each of these production scenarios with their probability of occurrence, we obtain an expected NPV for an initial 640-acre spacing of $6.67 MM. Similar analyses were done for initial spacing of 320, 160 and 80 acres and their estimated NPVs are $6.04 MM, $7.10 MM and $6.25 MM, respectively. Thus, the optimal Stage-1 spacing is 160 acres, in which no further downspacing is required. This example demonstrates the value when a dynamic strategy is used. A dynamic strategy takes advantage of the information gained during the initial stage to develop the optimal downspacing program.

Table 14 and Table 15 present the results for 3-year and 5-year Stage-1 lengths, respectively. The best initial spacing for the 3-year Stage-1 length is 160 acres and its estimated NPV is $6.63 MM. For 5-year Stage-1 length, the optimum is to start with 640-acre spacing and not downspace, in which case the expected NPV is $6.39MM. We observe from these results that extending the duration of Stage 1 beyond 1 year does not represent an economic benefit, which is consistent with and results from the decreasing correlation coefficients between Stage 2 and Stage 1 performance with increased Stage 1 duration previously discussed. The optimal development policy is a 1-year Stage 1 of

160 acres followed by no downspacing. These results are specific to the reservoir model and economic assumptions used in this work and cannot be generalized.

Table 16 to **Table 18** show the results if a better economic environment (higher price gas) is present. The gas price was assumed to be $9.0/Mcf. The results show the optimal development strategy is to start Stage 1 with a spacing of 80 acres, which will yield the highest estimated NPV ($17.87MM) for the project for all Stage-1 lengths. Once again the optimal length for Stage 1 is 1 year and no further downspacing is required (duly noting that downspacing below 80 acres was not investigated). The change in the optimal policy when the gas price is higher shows that the optimal development policy of a field might change depending on the economic environment. In fact, there is uncertainty involved in the economic parameters; however, they are not considered part of this study as my main focus was the modeling of subsurface uncertainty.

A close evaluation of the evaluation of the high price environment helps to demonstrate the value of an optimal dynamic strategy, which takes advantage of information gained during the first stage. For example, if the operator had to commit to 640-acre spacing from the beginning of the development plan and could not downspace, we calculate (not shown) that the ENPV would be $12.2 MM, or over $3.5 MM less. This $3.5 MM difference is the value of the information that is gained via the staged strategy. Thus, we see the value that can be gained through better use of information and better decision making.

In this section, a decision model was presented and was used to determine the optimal strategies for development of a tight gas reservoir. The decision model presented here provides recommendations to operators on the determination of the optimal development policy.

Table 13 — Optimal development strategy results for Stage-1 length of 1 year. Monetary values are per section

Stage 1 Spacing, acres	Probability	Observed DCP	Stage 2 Optimal Spacing acres	Stage 1 E[NPV], $MM	Stage 2 NPV, $MM	Total NPV, $MM	Estimated NPV, Optimal Policy, $MM
640	0.25	P90	640	0.94	14.64	15.58	6.67
	0.50	P50	160	0.94	3.51	4.45	
	0.25	P10	160	0.94	1.27	2.21	
320	0.25	P90	320	0.39	10.31	10.70	6.04
	0.50	P50	320	0.39	4.97	5.36	
	0.25	P10	320	0.39	2.37	2.76	
160	0.25	P90	160	0.43	10.55	10.98	7.10
	0.50	P50	160	0.43	6.24	6.67	
	0.25	P10	160	0.43	3.66	4.09	
80	0.25	P90	80	0.68	7.89	8.57	6.25
	0.50	P50	80	0.68	5.38	6.06	
	0.25	P10	80	0.68	3.63	4.31	

Table 14 — Optimal development strategy results for Stage-1 length of 3 years. Monetary values are per section

Stage 1 Spacing, acres	Probability	Observed DCP	Stage 2 Optimal Spacing, acres	Stage 1 E[NPV], $MM	Stage 2 NPV, $MM	Total NPV, $MM	Estimated NPV, Optimal Policy, $MM
640	0.25	P90	640	3.19	8.74	11.94	6.46
	0.50	P50	640	3.19	1.98	5.17	
	0.25	P10	320	3.19	0.38	3.57	
320	0.25	P90	320	2.75	5.62	8.37	5.85
	0.50	P50	320	2.75	2.75	5.50	
	0.25	P10	320	2.75	1.28	4.03	
160	0.25	P90	160	3.79	4.47	8.26	6.63
	0.50	P50	160	3.79	2.68	6.47	
	0.25	P10	160	3.79	1.54	5.33	
80	0.25	P90	80	4.28	1.56	5.85	5.24
	0.50	P50	80	4.28	0.92	5.20	
	0.25	P10	80	4.28	0.44	4.72	

Table 15 — Optimal development strategy results for Stage-1 length of 5 year. Monetary values are per section

Stage 1 Spacing acres	Probability	Observed DCP	Stage 2 Optimal Spacing, acres	Stage 1 E[NPV], $MM	Stage 2 NPV, $MM	Total NPV, $MM	Estimated NPV, Optimal Policy, $MM
640	0.25	P90	640	4.42	5.27	9.69	6.39
	0.50	P50	640	4.42	1.21	5.63	
	0.25	P10	640	4.42	0.17	4.59	
320	0.25	P90	320	4.00	3.05	7.06	5.67
	0.50	P50	320	4.00	1.50	5.50	
	0.25	P10	320	4.00	0.65	4.65	
160	0.25	P90	160	5.20	1.85	7.04	6.28
	0.50	P50	160	5.20	1.02	6.22	
	0.25	P10	160	5.20	0.45	5.65	
80	0.25	P90	80	5.18	(0.43)	4.75	4.53
	0.50	P50	80	5.18	(0.66)	4.52	
	0.25	P10	80	5.18	(0.85)	4.33	

Table 16 — Optimal development strategy results for Stage-1 length of 1 year with higher gas price ($9.0/Mcf). Monetary values are per section

Spacing acres	Stage 1 Probability	Observed DCP	Stage 2 Optimal Spacing, acres	Stage 1 E[NPV], $MM	Stage 2 NPV, $MM	Total NPV, $MM	Estimated NPV, Optimal Policy, $MM
640	0.25	P90	640	2.48	26.07	28.55	15.79
	0.50	P50	80	2.48	10.40	12.88	
	0.25	P10	80	2.48	6.35	8.83	
320	0.25	P90	160	2.31	19.15	21.46	14.15
	0.50	P50	80	2.31	10.89	13.20	
	0.25	P10	80	2.31	6.44	8.75	
160	0.25	P90	160	4.01	18.90	22.91	16.01
	0.50	P50	160	4.01	11.23	15.24	
	0.25	P10	160	4.01	6.64	10.65	
80	0.25	P90	80	7.69	14.31	22.00	17.87
	0.50	P50	80	7.69	9.84	17.53	
	0.25	P10	80	7.69	6.73	14.43	

Table 17 — Optimal development strategy results for Stage-1 length of 3 years with higher gas price ($9.0/Mcf). Monetary values are per section

Stage 1 Spacing acres	Probability	Observed DCP	Stage 2 Optimal Spacing, acres	Stage 1 E[NPV], $MM	Stage 2 NPV, $MM	Total NPV, $MM	Estimated NPV Optimal Policy, $MM
640	0.25	P90	640	6.53	15.64	22.17	14.07
	0.50	P50	160	6.53	5.56	12.08	
	0.25	P10	160	6.53	3.43	9.96	
320	0.25	P90	160	6.59	10.20	16.79	12.64
	0.50	P50	160	6.59	5.49	12.08	
	0.25	P10	160	6.59	3.00	9.59	
160	0.25	P90	160	10.14	8.33	18.47	15.58
	0.50	P50	160	10.14	5.16	15.30	
	0.25	P10	160	10.14	3.13	13.27	
80	0.25	P90	80	14.41	3.56	17.97	16.89
	0.50	P50	80	14.41	2.41	16.82	
	0.25	P10	80	14.41	1.55	15.96	

Table 18 — Optimal development strategy results for Stage-1 length of 5 years with higher gas price ($9.0/Mcf). Monetary values are per section

Spacing acres	Stage 1 Probability	Observed DCP	Stage 2 Optimal Spacing, acres	Stage 1 E[NPV], $MM	Stage 2 NPV, $MM	Total NPV, $MM	Estimated NPV, Optimal Policy, $MM
640	0.25	P90	640	8.73	9.52	18.25	13.02
	0.50	P50	160	8.73	2.95	11.69	
	0.25	P10	160	8.73	1.70	10.43	
320	0.25	P90	320	8.85	5.72	14.58	12.12
	0.50	P50	320	8.85	2.95	11.81	
	0.25	P10	320	8.85	1.44	10.30	
160	0.25	P90	160	12.72	3.87	16.59	15.23
	0.50	P50	160	12.72	2.40	15.12	
	0.25	P10	160	12.72	1.40	14.11	
80	0.25	P90	80	16.16	0.42	16.58	16.19
	0.50	P50	80	16.16	0.00	16.16	
	0.25	P10	80	16.16	(0.32)	15.84	

8.5. Economic Considerations (Present Value Ratio)

The results of the decision model for optimal development policy were evaluated using a performance indicator tool known as present value ratio (*PVR*), to consider situations in which capital is constrained. For this research, the evaluation was done calculating the *PVR* from the optimal Stage 2 spacing for production level determined from the *NPV* model. By definition, *PVR* is the ratio of the net present value (*NPV*) to the present value (*PV*) of capital investment. The *PVR* is represented by the following equation:

$$PVR = \frac{NPV}{PV\ of\ Capital\ Invesment} \quad \text{..... (8)}$$

The *PVR* shows net *PV* dollars generated per the *PV* of every capital investment (i.e. the capital investment is already recovered and the value of the *PVR* is the net gain over every dollar invested). *PVR* provides a measure of profitability per dollar invested. This is particular important consideration when faced with the selection of investments for a list containing more opportunities than the available funds can cover. In other words it can be used to evaluate the efficiency of an investment or to compare the efficiencies of a number of different investments when capital constraints are present. That is, if an investment does not have a positive *PVR*, or if there are other opportunities with a higher *PVR*, then the investment should be not be undertaken (Mian 2002).

Table 19 presents the results for the *PVR* evaluation for the optimal development policy previously determined for each Stage-1 length of 1 year for the low gas price environment ($5.50/Mcf). We observe in Table 19 that, even though the decision model

based on maximizing profitability *NPV* recommends using an optimal Stage-1 spacing of 160 acres followed by no Stage-2 downspacing (Table 13), the *PVR* evaluation shows that the optimum policy is Stage-1 spacing of 320 acres with no Stage-2 downspacing. Even though starting at initial spacing of 160 acres will result in an extra $1.06 MM of NPV, this action involves the investment of an additional $2MM which results in a lower PVR for this option (1.78 compared to 3.02 when 320 acres spacing is used), making the Stage-1 spacing of 320 acres with no Stage-2 downspacing the optimum policy specially if budget for the development plan is constrained. Other considerations as operational risk, such drilling schedules, expected drilling problems; safety risk will also need to be considered to determine which will be the best option.

Table 20 presents the results of *PVR* evaluation for Stage-1 length of 3 years and low gas price. Based on *NPV*, the best initial spacing for the 3-year Stage-1 length is 160 acres (Table 14) and its estimated *NPV* is $6.63 MM; however, the *PVR* for 160 acres is 1.66, which is much lower than the *PVR* of 5.25 for an initial spacing of 640 acres. The 640-acre initial spacing has an estimated *NPV* of $6.46 MM, which is only $0.17 MM lower than the *NPV* for the 160-acre initial spacing, with an investment of $2.77 MM less. It appears that choosing 640 acres as the initial spacing would be a better decision, particularly if capital is constrained. **Table 21** presents the results for a Stage-1 length of 5 years and low gas price. Based on *NPV*, the best initial spacing is 640 acres with a *NPV* of $6.39 MM (Table 15). This optimal development policy also results in the best *PVR*, 6.39, which makes this the clear best policy.

The *PVR* evaluation presented here shows that other factors need to be taken into consideration when making decisions on optimal development strategies. Besides maximizing profits (*NPV*), other economic aspects need to be accounted for as they can illustrate additional benefits. *NPV* evaluation itself does not give any indication of the size of the initial investment and could cause problems when choosing among several alternative investment of different size. This is the case when the *NPV* of two investments may be equal or close, but the amount of investment required by the two alternatives may vary widely.

PVR can be used in capital allocation as it provides a better picture of the investment ranking criteria. This is especially important when capital constrains exits. Capital additions should be analyzed in terms of their probable effect on return of investment. A capital decision should not be taken unless its analysis indicates that t will yield a return equal, or greater than the long-term company objective for return of investment. In the case of several investment options with constrained capital, only those investments that will maximize its worth should be considered. The selection of the projects from the investment opportunities being considered should be those that will yield the maximum return possible with the limited resources (capital). Finally, operational aspects such as drilling schedule, safety risk, drilling risk and economic uncertainties among others will also need to be included.

Table 19 — *PVR* evaluation for the optimal development strategy results for Stage-1 length of 1 year. Monetary values are per section

Stage 1			Stage 2			
Spacing, acres	Probability	Observed DCP	Optimal Spacing, acres	Estimated NPV Optimal Policy, $MM	Estimated PV of Capital Investment, $MM	PVR
640	0.25	P90	640	6.67	3.05	2.19
	0.50	P50	160			
	0.25	P10	160			
320	0.25	P90	320	6.04	2.00	3.02
	0.50	P50	320			
	0.25	P10	320			
160	0.25	P90	160	7.10	4.00	1.78
	0.50	P50	160			
	0.25	P10	160			
80	0.25	P90	80	6.25	8.00	0.78
	0.50	P50	80			
	0.25	P10	80			

Table 20 — *PVR* evaluation for the optimal development strategy results for Stage-1 length of 3 years. Monetary values are per section

Stage 1			Stage 2			
Spacing, acres	Probability	Observed DCP	Optimal Spacing, acre	Estimated NPV Optimal Policy, $MM	Estimated PV of Capital Investment, $MM	PVR
640	0.25	P90	640	6.46	1.23	5.25
	0.50	P50	640			
	0.25	P10	320			
320	0.25	P90	320	5.85	2.00	2.93
	0.50	P50	320			
	0.25	P10	320			
160	0.25	P90	160	6.63	4.00	1.66
	0.50	P50	160			
	0.25	P10	160			
80	0.25	P90	80	5.24	8.00	0.66
	0.50	P50	80			
	0.25	P10	80			

Table 21 — *PVR* evaluation for the optimal development strategy results for Stage-1 length of 5 years. Monetary values are per section

Stage 1			Stage 2			
Spacing, acres	Probability	Observed DCP	Optimal Spacing, acres	Estimated NPV Optimal Policy, $MM	Estimated PV of Capital Investment, $MM	PVR
640	0.25	P90	640	6.39	1.00	6.39
	0.50	P50	640			
	0.25	P10	640			
320	0.25	P90	320	5.67	2.00	2.84
	0.50	P50	320			
	0.25	P10	320			
160	0.25	P90	160	6.28	4.00	1.57
	0.50	P50	160			
	0.25	P10	160			
80	0.25	P90	80	4.53	8.00	0.57
	0.50	P50	80			
	0.25	P10	80			

9. CONCLUSIONS AND RECOMMENDATIONS

9.1. Conclusions

In this work, I developed a probabilistic multi-well reservoir model that incorporates uncertainty in key reservoir parameters and allows the prediction of production profiles as a function of well spacing and different development scenarios for a tight gas reservoir. The discounted production profiles obtained from the simulation results were used to integrate the reservoir model with a Bayesian decision model that, through evaluation of expected net present value, determines the well spacing that maximizes profitability. Besides its ability to model production uncertainty and spatial dependencies between wells, the reservoir model is distinguished from existing technologies and a previous probabilistic single-well model developed for the same area by incorporation of multiple wells in a section and the use of detailed geostatistical characterization to represent reservoir properties in the form of areal maps rather than using a constant property value obtained from a distribution.

The integrated reservoir and decision model were applied to UGR's Deep Basin tight gas asset in the Berland River area, Alberta, Canada, to determine the optimal well spacing in the area. I modeled an illustrative decision context that included two development decisions, the primary spacing and the secondary spacing based on primary development production results. The results were evaluated for different Stage 1 durations to assess the trade-off between stage duration and well spacing.

The decision model was evaluated under two different price environments. In the current low price environment, the optimal development strategy for Stage-1 lengths of 1 and 3 years is 160 acres with no further downspacing. When the stage length is increased to 5 years, the optimum is to start with 640-acre spacing with no further downspacing. When a high environment price is used, the recommendation is to start with a spacing of 80 acres and not downspace for all Stage-1 lengths. The results showed that in both cases, extending the duration of Stage 1 beyond 1 year does not represent an economic benefit. This is thought to be related to the onset of depletion effects in Stage 1 that could be related to relatively high values of permeability in the Gething formation for a tight gas reservoir. The results of this research are specific to the reservoir area modeled and other assumptions made. Generalizing these results to other tight gas reservoir is not recommended.

We have shown that in sequential development plans, the primary production results provide information that can be use to make more informed decisions. For the particular case in this work, it was shown that for the high price environment, if the operator has to commit to 640-acre spacing and cannot downspace, the ENPV would be over $3.5MM less that if a dynamic strategy was used. This $3.5 MM difference is the value of the information that is gained via the staged strategy. The value of a primary development plan is then the value of the primary production plus the value of the information it provides that can be used to decide on the optimal downspacing program. Thus, we see that value can be gained through better use of information and better decision making. I anticipate that use of integrated reservoir and decision modeling tools

and the dynamic development strategies they generate will help operators to quickly achieve the optimal well spacing much earlier in the lives of unconventional reservoirs.

The use of geostatistical maps to model the heterogeneity in the multi-well reservoir model provides a more realistic modeling of the uncertainty in reservoir properties and hence a better handling of the uncertainty in production performance. Since each well's performance is simulated in the model, aspects such as pressure interference and dependencies between reservoir properties are better reproduced. The single-well reservoir model previously developed for the same area reduces the reservoir to a single layer with homogeneous properties and it was shown that it overestimates the uncertainty and could provide errors in the production, leading to suboptimal decisions.

9.2. Recommendations for Future Work

The reservoir model was developed specifically for the Gething D formation in the Berland River Area in Alberta, Canada. Even though the results demonstrate an approximation of real production performance for a tight gas asset, it would be helpful to develop similar models for other unconventional gas assets, including shale gas, to validate the approach presented in this study with more real field examples.

The reservoir model was developed for the evaluation of one section only from the reservoir. An extension of this study could be to evaluate simultaneously the performance of multiple sections to provide the basis for an assessment of optimal number, length and locations of pilot downspacings.

The uncertainties in economics and marketing were not incorporated in this study. A more realistic evaluation that will lead to more informed decisions regarding the optimal development policy for the field could be explored by incorporating the uncertainty in the economic parameters.

NOMENCLATURE

Bcf	Billion Cubic Feet
bcm	Billion Cubic Meters
BDF	Boundary Dominated Flow
CDF	Cumulative Distribution Function
CMG	Computer Modeling Group
DA	Decision Analysis
DCA	Decline Curve Analysis
ENPV	Estimated Net Present Value
IMEX	CMG's g Adaptive Implicit-Explicit Black-Oil Simulator
MC	Monte Carlo Simulation
Mcf	Thousand of Cubic Feet
MM	Million
MMscf	Million Cubic Feet
NPV	Net Present Value
NTG	Net to Gross Ratio
PETREL	Schlumberger's Windows Based Software for 3D Visualization, 3D Mapping and 3D Reservoir Modeling and Simulation
PV	Present Value
PVR	Present Value Ratio
P90	90^{th} Percentile

P50	50^{th} Percentile
P10	10^{th} Percentile
SGS	Sequential Gaussian Simulation
sstvd	Subsea True Vertical Depth
UGR	Unconventional Gas Resources
Vsh	Volume of Shale
VBA	Visual Basic Application for MS Excel
@RISK	Stochastic Modeling Tool from the Palisade Corporation
ϕ_{gas}	Gas Porosity
k_{gas}	Gas Permeability
k_f	Fracture Conductivity
k	Formation Permeability
L_f	Fracture Length
w	Fracture Width
F_{cD}	Dimensionless Fracture Conductivity
q_i	Initial Production Rate
q	Gas Flow Rate as a Function of Time t
t	Time
t_o	Transition Point in Time Hyperbolic to Exponential Decline
b	Hyperbolic Decline Exponent
D_i	Initial Decline Rate
D	Exponential Decline Rate

$\mu_{2/1}(a)$	Expected Discounted Cumulative Production at Stage-2 Giving the Discounted Cumulative Production of Stage-1,
$\rho_{1,2}$	Correlation Coefficient Between Stages
$\frac{\sigma_2}{\sigma_1}$	Ratio Between Standard Deviation at Each Stage,
μ_2	Expected Value for Discounted Cumulative Production for Stage-2
μ_1	Expected Value for Discounted Cumulative Production for Stage-1

REFERENCES

Acosta, W.J. and Mata, T. 2005. Risk Analysis in the Determination of the Best Exploitation Strategy Using a Calibrated Reservoir-Simulation Model. Paper SPE 94804 presented at the SPE Latin American and Caribbean Petroleum Engineering Conference, Rio de Janeiro, Brazil, 20-23 June. DOI: 10.2118/94804-MS.

Arps, J.J. 1945. Analysis of Decline Curves. *Transactions of the American Institute of Mining and Metallurgical Engineers* **160**: 228-247.

Bickel, J.E. and Smith, J.E. 2006. Optimal Sequential Exploration: A Binary Learning Model. *Decision Analysis* **3** (1): 16-32. DOI: 10.1287/deca.1050.0052.

Cheng, Y., Lee, W.J., and McVay, D.A. 2008 a). Improving Reserves Estimates from Decline-Curve Analysis of Tight and Multilayer Gas Wells. *SPE Reservoir Evaluation & Engineering* **11** (5): 912-920. SPE-108176-PA. DOI: 10.2118/108176-PA.

Cheng, Y., Lee, W.J., and McVay, D.A. 2008 b). Quantification of Uncertainty in Reserve Estimation from Decline Curve Analysis of Production Data for Unconventional Reservoirs. *Journal of Energy Resources Technology* **130** (4): 043201. 6 pages. DOI: 10.1115/1.3000096.

Cheng, Y., McVay, D.A., Ayers, W.B. et al. 2008. Simulation-Based Technology for Rapid Assessment of Redevelopment Potential in Marginal Gas Fields - Technology Advances and Validation in Garden Plains Field, Western Canada Sedimentary Basin. *Spe Reservoir Evaluation & Engineering* **11** (3): 521-534. SPE-100583-PA. DOI: 10.2118/100583-PA.

Cheng, Y., McVay, D.A., Wang, J. et al. 2006. Simulation-Based Technology for Rapid Assessment of Redevelopment Potential in Stripper-Gas-Well Fields--Technology Advances and Validation in the Garden Plains Field, Western Canada Sedimentary Basin. Paper SPE 100583 presented at the SPE Gas Technology Symposium, Calgary, Alberta, Canada. 15-17 May. DOI: 10.2118/100583-MS.

Fattah, K.A. 2006. Predicting Production Performance Using a Simplified Model: Neither Hyperbolic nor Exponential Models Fully Explain Decline. So, Why Not Combine Them? *World Oil* **227** (4): 147-152.

Gao, H. and McVay, D.A. 2004. Gas Infill Well Selection Using Rapid Inversion Methods. Paper SPE 90545 presented at the SPE Annual Technical Conference and Exhibition, Houston, Texas, 26-29 September. DOI: 10.2118/90545-MS.

Gonzalez, R.J., Sultana, A., Oudinot, A.Y., and Reeves S.R. 2006. Incorporating Geostatistical Methods with Monte Carlo Procedures for Modeling Coalbed Methane Reservoirs. Paper 0638 presented at the International Coalbed Methane Symposium, Tuscaloosa, Alabama, 22-26 May. **0638**.

Guan, L. and Du, Y. 2004. Fast Method Finds Infill Drilling Potentials in Mature-Tight Reservoirs. Paper SPE 91755 presented at the SPE International Petroleum Conference in Mexico, Puebla, Mexico, 7-9 November. DOI: 10.2118/91755-MS.

Guan, L., McVay, D.A., Jensen, J.L. et al. 2002. Evaluation of a Statistical Infill Candidate Selection Technique. Paper SPE 75718 presented at the SPE Gas Technology Symposium, Calgary, Alberta, Canada, 30 April-2 May. DOI: 10.2118/75718-MS.

Guyaguler, B. and Horne, R.N. 2001. Uncertainty Assessment of Well Placement Optimization. Paper SPE 71625 presented at the SPE Annual Technical Conference and Exhibition, New Orleans, Louisiana, 30 September-3 October DOI: 10.2118/71625-MS.

Hietala, R.W. and Connolly, E.T. 1984. Integrated Rock-Log Calibration in the Elmworth Field, Alberta, Canada: Part Ii: Well Log Analysis Methods and Techniques, in J.A. Masters, Ed., *Volume M 38: Elmworth-Case Study of a Deep Basin Gas Field*. 215 - 242, Tulsa, Oklahoma: AAPG Special Volumes, AAPG.

Hudson, J.W., Jochen, J.E., and Jochen, V.A. 2000. Practical Technique to Identify Infill Potential in Low-Permeability Gas Reservoirs Applied to the Milk River

Formation in Canada. Paper SPE 59779 presented at the SPE/CERI Gas Technology Symposium, Calgary, Alberta, Canada, 3-5April. DOI: 10.2118/59779-MS.

Hudson, J.W., Jochen, J.E., and Spivey, J.P. 2001. Practical Methods to High-Grade Infill Opportunities Applied to the Mesaverde, Morrow, and Cotton Valley Formations. Paper SPE 68598 presented at the SPE Hydrocarbon Economics and Evaluation Symposium, Dallas, Texas, 2-3 April. DOI: 10.2118/68598-MS.

Hurst, A., Brown, G.C., and Swanson, R.I. . 2000. Swanson's 30-40-30 Rule. *AAPG Bulletin* **84** (12): 1883-1891. DOI: 10.1306/8626C70D-173B-11D7-8645000102C1865D.

Kalla, S. and White, C.D. 2005. Efficient Design of Reservoir Simulation Studies for Development and Optimization. Paper SPE 95456 presented at the SPE Annual Technical Conference and Exhibition, Dallas, Texas, 9-12 October. DOI: 10.2118/95456-MS.

King, G.R., Lee, S., Alexandre, P. et al. 2005. Probabilistic Forecasting for Mature Fields with Significant Production History: A Nemba Field Case Study. Paper SPE 95869 presented at the SPE Annual Technical Conference and Exhibition, Dallas, Texas, 9-12 October. DOI: 10.2118/95869-MS

Kupchenko, C.L., Gault, B.W., and Mattar, L. 2008. Tight Gas Production Performance Using Decline Curves. Paper SPE 114991 presented at the CIPC/SPE Gas Technology Symposium 2008 Joint Conference, Calgary, Alberta, Canada, 16-19 June. DOI: 10.2118/114991-MS.

Manceau, E., Mezghani, M., Zabalza-Mezghani, I. et al. 2001. Combination of Experimental Design and Joint Modeling Methods for Quantifying the Risk Associated with Deterministic and Stochastic Uncertainties - an Integrated Test Study. Paper SPE 71620 presented at the SPE Annual Technical Conference and Exhibition, New Orleans, Louisiana, 30 September-3 October. DOI: 10.2118/71620-MS.

Masters, J.A. 1979. Deep Basin Gas Trap, Western Canada. *AAPG Bulletin* **63** (2): 152-181.

Mattar, L. 2008. Production Analysis and Forecasting of Shale Gas Reservoirs: Case History-Based Approach. Paper SPE 119897 presented at the SPE Shale Gas Production Conference, Fort Worth, Texas, 16-18 November. DOI: 10.2118/119897-MS.

McCain, W.D., Voneiff, G.W., Hunt, E.R. et al. 1993. A Tight Gas Field Study: Carthage (Cotton Valley) Field. Paper SPE 26141 presented at the SPE Gas Technology Symposium, Calgary, Alberta, Canada, 28-30 June. DOI: 10.2118/26141-MS.

McKinney, P.D., Rushing, J.A., and Sanders, L.A. 2002. Applied Reservoir Characterization for Maximizing Reserve Growth and Profitability in Tight Gas Sands: A Paradigm Shift in Development Strategies for Low-Permeability Gas Reservoirs. Paper SPE 75708 presented at the SPE Gas Technology Symposium, Calgary, Alberta, Canada, 30 April-2 May. DOI: 10.2118/75708-MS.

Megill, R.E. 1984. *An Introduction to Risk Analysis, Second Edition.* Tulsa, Oklahoma: PennWell Publishing Company. Original Edition. ISBN.

Mian, M.A. 2002. Project Economics and Decision Analysis, Volume I: Deterministic Models, Tulsa, Oklahoma, USA: PennWell Publishing Company.

Mishra, S., Choudhary, M.K., and Datta-Gupta, A. 2002. A Novel Approach for Reservoir Forecasting under Uncertainty. *SPE Reservoir Evaluation & Engineering* **5** (1): 42-48. SPE-75353-PA. DOI: 10.2118/75353-PA.

Newsham, K.E. and Rushing, J.A. 2001. An Integrated Work-Flow Model to Characterize Unconventional Gas Resources: Part I - Geological Assessment and Petrophysical Evaluation. Paper SPE 71351 presented at the SPE Annual Technical Conference and Exhibition, New Orleans, Louisiana, 30 September-3 October. DOI: 10.2118/71351-MS.

Oudinot, A.Y., Koperna, G.J., and Reevs, S.R. . 2005. Development of a Probabilistic Forecasting and History Matching Model for a Coalbed Methane Reservoirs. Paper 0528 presented at the International Coalbed Methane Symposium, Tuscaloosa, Alabama, 16-20 May. **0528**.

Rushing, J.A. and Newsham, K.E. 2001. An Integrated Work-Flow Model to Characterize Unconventional Gas Resources: Part Ii - Formation Evaluation and Reservoir Modeling. Paper SPE 71352 presented at the SPE Annual Technical Conference and Exhibition, New Orleans, Louisiana, 30 September-3 October. DOI: 10.2118/71352-MS.

Schepers, K.C., Gonzalez, R.J., Koperna, G.J. et al. 2009. Reservoir Modeling in Support of Shale Gas Exploration. Paper SPE 123057 presented at the Latin American and Caribbean Petroleum Engineering Conference, Cartagena de Indias, Colombia, 31 May-3- June. DOI: 10.2118/123057-MS.

Smith, D.G., Zorn, C.E., and Sneider, R.M. 1984. The Paleogeography of the Lower Cretaceous of Western Alberta and Northeastern British Columbiain and Adjacent to the Deep Basin of the Elmworth Area. *AAPG Special Volumes.* **Volume M 38** (Elmworth: Case Study of a Deep Basin Gas Field): Pages 79 - 114.

Teufel, L.W., Chen, H.-Y., Engles, T.W. et al. 2004. Optimization of Infill Drilling in Naturally-Fractured Tight Gas Reservoirs: Phase Ii, Final Report, Contract No. DOE-FC26-98FT40486. US DOE:Washington, D.C. DOI: 10.2172/828437.

Turkarslan, G. 2010. Optimizing Development Strategies to Increase Reserves in Unconventional Gas Reservoir. *Thesis. Texas A&M University, College Station, Texas.*

Turkarslan, G., McVay, D.A., Bickel, J.E. et al. 2010. Integrated Reservoir and Decision Modeling to Optimize Spacing in Unconventional Gas Reservoirs. Paper SPE 137816 presented at the Canadian Unconventional Resources and International Petroleum Conference, Calgary, Alberta, Canada, 19-21 October. DOI: 10.2118/137816-MS.

Twartz, S.K., Gorjy, F., and Milne, I.G. 1998. A Multiple Realisation Approach to Managing Uncertainty in the North Rankin Gas Condensate Field, Western Australia. Paper SPE 50078 presented at the SPE Asia Pacific Oil and Gas Conference and Exhibition, Perth, Australia, 12-14 October. DOI: 10.2118/50078-MS.

Voneiff, G.W. and Cipolla, C. 1996. A New Approach to Large-Scale Infill Evaluations Applied to the Ozona (Canyon) Gas Sands. Paper SPE 35203 presented at the Permian Basin Oil and Gas Recovery Conference, Midland, Texas, 27-29 March. DOI: 10.2118/35203-MS.

White, C.D., Willis, B.J., Narayanan, K. et al. 2000. Identifying Controls on Reservoir Behavior Using Designed Simulations. Paper SPE 62971 presented at the SPE Annual Technical Conference and Exhibition, Dallas, Texas, 1-4 October. DOI: 10.2118/ 62971-MS.

Wongnapapisan, B., Flew, S., Boyd, F. et al. 2004. Optimising Brown Field Redevelopment Options Using a Decision Risk Assessment: Case Study-Bokor Field, Malaysia. Paper SPE 87047 presented at the SPE Asia Pacific Conference on Integrated Modelling for Asset Management, Kuala Lumpur, Malaysia, 29-30 March. DOI: 10.2118/87047-MS.

Zahid, S., Bhatti, A.A., Khan, H.A. et al. 2007. Development of Unconventional Gas Resources: Stimulation Perspective. Paper SPE 107053 presented at the Production and Operations Symposium, Oklahoma City, Oklahoma, 31 March-3 April. DOI: 10.2118/107053-MS.

VITA

Name: Rubiel Raul Ortiz Prada

Address: Harold Vance Department of Petroleum Engineering

Texas A&M University

3116 TAMU - 507 Richardson Building

College Station, TX 77843-3116

Email Address: pradort@hotmail.com

Education: B.S., Petroleum Engineering, Universidad Industrial de Santander, Bucaramanga, Colombia, 1995

M.S., Petroleum Engineering, Texas A&M University, 2010